

**Studies on Aerobic Oxidation of Thiols by Riboflavin-Derived
Photocatalysts and Chiral Sensing Using Their Supramolecular Gels**

Marina OKA

岡 真里奈

**Graduate School of Natural Science and Technology
Shimane University**

Studies on Aerobic Oxidation of Thiols by Riboflavin-Derived Photocatalysts and Chiral Sensing Using Their Supramolecular Gels

Table of Contents

Chapter 1	General Introduction	1
Chapter 2	Aerobic oxidative hetero-coupling of thiols using phototropin-inspired flavin photocatalysis	21
Chapter 3	Flavin photocatalyzed S-N bond formation by dehydrogenative coupling of thiols and amines	49
Chapter 4	Aerobic oxidative homo-coupling of thiols by flavin-iodine organocatalysis	67
Chapter 5	Colorimetric chiral sensing using flavin/melamine supramolecular organogels	89
List of Publications		139
Acknowledgment		141

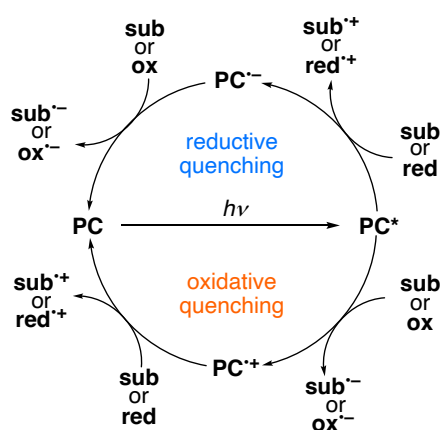
Chapter 1

General Introduction

Oxidation is one of the most important chemical reactions; however, it is also known for having a high environmental impact. Oxidation processes commonly necessitate large quantities of relatively expensive and difficult-to-handle oxidants to remove electrons from the substrates, generating oxidant-derived waste after the reaction. Therefore, it is desirable to develop environmentally friendly oxidation methods from the viewpoint of green and sustainable chemistry. Recently, oxidation using molecular oxygen (O_2) as the terminal oxidant has been actively studied. O_2 is considered an ideal oxidant because it is abundant in the atmosphere, can be used continuously, and only water is generated as a byproduct during the oxidation process.¹ However, the use of O_2 with weak oxidizing power requires activation, which conventionally requires high-temperature and high-pressure conditions. Thus, aerobic oxidation is accompanied by the acceleration of side reactions, resulting in low chemoselectivity and atom efficiency. Therefore, there is a need for the development of environmentally friendly and highly selective catalytic methods for aerobic oxidation under mild conditions.

Photoredox processes using visible-light irradiation are of growing interest in organic synthesis.² Visible light is a clean, easy-to-handle, and abundant source of energy, and thus has significant potential for developing sustainable and environmentally friendly protocols. Generally, photoredox reactions proceed via a catalytic cycle, as illustrated in Scheme 1. In an oxidative quenching cycle, the excited photoredox catalyst (**PC***) is quenched by the donation of an electron to the substrate (**sub**) or oxidant (**ox**). In a reductive quenching cycle, **PC*** is quenched by the acceptance of an electron from the

sub or reductant (**red**). Transition metal complexes, such as $\text{Ru}(\text{bpy})_3^{2+}$ and $\text{Ir}(\text{ppy})_3$, are often used as photoredox catalysts (Figure 1).³ These metal complexes have excellent photophysical properties in visible-photocatalysis, yet they come with disadvantages such as high cost and relative toxicity. Organic photocatalysts, including acridinium dye,⁴ eosin Y,⁵ and quinone⁶, have been recognized as attractive alternatives to transition metal complexes in photocatalytic reactions.^{2b,c,7} These are usually inexpensive, have low toxicity, are easy-to-handle, and are expected to demonstrate excellent activity owing to their high oxidizing power. Flavin compounds, including riboflavin, commonly known as vitamin B₂, have attracted attention as unique photocatalysts that promote various oxidation reactions.⁸ Flavin photocatalyzed oxidation typically proceeds in a reductive quenching cycle. The excited flavin receives electrons from the electron-rich substrate and produces reactive radical species that undergo further transformations. Subsequently, the initial flavin is regenerated by a reaction with a sacrificial oxidant, usually O₂. Therefore, flavin photocatalysts are expected to facilitate O₂-driven oxidation under mild conditions.



Scheme 1. Oxidative and reductive quenching cycle of photocatalysts.

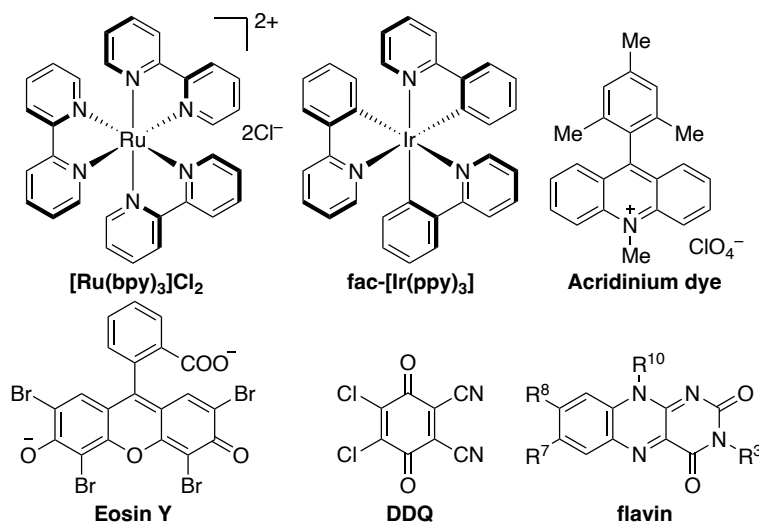


Figure 1. Structures of typical photoredox catalysts.

Riboflavin is a functional organic molecule that exhibits unique redox and optical properties originating from its π -conjugated system.⁹ In vivo, it exists as cofactors such as flavin mononucleotide (**FMN**) and flavin adenine dinucleotide (**FAD**, Figure 2). Flavin compounds play pivotal roles in metabolism, energy production, neurotransmitter regulation, and phototransduction through their association with proteins.¹⁰ Flavin monooxygenase (**FMO**) is the biological enzyme responsible for aerobic oxygenation. Its active center, the riboflavin moiety, receives two electrons from reducing coenzyme NAD(P)H. The resulting ‘reduced form’ of riboflavin carries out oxygenation reactions through the activation of O₂ (Scheme 2). Flavin catalysts are organocatalysts developed to mimic the oxidation function of **FMO** and are known to facilitate two types of oxidation reactions: i) dehydrogenative oxidation and ii) oxygenation reactions, utilizing O₂ as an oxidant.¹¹ These flavin-catalyzed aerobic oxidations are characterized by chemoselective oxidation reactions proceeding under mild conditions.¹² However, in contrast to the numerous successes in the oxygenation reactions, the dehydrogenative oxidation of substrates such as alcohols and thiols is inefficient and challenging to

proceed smoothly due to the weak oxidative power of flavin catalysts.

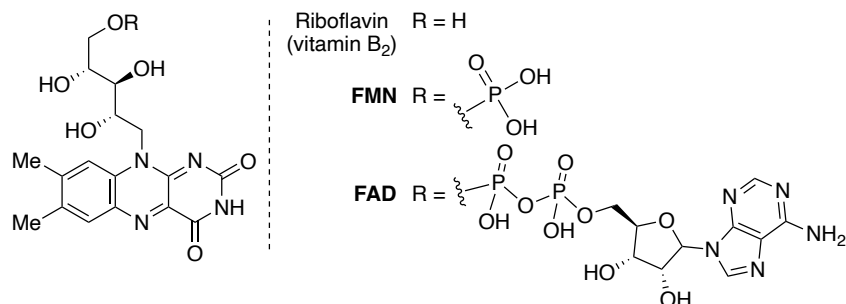
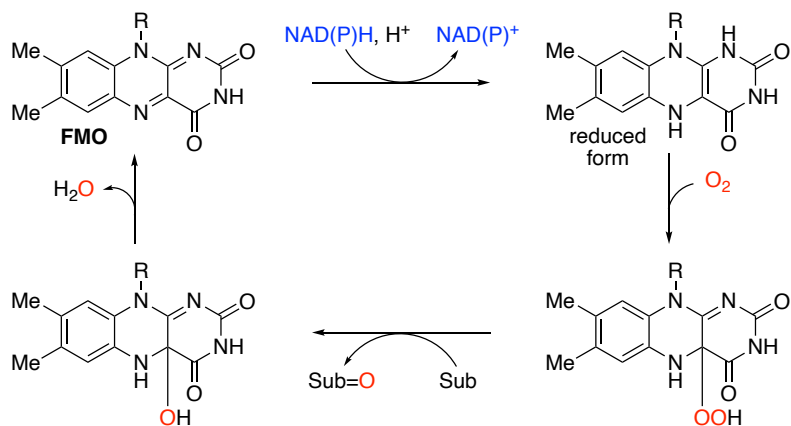


Figure 2. Structures of riboflavin derivatives.



Scheme 2. Catalytic cycle of flavin monooxygenase

Flavin compounds possess absorption in the visible light region and exhibit specific luminescence properties originating from the π -conjugated system. Upon excitation by blue light, the oxidizing power dramatically increased. For example, riboflavin tetraacetate (**TARF**), obtained by acetylation of the four hydroxyl groups of riboflavin and often used as a photocatalyst, increases its oxidizing power under light irradiation. Its singlet excited state reduction potential is 1.67 V vs. saturated calomel electrode (SCE), in contrast to its ground state reduction potential of -0.81 V vs. SCE (Figure 3).¹³ Since

the redox potential of electron-rich 4-methoxybenzyl alcohol is 1.57 V vs. SCE,¹⁴ the excited flavin catalyst is expected to promote oxidation, which is difficult for the flavin catalyst in its ground state. Furthermore, it has been reported that coordination of flavins with metal ions (2.54 V vs. SCE for scandium)¹⁵ or introduction of electron-withdrawing groups into the flavin framework (values up to 2.67 V vs. SCE)¹⁶ can provide flavins with high reduction potential. These flavin catalysts with increasing oxidizing power are expected to be applied to the oxidation of various non-activated benzylic substrates, such as toluene (2.20 V vs. SCE) and ethylbenzene (2.14 V vs. SCE), as well as substrates containing heteroatoms or electron-withdrawing groups.

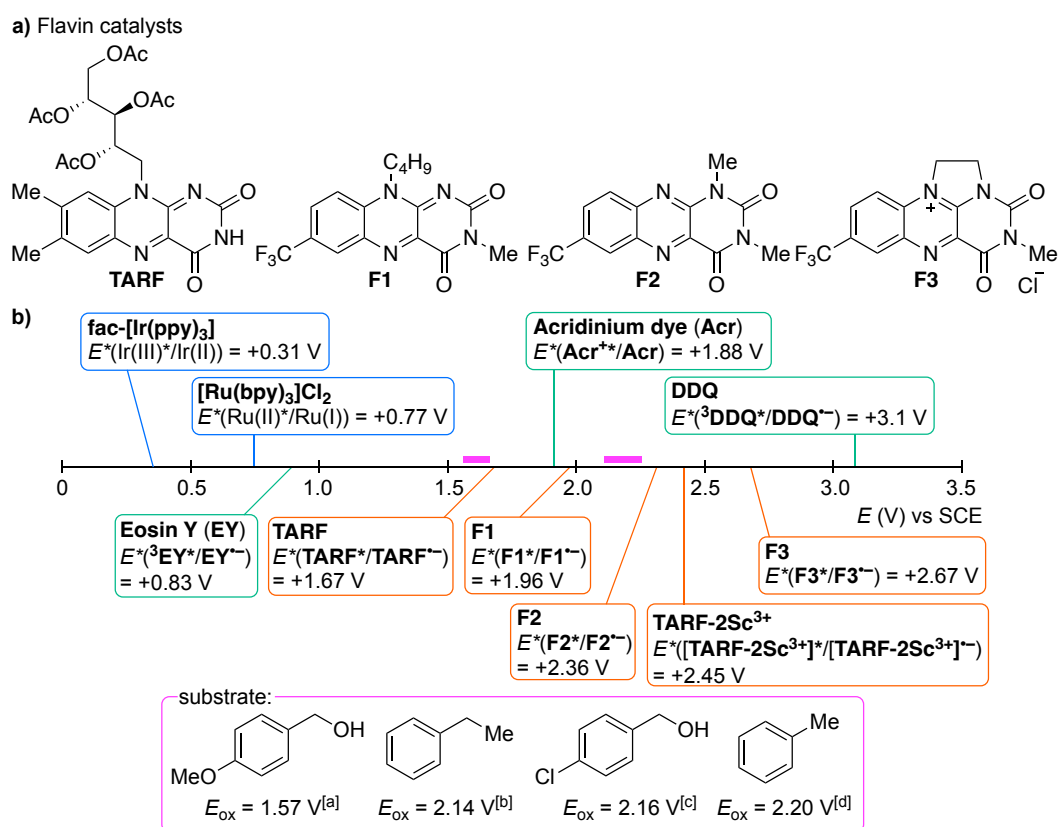
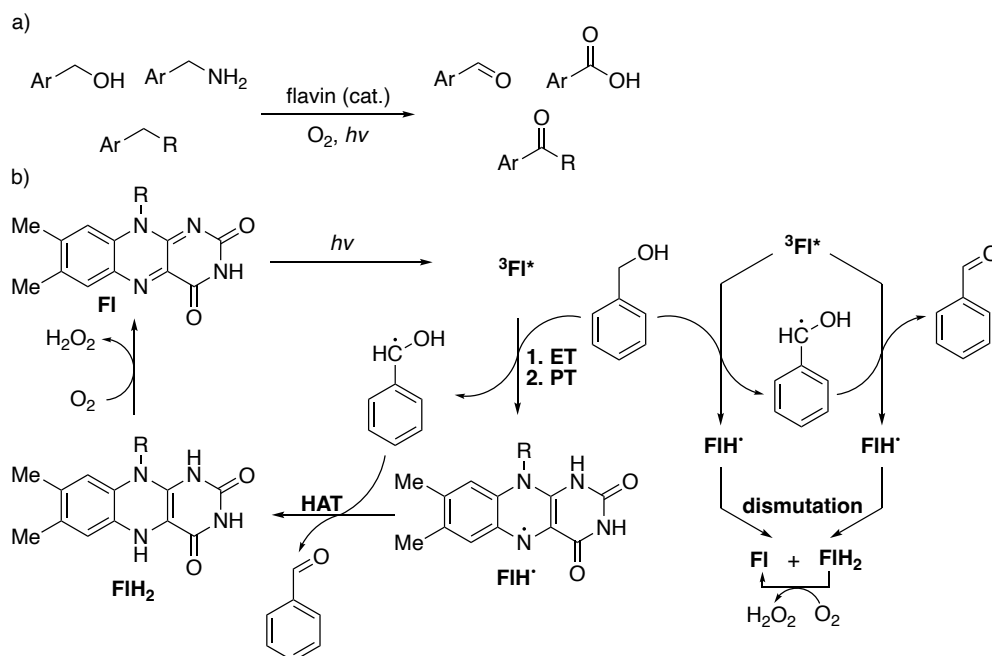


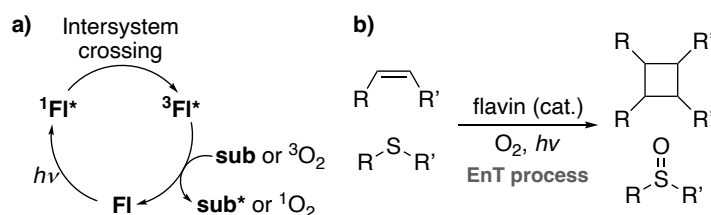
Figure 3. (a) Structures of flavin-based photocatalysts and (b) excited-state reduction potentials of them and other photoredox catalysts. ^[a]ref. 14 ^[b]ref. 15 ^[c]ref. 16a ^[d]ref. 17

Flavin photocatalysts facilitate oxidation through one- and two-electron transfer (ET) mechanisms. The oxidation of benzylic substrates such as benzyl alcohol,¹⁸ benzylamine,¹⁹ and alkylbenzene^{16,20} to aldehydes, ketones, and carboxylic acids has been actively studied (Scheme 3a). Among them, the mechanism of dehydrogenative oxidation of benzyl alcohol has been investigated in detail through subpico- to micro-second transient absorption experiments and LED illuminated NMR studies. Flavin undergoes oxidation through the catalytic cycle illustrated in Scheme 3b.²¹ In addition to benzylic oxidation, numerous other examples have been reported, including esterification of carboxylic acids and alcohols,²² photooxidative coupling of aldehydes and amines,²³ allylation of N-substituted tetrahydroisoquinolines,²⁴ cyanation of aliphatic carboxylic acids,²⁵ and cyclization of thiobenzanilides to benzothiazoles.²⁶



Scheme 3. (a) Flavin photocatalyzed reactions and (b) the mechanism for the oxidation of benzyl alcohol. ET: electron transfer, PT: proton transfer, HAT: hydrogen atom transfer.

The triplet excited state of flavin, which has a long lifetime, also promotes an energy-transfer process (EnT), known as a photosensitizing reaction. In the triplet excited state, the flavin transfers energy to the substrate, thereby the excited substrate allows the chemical reaction to proceed (Scheme 4). As an example of energy transfer with flavin, the intramolecular [2+2] photocycloaddition of styrene dienes has been reported.²⁷ This is due to the direct excitation of the substrate by energy transfer from flavin in the triplet state, facilitating subsequent cyclization. Another known example of photosensitization involves the generation of singlet oxygen $^1\text{O}_2$, which proceeds independently of the substrate. $^1\text{O}_2$, which is efficiently produced by energy transfer from flavin,²⁸ has been reported to be involved in various oxygenation reactions such as oxygenation of sulfides²⁹ and benzyl C-H bonds.³⁰ A further example of a reaction combining EnT and ET is the synthesis of coumarins via *E-Z* isomerization of (*E*)-cinnamic acid and subsequent cyclization.³¹ However, to the best of the author's knowledge, there have been no examples of S-S or S-N bond formation via oxidation of thiols using flavin photocatalysts, although numerous examples of flavin-photocatalyzed oxidations have been reported.



Scheme 4. (a) Catalytic cycle of flavin involving energy transfer (EnT) process and (b) [2+2] photocycloaddition and sulfoxidation promoted by the EnT mechanism flavin catalysts.

Organosulfur compounds find extensive application in organic synthesis, pharmaceuticals, pesticides, and insecticides, marking them as most important compounds. Among them, numerous compounds containing sulfur heteroatoms, that is S-X (X=S, N, P, O, etc.) bonds, have attracted widespread attention because of their remarkable functions, including biological activities.³² Typical organosulfur compounds are presented in Figure 4. Disulfides are important functional groups found in pharmaceuticals including antiviral and anticancer agents,³³ marine natural products,³⁴ foods,³⁵ and functional polymers.³⁶ Disulfides are also used as catalysts,³⁷ intermediates for organic synthesis,³⁸ and functional group protection.³⁹ Sulfoxides commonly obtained by oxygenation of sulfides have also been reported in numerous pharmacologically active substances, such as proton pump inhibitors⁴⁰ and the natural product sulforaphane, which has anticancer activity.⁴¹ In addition to pharmaceuticals, organosulfur compounds containing S-N bonds, such as sulfenamides and sulfonamides, are widely used in synthetic and industrial applications, such as reaction reagents in the synthesis of various organosulfur compounds⁴² and vulcanization accelerators in the rubber industry.⁴³ Therefore, it is necessary to develop an efficient method for the green synthesis of these organosulfur compounds from inexpensive and readily available thiols and sulfides.

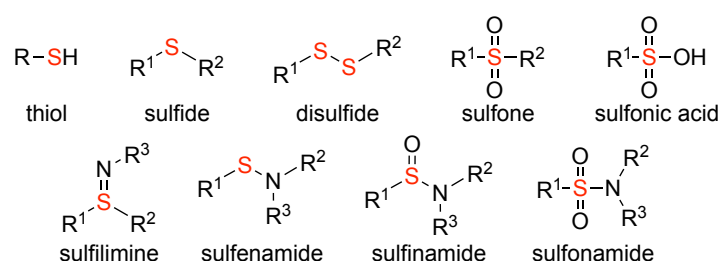


Figure 4. Various organosulfur compounds

In addition to their applications as organocatalysts for green catalytic reactions,^{8a,c,12,44} flavin compounds are expected to function as key building blocks for both functional polymers and supramolecules. Supramolecular gels formed from flavin derivatives represent novel soft materials exhibiting unique functions that combine the properties of supramolecular gels and riboflavin derivatives. Several flavin-based supramolecular gels have been reported thus far.⁴⁵ Nandi *et al.* found that the combination of riboflavin with melamine or methylcellulose forms a hydrogel through hydrogen bonding, which enhances the photoluminescence properties.^{45a-d} Naota *et al.* reported supramolecular organogels containing tetraoctadecanoyl riboflavin^{45g}. Upon ultrasonication, the supramolecular gels formed in organic solvents exhibited high catalytic activity and substrate specificity for the aerobic hydrogenation of alkenes. Hydrogels with dipeptide-functionalized flavins have also been reported to serve as photocatalysts for the oxidation of sulfides.^{45h} However, to the best of the author's knowledge, only a few studies have focused on the chirality of riboflavin.

Based on this information, the author studied the following four areas of riboflavin-derived photocatalysts for the aerobic oxidation of thiols and their supramolecular gels for chiral sensing.

- (1) Aerobic oxidative hetero-coupling of thiols using phototropin-inspired flavin photocatalysis
- (2) Flavin photocatalyzed S-N bond formation by dehydrogenative coupling of thiols and amines
- (3) Aerobic oxidative homo-coupling of thiols by flavin-iodine coupled organocatalysis

(4) Colorimetric chiral sensing using flavin/melamine-based supramolecular organogels

These studies will be described in the following chapters.

Chapter 2 describes the synthesis of unsymmetrical disulfides by aerobic oxidative heterocoupling of two thiols using flavin photocatalysis (Figure 5).⁴⁶ Inspired by the photochemical process of phototropin, the formation of a flavin-thiol adduct, which mimics the phototropin photoreceptor, was catalytically reproduced by simple riboflavin tetraacetate (**FI**), which can be synthesized from commercially available riboflavin (vitamin B₂) by single-step acetylation. The corresponding unsymmetrical disulfides were selectively produced by the flavin-catalyzed reaction of two different thiols under visible light irradiation in air. This system was used to perform heterocoupling between two different alkyl thiols, which is difficult using conventional methods, and the corresponding alkyl-alkyl unsymmetrical disulfides were selectively obtained. In particular, there has been no reported example of the selective heterocoupling of secondary and tertiary alkyl thiols, and this reaction is the first synthetic method to proceed under metal-free and mild conditions at 25 °C. Control experiments and time-resolved absorption measurements were conducted to investigate the reaction mechanism, which indicated that the reaction proceeded via the formation of a flavin-thiol adduct.

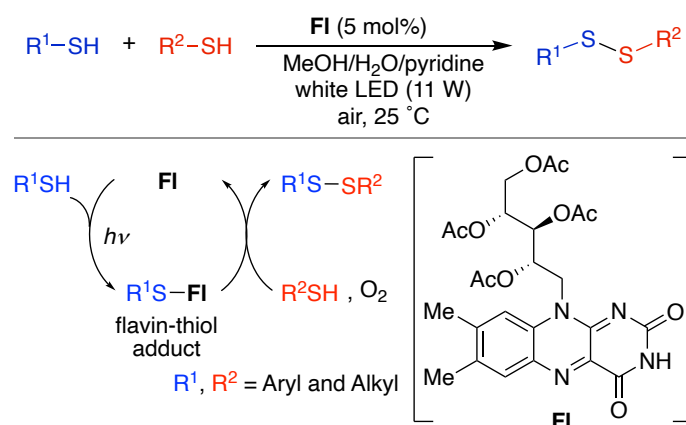
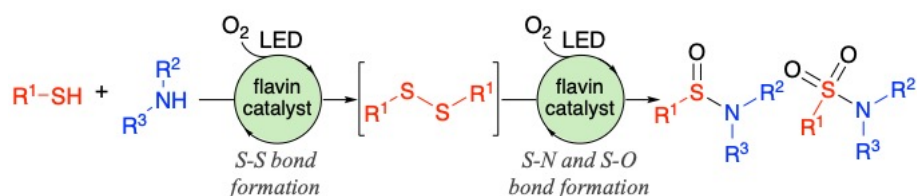


Figure 5. Flavin photocatalyzed hetrocoupling of two thiols for the synthesis of unsymmetrical disulfides

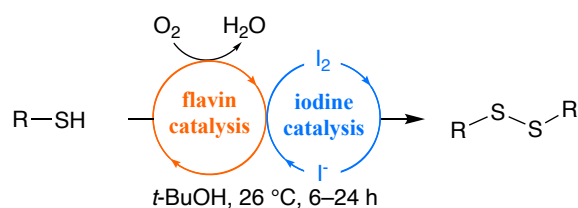
In chapter 3, the author developed a method for the synthesis of sulfinamides and sulfonamides via aerobic oxidative multi-step S-S, S-N, and S-O bond formation by coupling thiols and amines using flavin photocatalyst (Scheme 5).⁴⁷ In the presence of amines, the flavin photocatalyzed oxidation of thiols enhanced the conversion to disulfides. Moreover, the flavin catalyst acted as a photosensitizer under visible-light irradiation to promote the formation of S-N and S-O bonds (oxygenation). This reaction is a green method driven by an environmentally friendly oxidant, air (1 atm), under mild metal-free conditions.



Scheme 5. Aerobic oxidative S-S, S-N, and S-O bond formation by coupling of thiols and amines

In Chapter 4, the author demonstrated that the combination of easily prepared flavin

and iodine catalysts could achieve efficient homocoupling of thiols, thus providing a simple and environmentally friendly synthetic method for disulfides (Scheme 6).⁴⁸ Flavin catalytically facilitates the oxidative transformation of I^- to I_2 through the activation of molecular oxygen as well as the oxidation of thiols to disulfides. While the flavin-catalyzed photooxidation of thiols described in Chapter 2 required visible-light irradiation and basic conditions, this flavin-iodine-catalyzed system allowed the smooth oxidation of thiols without light irradiation and was independent of the acidity of the reaction system. Therefore, this reaction can be applied to various thiols, including those with acidic carboxyl groups and basic amino groups.



Scheme 6. Aerobic oxidation of thiols using flavin-iodine coupled catalysis

In Chapter 5, the author describes colorimetric chiral sensing using supramolecular organogels formed from flavin and melamine derivatives (Figure 6).⁴⁹ A novel chiral supramolecular gel was formed by the stepwise self-assembly of a carbamoylated riboflavin and an achiral melamine derivative in organic solvents. The obtained supramolecular gels were successfully employed as photostimulated chiral sensors for optically active alcohols, enabling visible colorimetric detection of chirality. Owing to the induced supramolecular chirality and flavin photocatalysis, the photooxidation of chiral alcohols occurs enantioselectively, resulting in a color change of the gel from yellow to green.

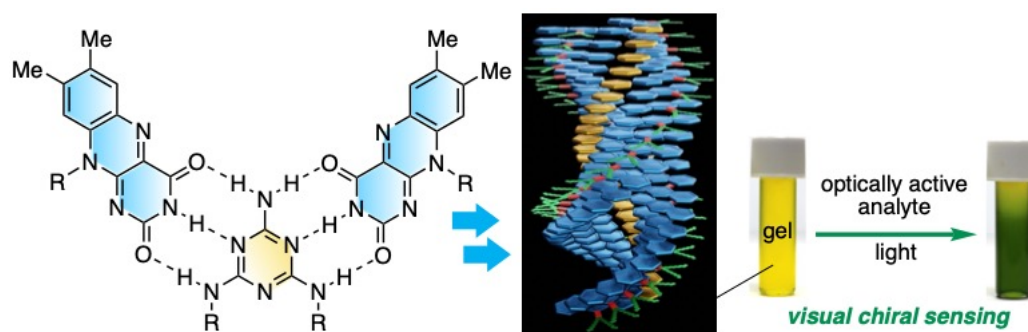


Figure 6. Visible colorimetric chiral sensing with flavin/melamine-based chiral supramolecular organogels.

References

- [1] (a) Hill, C. L. *Nature* **1999**, *401*, 436-437. (b) Campbell, A. N.; Stahl, S. S. *Acc. Chem. Res.* **2012**, *45*, 851-863. (c) Bryliakov, K. P. *Chem. Rev.* **2017**, *117*, 11406-11459.
- [2] (a) Tucker, J. W.; Stephenson, C. R. J. *J. Org. Chem.* **2012**, *77*, 1617-1622. (b) Reckenthäler, M.; Griesbeck, A. G. *Adv. Synth. Cat.* **2013**, *355*, 2727-2744. (c) Romero, N. A.; Nicewicz, D. A. *Chem. Rev.* **2016**, *116*, 10075-10166.
- [3] (a) Prier, C. K.; Rankic, D. A.; MacMillan, D. W. C. *Chem. Rev.* **2013**, *113*, 5322-5363. (b) Shaw, M. H.; Twilton, J.; MacMillan, D. W. C. *J. Org. Chem.* **2016**, *81*, 6898-6926.
- [4] Fukuzumi, S.; Ohkubo, K.; Suenobu, T. *Acc. Chem. Res.* **2014**, *47*, 1455-1464.
- [5] Yang, X.-J.; Chen, B.; Zheng, L.-Q.; Wu, L.-Z.; Tung, C.-H. *Green Chem.* **2014**, *16*, 1082-1086.
- [6] Ohkubo, K.; Fujimoto, A.; Fukuzumi, S. *J. Am. Chem. Soc.* **2013**, *135*, 5368-5371.
- [7] (a) Xuan, J.; Xiao, W.-J. *Angew. Chem. Int. Ed.* **2012**, *51*, 6828-6838. (b) Narayanam, J. M. R.; Stephenson, C. R. J. *Chem. Soc. Rev.* **2011**, *40*, 102-113. (c) Rueping, M.; Vila, C.; Szadkowska, A.; Koenigs, R. M.; Fronert, J. *ACS Catal.* **2012**, *2*, 2810-2815. (d) Hari, D. P.; König, B. *Angew. Chem. Int. Ed.* **2013**, *52*, 4734-4743. (e) Xi, Y.; Yi, H.; Lei, A. *Org. Biomol. Chem.* **2013**, *11*, 2387-2403. (f) Marzo, L.; Pagire, S. K.; Reiser, O.; König, B. *Angew. Chem. Int. Ed.* **2018**, *57*, 10034-10072.
- [8] (a) König, B.; Kümmel, S.; Svobodová, E.; Cibulka, R. *Phys. Sci. Rev.* **2018**, *3*. (b) Srivastava, V.; Singh, P. K.; Srivastava, A.; Singh, P. P. *RSC Adv.* **2021**, *11*, 14251-14259. (c) Cibulka, R.; Fraaije, M. W. *Flavin-Based Catalysis: Principles and Applications*; Wiley, 2021.

- [9] Walsh, C. *Acc. Chem. Res.* **1980**, *13*, 148-155.
- [10] Walsh, C. T.; Wencewicz, T. A. *Nat. Prod. Rep.* **2013**, *30*, 175-200.
- [11] Imada, Y.; Iida, H.; Ono, S.; Murahashi, S.-I. *J. Am. Chem. Soc.* **2003**, *125*, 2868-2869.
- [12] (a) Cibulka, R. *Eur. J. Org. Chem.* **2015**, *2015*, 915-932. (b) Iida, H.; Imada, Y.; Murahashi, S. I. *Org. Biomol. Chem.* **2015**, *13*, 7599-7613.
- [13] Mühlendorf, B.; Wolf, R. *Chem. Commun.* **2015**, *51*, 8425-8428.
- [14] Fukuzumi, S.; Kuroda, S. *Res. Chem. Intermed.* **1999**, *8*, 789-811.
- [15] Fukuzumi, S.; Yasui, K.; Suenobu, T.; Ohkubo, K.; Fujitsuka, M.; Ito, O. *J. Phys. Chem. A* **2001**, *105*, 10501-10510.
- [16] (a) Zelenka, J.; Svobodová, E.; Tarábek, J.; Hoskovcová, I.; Boguschová, V.; Bailly, S.; Sikorski, M.; Roithová, J.; Cibulka, R. *Org. Lett.* **2019**, *21*, 114-119. (b) Tolba, A. H.; Vávra, F.; Chudoba, J.; Cibulka, R. *Eur. J. Org. Chem.* **2020**, *2020*, 1579-1585.
- [17] Fukuzumi, S.; Ohkubo, K.; Suenobu, T.; Kato, K.; Fujitsuka, M.; Ito, O. *J. Am. Chem. Soc.* **2001**, *123*, 8459-8467.
- [18] (a) Fukuzumi, S.; Kuroda, S.; Tanaka, T. *J. Am. Chem. Soc.* **1985**, *107*, 3020-3027. (b) Cibulka, R.; Vasold, R.; König, B. *Chem. –Eur. J.* **2004**, *10*, 6224-6231. (c) Svoboda, J.; Schmaderer, H.; König, B. *Chem. –Eur. J.* **2008**, *14*, 1854-1865. (d) Schmaderer, H.; Hilgers, P.; Lechner, R.; König, B. *Adv. Synth. Catal.* **2009**, *351*, 163-174.
- [19] König, B.; Lechner, R. *Synthesis* **2010**, *2010*, 1712-1718.
- [20] (a) Lechner, R.; Kümmel, S.; König, B. *Photochem. Photobiol. Sci.* **2010**, *9*, 1367-1377. (b) Mühlendorf, B.; Wolf, R. *Angew. Chem. Int. Ed.* **2016**, *55*, 427-430.
- [21] (a) Megerle, U.; Wenninger, M.; Kutta, R. J.; Lechner, R.; König, B.; Dick, B.; Riedle,

- E. Phys. Chem. Chem. Phys.* **2011**, *13*, 8869-8880. (b) Feldmeier, C.; Bartling, H.; Magerl, K.; Gschwind, R. M. *Angew. Chem. Int. Ed.* **2015**, *54*, 1347-1351.
- [22] März, M.; Kohout, M.; Neveselý, T.; Chudoba, J.; Prukała, D.; Niziński, S.; Sikorski, M.; Burdziński, G.; Cibulka, R. *Org. Biomol. Chem.* **2018**, *16*, 6809-6817.
- [23] Hassan Tolba, A.; Krupicka, M.; Chudoba, J.; Cibulka, R. *Org. Lett.* **2021**, *23*, 6825-6830.
- [24] Song, Y.; Wang, X.; Wang, L.; Dong, Z.; Fan, S.; Huang, P.; Zeng, J.; Cheng, P. *Tetrahedron Lett.* **2021**, *78*, 153286.
- [25] Ramirez, N. P.; Konig, B.; Gonzalez-Gomez, J. C. *Org. Lett.* **2019**, *21*, 1368-1373.
- [26] Bouchet, L. M.; Heredia, A. A.; Argüello, J. E.; Schmidt, L. C. *Org. Lett.* **2020**, *22*, 610-614.
- [27] (a) Mojz, V.; Svobodová, E.; Straková, K.; Neveselý, T.; Chudoba, J.; Dvořáková, H.; Cibulka, R. *Chem. Commun.* **2015**, *51*, 12036-12039. (b) Mojz, V.; Pitrová, G.; Straková, K.; Prukala, D.; Brazevic, S.; Svobodová, E.; Hoskovcová, I.; Burdziński, G.; Slanina, T.; Sikorski, M.; Cibulka, R. *Chemcatchem* **2018**, *10*, 849-858.
- [28] Sikorska, E.; Sikorski, M.; Steer, R. P.; Wilkinson, F.; Worrall, D. R. *J. Chem. Soc., Faraday Trans.* **1998**, *94*, 2347-2353.
- [29] Dad'ova, J.; Svobodová, E.; Sikorski, M.; König, B.; Cibulka, R. *Chemcatchem* **2012**, *4*, 620-623.
- [30] Lesieur, M.; Genicot, C.; Pasau, P. *Org. Lett.* **2018**, *20*, 1987-1990.
- [31] (a) Metternich, J. B.; Gilmour, R. *J. Am. Chem. Soc.* **2016**, *138*, 1040-1045. (b) Metternich, J. B.; Gilmour, R. *J. Am. Chem. Soc.* **2015**, *137*, 11254-11257. (c) Morack, T.; Metternich, J. B.; Gilmour, R. *Org. Lett.* **2018**, *20*, 1316-1319.
- [32] (a) Guarino, V. R.; Karunaratne, V.; Stella, V. J. *Bioorg. Med. Chem. Lett. Letters*

- 2007**, *17*, 4910-4913. (b) Kumar, T. S.; Zhou, S.-Y.; Joshi, B. V.; Balasubramanian, R.; Yang, T.; Liang, B. T.; Jacobson, K. A. *J. Med. Chem.* **2010**, *53*, 2562-2576. (c) Rosas-Hernández, A.; Steinlechner, C.; Junge, H.; Beller, M. *Top. Curr. Chem.* **2017**, *376*, 1. (d) O'Driscoll, M.; Greenhalgh, K.; Young, A.; Turos, E.; Dickey, S.; Lim, D. V. *Bioorg. Med. Chem.* **2008**, *16*, 7832-7837. (e) Ilardi, E. A.; Vitaku, E.; Njardarson, J. T. *J. Med. Chem.* **2014**, *57*, 2832-2842. (f) Viswanatharaju Ruddraraju, K.; Parsons, Z. D.; Lewis, C. D.; Gates, K. S. *J. Org. Chem.* **2017**, *82*, 776-780.
- [33] (a) Fujiwara, M.; Watanabe, H.; Matsui, K. *J. Biochem.* **1954**, *41*, 29-39. (b) Lindquist, N.; Fenical, W. *Tetrahedron Lett.* **1990**, *31*, 2389-2392. (c) Block, E.; Ahmad, S.; Catalfamo, J. L.; Jain, M. K.; Apitz-Castro, R. *J. Am. Chem. Soc.* **2002**, *124*, 7045-7055. (d) Scharf, D. H.; Remme, N.; Habel, A.; Chankhamjon, P.; Scherlach, K.; Heinekamp, T.; Hortschansky, P.; Brakhage, A. A.; Hertweck, C. *J. Am. Chem. Soc.* **2011**, *133*, 12322-12325. (e) Chankhamjon, P.; Boettger-Schmidt, D.; Scherlach, K.; Urbansky, B.; Lackner, G.; Kalb, D.; Dahse, H. M.; Hoffmeister, D.; Hertweck, C. *Angew. Chem. Int. Ed.* **2014**, *53*, 13409-13413. (f) Silva, F.; Khokhar, S. S.; Williams, D. M.; Saunders, R.; Evans, G. J. S.; Graz, M.; Wirth, T. *Angew. Chem. Int. Ed.* **2018**, *57*, 12290-12293.
- [34] (a) Holland-Nell, K.; Meldal, M. *Angew. Chem. Int. Ed.* **2011**, *50*, 5204-5206. (b) Fung, E.; Chua, K.; Ganz, T.; Nemeth, E.; Ruchala, P. *Bioorg. Med. Chem. Lett.* **2015**, *25*, 763-766.
- [35] Block, E. *Angew. Chem. Int. Ed.* **1992**, *31*, 1135-1178.
- [36] Xiao, X.; Xue, J.; Jiang, X. *Nature Commun.* **2018**, *9*, 2191.
- [37] Deng, Y.; Wei, X.-J.; Wang, H.; Sun, Y.; Noël, T.; Wang, X. *Angew. Chem. Int. Ed.* **2017**, *56*, 832-836.

- [38] Beletskaya, I.; Moberg, C. *Chem. Rev.* **1999**, *99*, 3435-3462.
- [39] Stachel, H.-D.; Zimmer, B.; Eckl, E.; Semmlinger, K.; Weigand, W.; Wunsch, R.; Mayer, P. *Helv. Chim. Acta* **2005**, *88*, 1208-1220.
- [40] Hetzel, D. J.; Dent, J.; Reed, W. D.; Narielvala, F. M.; Mackinnon, M.; McCarthy, J. H.; Mitchell, B.; Beveridge, B. R.; Laurence, B. H.; Gibson, G. G.; Grant, A. K.; Shearman, D. J. C.; Whitehead, R.; Buckle, P. J. *Gastroenterology* **1988**, *95*, 903-912.
- [41] (a) Juge, N.; Mithen, R. F.; Traka, M. *Cell. Mol. Life Sci.* **2007**, *64*, 1105. (b) Kokotou, M. G.; Revelou, P.-K.; Pappas, C.; Constantinou-Kokotou, V. *Food Chem.* **2017**, *237*, 566-573.
- [42] (a) Briggs, E. L.; Tota, A.; Colella, M.; Degennaro, L.; Luisi, R.; Bull, J. A. *Angew. Chem. Int. Ed.* **2019**, *58*, 14303-14310. (b) Andresini, M.; Spennacchio, M.; Romanazzi, G.; Ciriaco, F.; Clarkson, G.; Degennaro, L.; Luisi, R. *Org. Lett.* **2020**, *22*, 7129-7134. (c) Gigant, N.; Drège, E.; Retailleau, P.; Joseph, D. *Chem. –Eur. J.* **2015**, *21*, 15544-15547. (d) Richards-Taylor, C. S.; Martínez-Lamenca, C.; Leenaerts, J. E.; Trabanco, A. A.; Oehlich, D. *J. Org. Chem.* **2017**, *82*, 9898-9904. (e) Tilby, M. J.; Dewez, D. F.; Pantaine, L. R. E.; Hall, A.; Martinez-Lamenca, C.; Willis, M. C. *ACS Catal.* **2022**, *12*, 6060-6067. (f) Gomez-Palomino, A.; Cornella, J. *Angew. Chem. Int. Ed.* **2019**, *58*, 18235-18239.
- [43] (a) Rong, G.; Chen, Y.; Wang, L.; Li, J.; Wang, J.; Panzer, M. J.; Pang, Y. *J. Appl. Polym. Sci.* **2014**, *131*. (b) Charoeythornkhajhornchai, P.; Samthong, C.; Somwangthanoj, A. *J. Appl. Polym. Sci.* **2017**, *134*, 44822.
- [44] Murahashi, S. I. *Angew. Chem. Int. Ed.* **1995**, *34*, 2443-2465.
- [45] (a) Manna, S.; Saha, A.; Nandi, A. K. *Chem. Commun.* **2006**, 4285-4287. (b) Saha, A.; Manna, S.; Nandi, A. K. *Langmuir* **2007**, *23*, 13126-13135. (c) Saha, A.; Manna,

S.; Nandi, A. K. *Soft Matter* **2009**, *5*. (d) Bairi, P.; Roy, B.; Nandi, A. K. *Chem. Commun.* **2012**, *48*, 10850-10852. (e) Fitzpatrick, B.; Creran, B.; Cooke, G.; Rotello, V. M. *Macromol. Chem. Phys.* **2012**, *213*, 1758-1767. (f) Bachl, J.; Hohenleutner, A.; Dhar, B. B.; Cativiela, C.; Maitra, U.; König, B.; Díaz, D. D. *J. Mater. Chem. A* **2013**, *1*. (g) Kawamorita, S.; Fujiki, M.; Li, Z.; Kitagawa, T.; Imada, Y.; Naota, T. *ChemCatChem* **2019**, *11*, 878-884. (h) Cariello, M.; Dietrich, B.; Thomson, L.; Gauci, V.; Boyer, A.; Sproules, S.; Cooke, G.; Seddon, A.; Adams, D. J. *Chem. –Eur. J.* **2022**, *28*, e202201725.

[46] Oka, M.; Katsube, D.; Tsuji, T.; Iida, H. *Org. Lett.* **2020**, *22*, 9244-9248.

[47] Oka, M.; Takeda, A.; Iida, H. *Chem. Lett.*, **2024**, DOI: 10.1093/chemle/upad057

[48] Oka, M.; Kozako, R.; Iida, H. *Synlett* **2021**, *32*, 1227-1230.

[49] Oka, M.; Kozako, R.; Teranishi, Y.; Yamada, Y.; Miyake, K.; Fujimura, T.; Sasai, R.; Ikeue, T.; Iida, H. *Chem. –Eur. J.* **2024**, e202303353.

Chapter 1

Chapter 2

Aerobic oxidative hetero-coupling of thiols using phototropin-inspired flavin photocatalysis

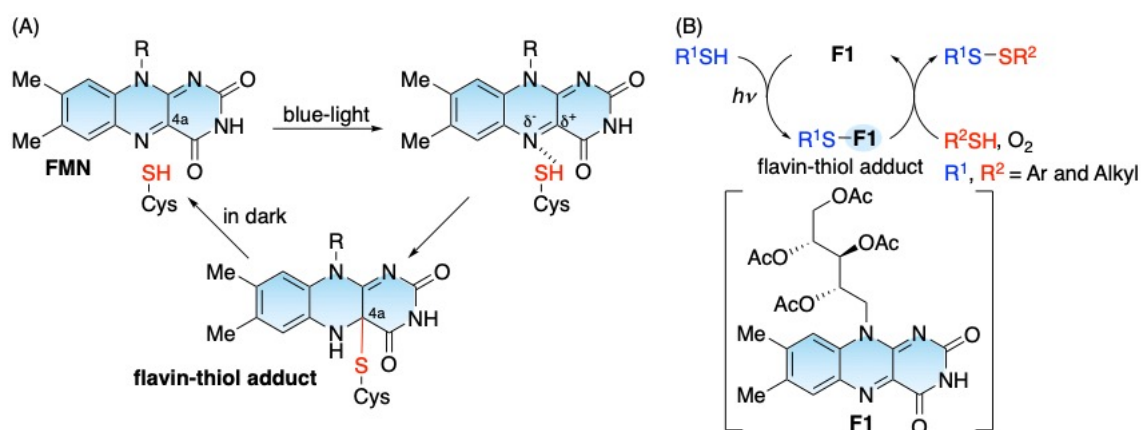
- 2-1 Abstract
- 2-2 Introduction
- 2-3 Results and Discussion
- 2-4 Conclusion
- 2-5 Experimental Section
- 2-6 References and Notes

2-1 Abstract

Inspired by the photochemical process of phototropin, a blue light receptor protein in plants, the author developed a novel flavin-based photocatalytic approach for the chemoselective oxidative heterocoupling of two thiols. This system simplifies the synthesis of unsymmetrical disulfides. Using photo- and redox organocatalysis of flavin derivatives, readily synthesized from commercially available riboflavin, the oxidation of thiols occurs under mild conditions and irradiation with visible light using O₂, which is abundant and known as a green oxidant.

2-2 Introduction

Higher plants have a unique blue light receptor protein called phototropin, which plays a role in optimizing and controlling the light response of plants.¹ A plant bending its stem toward a light source is an example of a phototropin-mediated process. Phototropins typically comprise two light-oxygen-voltage-sensing domains (LOV domains), which are noncovalently bound to a chromophore, flavin mononucleotide (FMN).² Upon exposure to blue light, FMN is excited and interacts with a protein cysteine to form a flavin–thiol adduct connecting the C(4a) carbon of the FMN cofactor to the thiol group of cysteine (Scheme 1A).³ The formed adducts then revert to their initial form in the dark. Although this photochemical process has been actively studied in biology and biochemistry, it has not received much attention in organic synthesis. The author hypothesized that the flavin–thiol adducts formed by visible light irradiation could be used as a reaction intermediate in the synthesis of sulfur-containing compounds in organic chemistry. Inspired by this photochemical process, the author presents a novel green method for synthesizing unsymmetrical disulfides. An organocatalyst derived from riboflavin (**F1**) facilitates the chemoselective synthesis of unsymmetrical disulfides from two different thiols under air and visible light irradiation, using flavin–thiol adduct formation as a key step (Scheme 1B). Riboflavin and its derivatives have recently attracted attention as promising redox organocatalysts that facilitate various catalytic oxidations^{4,5} and have also been applied to nonthermal photocatalytic oxidations.^{6,7} The application of flavin catalysts has been recognized as an attractive approach for designing green and sustainable transformations. However, flavin-based photocatalytic synthesis of disulfides has not yet been developed.



Scheme 1. (A) Photoreaction of phototropin and (B) heterocoupling of thiols using F1.

Disulfides, in which two sulfur atoms are covalently bonded, are important in biological,⁹ pharmaceutical,¹⁰ and materials chemistry.¹¹ Among them, unsymmetrical disulfides (R¹S-SR²) are often found in pharmacologically active compounds, such as antibiotic and anti-thrombotic activity (Figure 1)¹². Therefore, the development of a facile approach to the synthesis of unsymmetrical disulfides has attracted considerable attention. However, while various synthetic methods have been developed for synthesizing symmetrical disulfides (R¹S-SR¹), the effective synthetic strategies for unsymmetrical disulfides have been limited.¹³ Over the past several years, nucleophilic substitution reactions¹⁴ and thiol-disulfide exchange reactions¹⁵ have been reported in synthesizing unsymmetrical disulfides (Scheme 2A). However, this requires the prefunctionalization of thiols, which is a two-step process. In addition, the direct oxidative coupling of two different thiols using metal catalysts¹⁶ or oxidants¹⁷ has received much attention as the most atomic-economical and ideal method (Scheme 2B). Metal-catalyzed heterocoupling reactions typically require large amounts of metals because sulfur atoms are strongly coordinated with metals. Heterocoupling reactions using oxidants have the environmental problem of requiring excess oxidants and the chemoselectivity problem of difficulty

controlling the homocoupling, which produces symmetrical disulfides as byproducts. Recently, the heterocoupling of thiols by electrochemical anodic oxidation has been reported¹⁸; however, the substrate scope remains a problem, and the development of a chemoselective and green method is desired.

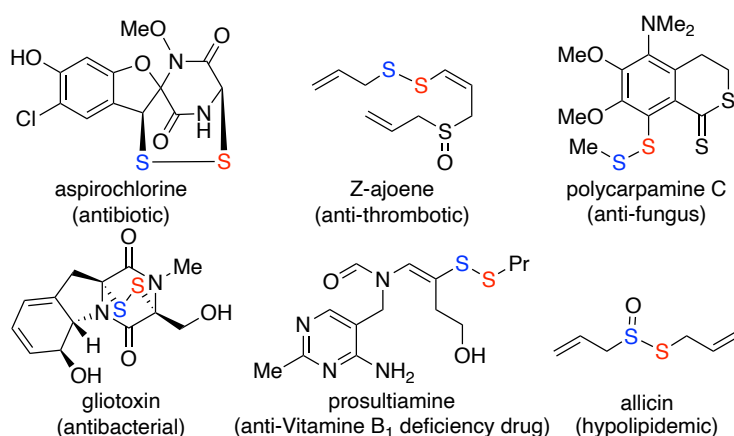
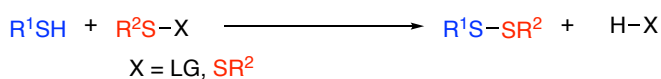
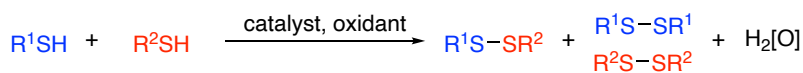


Figure 1. Some pharmaceutically unsymmetrical disulfides.

(A) Substitution reaction



(B) Oxidative hetero-coupling

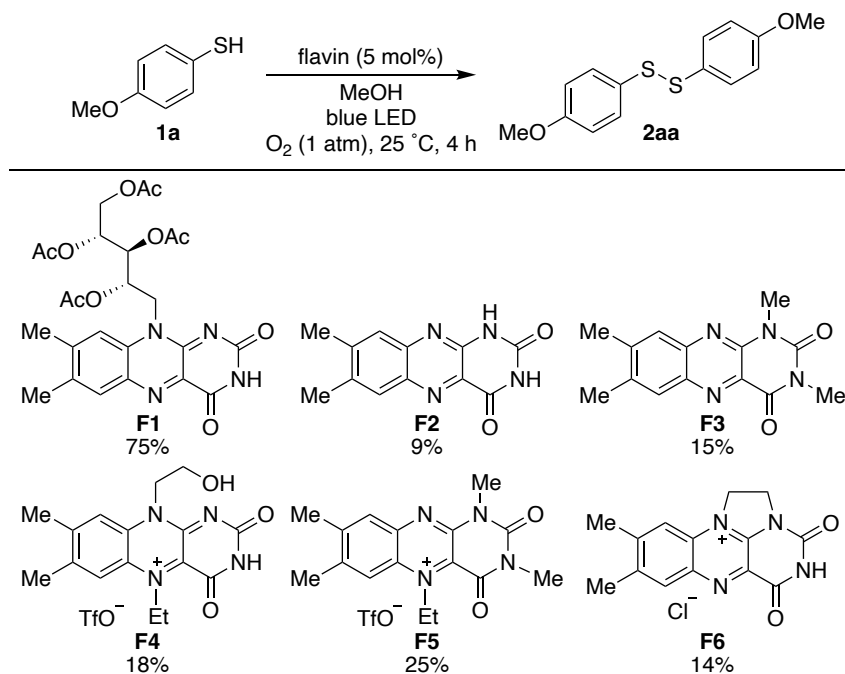


Scheme 2. Synthesis methods of unsymmetrical disulfides.

2-3 Results and Discussion

First, the catalytic activity of the flavin compounds in the photocatalytic oxidation of thiols to symmetrical disulfides was investigated (Table 1). Homocoupling of 4-methoxybenzenthionol (**1a**) was performed using readily available flavin compounds as photocatalysts in MeOH under blue LED irradiation and oxygen (1 atm) at 25 °C for 4 h. Various neutral flavins (**F1–3**) and cationic flavinium salts (**F4–6**) were studied, and the oxidation of **1a** most proceeded when **F1**, which is easily synthesized by the acetylation of riboflavin, was used to obtain the corresponding disulfide **2aa** in 75% yield. Alloxazines **F2** and **F3** and cationic flavinium salts **F4–6** showed low catalytic activity in 9%–25% yields.

Table 1. Effect of flavin catalysts on homocoupling of **1a**.

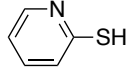


Conditions: **1a** (0.01 M), flavin (5 mol%), and MeOH with blue LED (7.2 W) under O₂ (1 atm) at 25 °C for 4 h. The yield was determined by GC using tetraethylene glycol dimethyl ether as an internal standard.

The reaction of 2-mercaptopyridine (**1b**) in MeOH/H₂O (1:1, v/v) using **F1** as the photocatalyst afforded **1bb** quantitatively in 2 h (Table 2, entry 1). Aerobic oxidative coupling did not proceed in the absence of **F1**, without white LED irradiation, or under N₂ atmosphere (entries 2–4), indicating the photocatalysis of **F1** and the need for O₂. Notably, this oxidative transformation was chemoselective, and no over-oxidized byproducts, including sulfides, sulfoxides, or pyridine N-oxide, were observed (entry 1). The coupling of **1a** with a relatively electron-rich unit was obtained in low yield (19%) in MeOH/H₂O (1:1, v/v), but **2aa** was obtained in 84% yield in MeOH/H₂O/pyridine (1:1:0.01, v/v), suggesting that a small amount of pyridine accelerated the coupling reaction (entries 5 and 6). This is likely because thiols become anionic under basic conditions, thereby increasing their nucleophilicity. By contrast, the reaction did not proceed with tert-butyl mercaptan (**1c**), probably owing to the moderate oxidizing power of the flavin catalyst (entry 7)¹⁹. This moderate oxidizing power of the flavin photocatalyst was expected to positively affect chemoselective heterocoupling, and the synthesis of unsymmetrical disulfides with equimolar amounts of thiols **1b** and **1c** was attempted. The desired unsymmetrical disulfide **2bc** was obtained chemoselectively in 82% yield, whereas symmetrical disulfides, which formed byproducts, were hardly obtained (entry 8).

Table 2. Synthesis of symmetrical disulfides and unsymmetrical disulfides.^a

$$\begin{array}{ccc}
 \text{R}^1\text{-SH} & \xrightarrow[\text{air, 25 }^\circ\text{C}]{\text{F1 (5 mol\%)} \\ \text{white LED}} & \text{R}^1\text{-S-S-R}^1 \\
 \mathbf{1x} & & \mathbf{2xx} \\
 \\
 \text{R}^1\text{-SH} + \text{R}^2\text{-SH} & \longrightarrow & \text{R}^1\text{-S-S-R}^2 \\
 \mathbf{1x} \quad \mathbf{1y} & & \mathbf{2xy}
 \end{array}$$

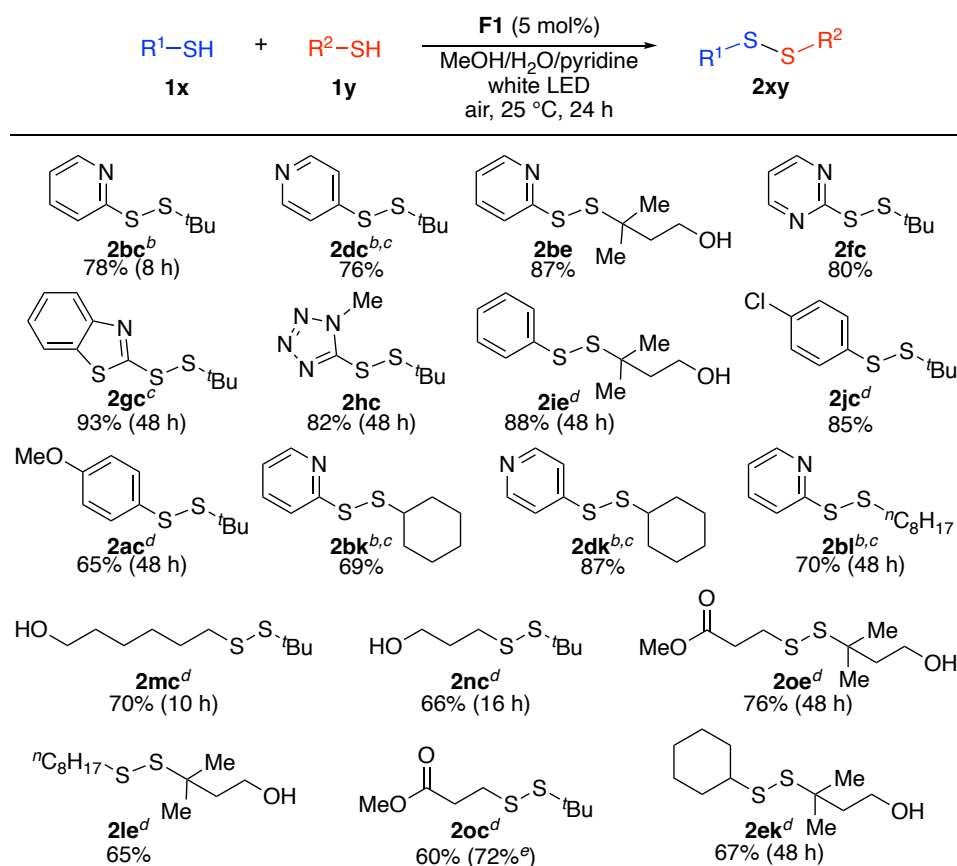
entry	R ¹ -SH	R ² -SH	solvent	time (h)	product yield
1		–	MeOH:H ₂ O 1:1 (v/v)	2	2bb >99%
2 ^b	1b	–	MeOH:H ₂ O 1:1 (v/v)	2	2bb 11%
3 ^c	1b	–	MeOH:H ₂ O 1:1 (v/v)	2	2bb 2%
4 ^d	1b	–	MeOH:H ₂ O 1:1 (v/v)	2	2bb 1%
5	1a	–	MeOH:H ₂ O 1:1 (v/v)	2	2aa 19%
6	1a	–	MeOH:H ₂ O:pyridine 1:1:0.01 (v/v)	2	2aa 84%
7	^t Bu-SH 1c	–	MeOH:H ₂ O:pyridine 1:1:0.01 (v/v)	2	2cc 15%
8 ^e	1b	1c	MeOH:H ₂ O 1:1 (v/v)	6	2bc (2bb 2%) 82% (2cc <1%)

^aConditions: **1x** (0.05 M), **F1** (5 mol%), and solvent, with white LED under air (1 atm) at 25 °C for 2 h. The yield was determined by GC using tetraethylene glycol dimethyl ether as an internal standard. ^bWithout **F1**. ^cWithout irradiation. ^dUnder N₂. ^e**1x** (0.05 M), **1y** (0.05 M), **F1** (5 mol%), and MeOH/H₂O (1:1, v/v) were mixed in air (1 atm) at 25 °C for 6 h. The yield was determined by GC using tetraethylene glycol dimethyl ether as an internal standard.

Next, the substrate scope of the thiol heterocoupling reaction was investigated (Table 3). The heterocoupling between various heteroarylthiols (**1b,d,f–h**) and tert-alkanethiols (**1c,e**) successfully yielded the corresponding products in 76%–93% yields. Arylthiols **1i**, **1j**, and **1a** reacted with **1c** and **1e** and furnished unsymmetrical disulfides in 65%–88% yields, whereas the arylthiol with an electron-rich substituent (**1a**) showed relatively

lower reactivity than electron-poor arylthiols. In addition to tert-alkanethiols, the heterocoupling reaction proceeded with secondary and primary alkanethiols (**1k**, **1l**) to give **2bk**, **2dk**, and **2bl** in 69%–87% yields. Most examples reported thus far have been limited to the heterocoupling of aryl and alkanethiols, which differ mainly in their reactivity. Because the two alkanethiols have relatively analogous reactivities, the chemoselective synthesis of the unsymmetrical alkyl–alkyl disulfides has been challenging.^{16b} Based on these challenges, it is remarkable that the current photocatalytic method was able to transform two alkanethiols (primary and tertiary) to the desired unsymmetrical alkyl–alkyl disulfides (**2mc,nc,oe,le**, and **oc**) in 65%–76% yields at ambient temperature. Unsymmetrical disulfide (**2ek**) was also obtained in 67% yield from the reaction between a secondary alkanethiol and a tertiary alkanethiol. The heterocoupling of secondary and tertiary alkanethiols has not been reported previously, and the author succeeded in developing the first green chemoselective method.

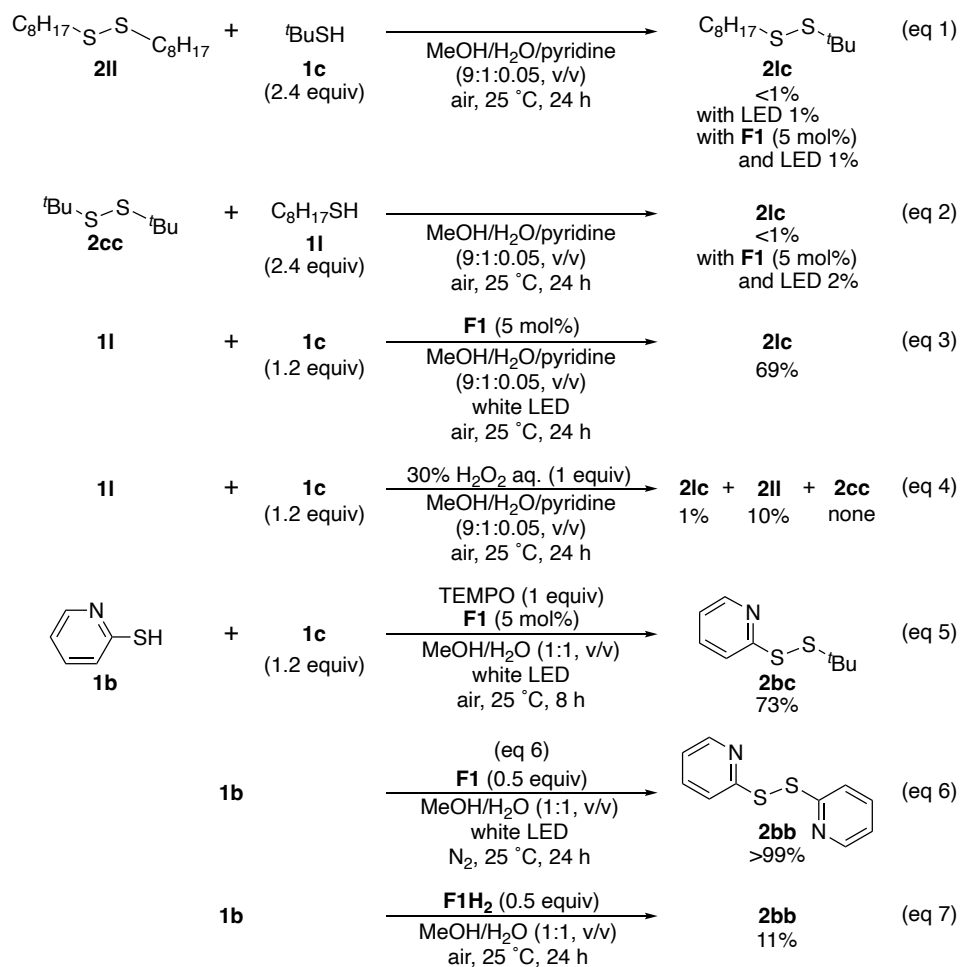
Table 3. Substrate scope of photocatalyzed oxidative heterocoupling



^aConditions: **1x** (0.05 M), **1y** (0.06 M), **F1** (5 mol%), and MeOH/H₂O/pyridine (1:1:0.01, v/v), with white LED (11 W) under air (1 atm) at 25 °C for 24 h. ^bWithout pyridine. ^cMeOH/H₂O/pyridine (9:1:0.05, v/v). ^dUsing **1x** (0.2 M), **1y** (0.24 M), and MeOH/H₂O/pyridine (9:1:0.05, v/v). ^eYield was determined by GC.

Control experiments were conducted to elucidate the reaction mechanism (Scheme 3). The heterocoupling reactions of thiols reported previously initially produce symmetrical disulfides R¹S–SR¹, followed by thiol–disulfide exchange to produce the corresponding unsymmetrical disulfide R¹S–SR².^{16b,c,18} However, using symmetrical alkyl–alkyl disulfides **2ll** and **2cc** as starting materials and reacting them with alkanethiols **1c** and **1l** did not yield the corresponding unsymmetrical alkyl–alkyl disulfide **2lc**, both in the

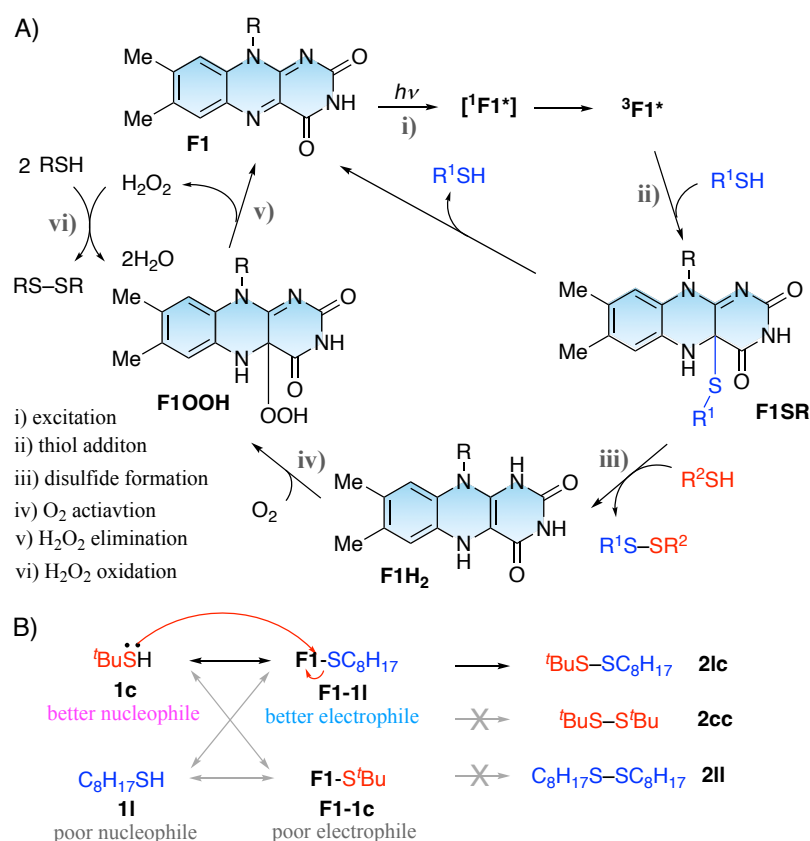
absence and presence of **F1** (eqs 1 and 2). This indicates that the thiol–disulfide exchange reaction with alkanethiols was not facilitated because the alkyl–alkyl disulfides were not highly reactive. By contrast, in this catalytic reaction system, **2lc** was obtained from two different alkyl thiols, **1l** and **1c** (eq 3). When H₂O₂ was used as the oxidant, the homocoupling product **2ll** was preferentially obtained instead of the heterocoupling product **2lc** (eq 4). As shown in eq 5, the addition of the radical scavenger 2,2,6,6-tetramethylpiperidine 1-oxyl (TEMPO) to the reaction mixture of **1b** and **1c** did not decrease the yield of unsymmetrical disulfide **2bc**. The result suggested that this catalytic reaction proceeds without the formation of thiyl radicals, in contrast to the previous processes.^{16b,c,18} Using 0.5 equiv of **F1** under nitrogen, **1b** was quantitatively converted to **2bb** (eq 6).



Scheme 3. Control experiments

Based on these experiments and previously reported literature, a mechanism for the transformation of the two thiols into unsymmetrical disulfides is proposed in Scheme 4A. **F1** is excited by visible light irradiation to $^3\mathbf{F1}^*$ via a $^1\mathbf{F1}^*$ intermediate (step i), and $^3\mathbf{F1}^*$ then forms an **FISR** similar to the LOV domain of phototropin by covalent bonding with a thiol (step ii).^{3a,20} **FISR** undergoes nucleophilic substitution from the thiol to form a disulfide and reduced flavin (**F1H₂**, Step iii). This may explain why the current flavin-catalyzed system succeeded in producing unsymmetrical disulfide **2Ic** (eq 3, Scheme 3), which was hardly promoted by the previous thiol–disulfide exchange reactions (eqs 1 and

2). If the reaction pathway of **F1SR** is similar to that of the flavin-thiol adduct formed in the LOV domain,^{3a,20} then it is possible that **F1SR** removes thiol and returns to **F1**. However, owing to the reversibility of this process, **F1SR** is continuously formed from **F1** and remains constant in the reaction mixture in the light steady state. Therefore, efficient promotion of the subsequent nucleophilic substitution of thiols by **F1SR** was achieved. The obtained **F1H₂** reacts with O₂ to form the hydroperoxy intermediate (**F1OOH**) and then returns to the initial **F1** by releasing H₂O₂ (steps iv and v).²¹ **1b** was slightly converted to **2bb** with **F1H₂** (0.5 eq) in air and the dark (eq 7), suggesting that H₂O₂ produced by **F1H₂** and O₂ may contribute to disulfide bond formation (step vi), but this is a minor process. As shown in Scheme 4B, during heterocoupling, two different thiols, **1c** and **1l**, usually yielded two corresponding flavin adducts (**F1-1c** and **F1-1l**), potentially producing three disulfides (**2lc**, **2cc**, and **2ll**) via four reaction pathways. However, owing to the mild reactivity of the photoinduced **F1SR**, chemoselective coupling is possible in this system. The relatively electron-rich thiol **1c** acts as an excellent nucleophile and preferentially nucleophilically attacks the relatively electron-deficient flavin adduct **F1-1l**.



Scheme 4. (A) Proposed photocatalyzed mechanism and (B) mechanism of heterocoupling reaction through flavin-thiol adducts.

To clarify the formation of flavin-thiol adducts in this reaction system, the reaction of **1l** was studied by nanosecond laser flash spectroscopy using **F1** under a nitrogen atmosphere (Figure 2A). Interestingly, the spectral changes were similar to those observed in the LOV domain of phototropin.^{3a,20} Upon laser irradiation, the characteristic absorption bands at approximately 360 and 450 nm of **F1** (Figure 2B) decreased, and a new absorption appeared in the 600–700 nm region within 20 ns (Figure 2Aa). This may be owing to absorption derived from the triplet state of flavin ($^3\text{F1}^*$). The triplet state disappeared within 10 μs , leaving the metastable intermediate state (Figure 2Ab). This intermediate state could originate from the flavin-thiol adduct (**F1SR**), which has an

absorption at 390 nm.^{3a,20} However, owing to the poor resolution of nanosecond laser flash spectroscopy, it cannot be excluded that the 4a-methoxy and hydroxy flavins (**F1OMe** and **F1OH**), whose absorption is expected to appear at approximately the same wavelength as **F1SR**, may have formed in the MeOH/H₂O solution.²² After 10 s, the metastable intermediate returned to its initial ground state (**F1**) (Figure 2c), likely due to the removal of thiol, MeOH, or H₂O from its adduct (**F1SR**, **F1OMe**, or **F1OH**). These results indicate that the formation of flavin intermediates is triggered by light, and this process is reversible.

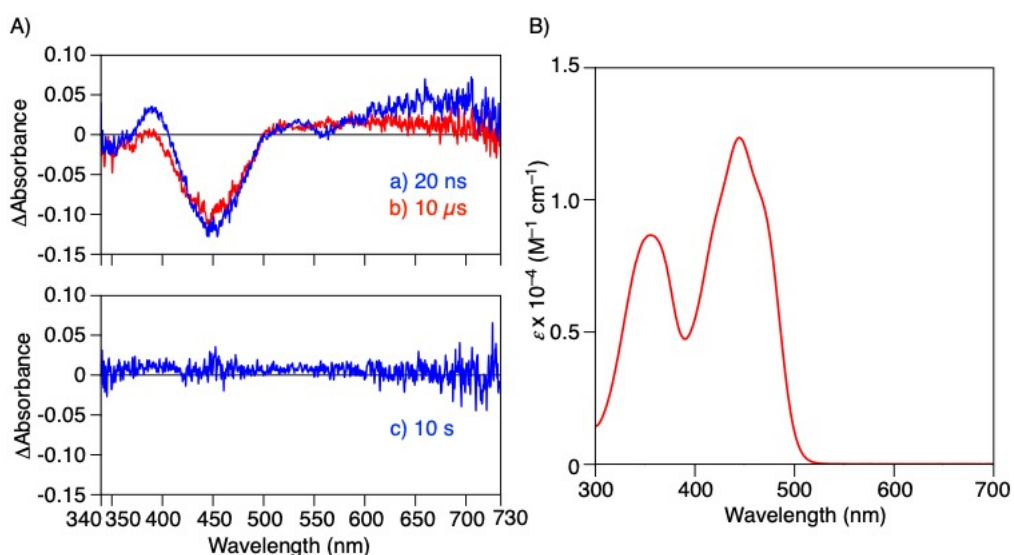


Figure 2. (A) Difference absorption spectra of **F1** (0.12 mM) with **11** (13 mM) in MeOH/H₂O/pyridine (9:1:0.05, v/v) under N₂. Spectra were collected at (a) 20 ns, (b) 10 μs, and (c) 10 s after excitation with a 355 nm laser pulse. (B) Absorption spectrum of **F1** in MeOH/H₂O/pyridine (9:1:0.05, v/v, 0.12 mM).

2-4 Conclusion

In conclusion, a novel approach for a chemoselective oxidative heterocoupling reaction using two thiols as starting materials was successfully developed. A simple flavin catalyst, readily synthesized from commercially available riboflavin, successfully formed a phototropin-like flavin-thiol adduct under visible-light irradiation, and its mild reactivity played an important role in the chemoselective synthesis of unsymmetrical disulfides. Owing to the redox and photo-organocatalysis of flavin, it is possible that this reaction system can be driven by O₂ and visible light at room temperature under metal-free conditions. Although slight limitations in efficiency and substrate scope are present at the current stage, this method using photoinduced flavin-thiol adducts as key intermediates provides a new methodology for the catalytic organic reactions of sulfur-containing compounds.

2-5 Experimental Section

General

The IR spectra were recorded on a JASCO FT/IR-660plus spectrophotometer (JASCO, Tokyo, Japan). The NMR spectra were measured using JEOL JNM-L400 and JNM ECX-500 spectrometers (JEOL, Akishima, Japan) operating at 400 and 500 MHz, respectively, for ^1H and 100 and 126 MHz, respectively, for ^{13}C using tetramethylsilane (TMS) or a solvent residual peak as the internal standard. The electrospray ionization mass (ESI-MS) spectra were recorded on a Bruker microTOFII mass spectrometer (Bruker, Billerica, MA) using the positive or negative mode ESI-TOF method for acetonitrile solutions and sodium formate as the reference. The GC measurements were performed on a Shimadzu GC-2014 gas chromatograph (Shimadzu, Kyoto, Japan) equipped with a flame ionization detector (FID) using a Supelco Equity-5 (30 m x 0.25 mm) column.

Materials

All starting materials were purchased from Aldrich (Milwaukee, WI), Wako Pure Chemical Industries (Osaka, Japan), Nacalai tesque (Kyoto, Japan), and Tokyo Kasei (TCI, Tokyo, Japan) and were used as received. Riboflavin tetraacetate (**F1**)²³ and its reduced form (**F1H₂**)²⁴ were synthesized according to the previously reported methods.

Experimental Procedures

Typical procedure for homocoupling of 1a. A mixture of 4-methoxybenzenethiol (**1a**, 140 mg, 1.00 mmol), **F1** (27.2 mg, 0.050 mmol), MeOH (10 mL), H₂O (10 mL), and pyridine (100 μL) was stirred and irradiated (white LED, 11 W) at 25 °C for 2 h under O₂. The yield of the desired disulfide **2aa** was determined by GC measurement. These results

are summarized in Table 2.

Typical procedure for synthesis of 2bc. A mixture of 2-pyridylthiol (**1b**, 111 mg, 1.00 mmol), tert-butylthiol (**1c**, 108 mg, 1.20 mmol), **F1** (27.2 mg, 0.050 mmol), MeOH (10 mL), and H₂O (10 mL) was stirred and irradiated (white LED, 11 W) at 25 °C for 8 h under O₂. After the solvent was removed by evaporation, the residue was purified by column chromatography (SiO₂, hexane/ethyl acetate = 100/0 to 4/1, v/v) to give **2bc** (155 mg, 78%) as a colorless oil. These results are summarized in Table 3.

Spectroscopic data of 2-(tert-butylidisulfanyl)pyridine (2bc):¹⁸ Column chromatography (SiO₂, hexane/ethyl acetate=100/0 to 4/1, v/v) afforded the desired product (155 mg, 78%) as a colorless oil. ¹H NMR (500 MHz, CDCl₃, 25 °C, δ): 8.44-8.40 (m, 1H), 7.79 (d, *J* = 8.0 Hz, 1H), 7.65-7.55 (m, 1H), 7.15-7.10 (m, 1H), 1.34 (s, 9H). ¹³C{¹H} NMR (126 MHz, CDCl₃, 25 °C, δ): 161.8, 149.3, 136.9, 120.5, 119.7, 49.4, 29.9.

Spectroscopic data of 4-(tert-butylidisulfanyl)pyridine (2dc):¹⁸ Column chromatography (SiO₂, chloroform/hexane=3/2 to 100/0, v/v) afforded the desired product (151 mg, 76%) as a colorless oil. ¹H NMR (500 MHz, CDCl₃, 25 °C, δ): 8.45 (d, *J* = 6.0 Hz, 2H), 7.48 (d, *J* = 6.0 Hz, 2H), 1.33 (s, 9H). ¹³C{¹H} NMR (126 MHz, CDCl₃, 25 °C, δ): 150.3, 149.4, 120.2, 49.9, 29.9.

Spectroscopic data of 3-methyl-3-(pyridin-2-ylidisulfanyl)butan-1-ol (2be): Column chromatography (SiO₂, hexane/ethyl acetate=100/0 to 1/1, v/v) afforded the desired

product (201 mg, 87%) as a colorless oil. IR (neat, cm^{-1}) 3354, 3048, 1576, 1560, 1447, 1417, 762, 718. ^1H NMR (500 MHz, CDCl_3 , 25 $^\circ\text{C}$, δ): 8.45-8.40 (m, 1H), 7.69 (d, $J = 7.5$ Hz, 1H), 7.61 (ddd, $J = 7.8, 7.8, 2.0$ Hz, 1H), 7.08 (ddd, $J = 7.3, 4.5, 1.1$ Hz, 1H), 3.81 (t, $J = 6.8$ Hz, 2H), 2.59 (br s, 1H), 1.90 (t, $J = 6.5$ Hz, 2H), 1.36 (s, 6H). $^{13}\text{C}\{^1\text{H}\}$ NMR (126 MHz, CDCl_3 , 25 $^\circ\text{C}$, δ): 160.8, 149.4, 137.0, 120.8, 120.4, 59.7, 51.1, 43.3, 28.1. HRMS (ESI-TOF) m/z : $[\text{M}+\text{H}]^+$ calcd for $\text{C}_{11}\text{H}_{15}\text{NOS}_2$, 230.0668; found, 230.0665.

Spectroscopic data of 2-(*tert*-butyldisulfanyl)pyrimidine (2fc):¹⁸ Column chromatography (SiO_2 , dichloromethane/methanol=100/0 to 10/1, v/v) afforded the desired product (160 mg, 80%) as a colorless oil. ^1H NMR (500 MHz, CDCl_3 , 25 $^\circ\text{C}$, δ): 8.61 (d, $J = 4.5$ Hz, 2H), 7.08 (t, $J = 4.8$ Hz, 1H), 1.37 (s, 9H). $^{13}\text{C}\{^1\text{H}\}$ NMR (126 MHz, CDCl_3 , 25 $^\circ\text{C}$, δ): 172.6, 158.0, 118.2, 49.4, 30.1.

Spectroscopic data of 2-(*tert*-butyldisulfanyl)benzothiazole (2gc):¹⁸ Column chromatography (SiO_2 , hexane) afforded the desired product (238 mg, 93%) as a white solid. ^1H NMR (500 MHz, CDCl_3 , 25 $^\circ\text{C}$, δ): 7.85 (d, $J = 8.0$ Hz, 1H), 7.80-7.76 (m, 1H), 7.45-7.39 (m, 1H), 7.34-7.29 (m, 1H), 1.43 (s, 9H). $^{13}\text{C}\{^1\text{H}\}$ NMR (126 MHz, CDCl_3 , 25 $^\circ\text{C}$, δ): 174.5, 155.0, 135.9, 126.3, 124.6, 122.2, 121.2, 50.4, 29.9.

Spectroscopic data of 5-(*tert*-butyldisulfanyl)-1-methyl-tetrazole (2hc):¹⁸ Column chromatography (SiO_2 , hexane/ethyl acetate=100/0 to 1/1, v/v) afforded the desired product (169 mg, 82%) as a colorless oil. ^1H NMR (500 MHz, CDCl_3 , 25 $^\circ\text{C}$, δ): 4.13 (s, 3H), 1.37 (s, 9H). $^{13}\text{C}\{^1\text{H}\}$ NMR (126 MHz, CDCl_3 , 25 $^\circ\text{C}$, δ): 153.6, 50.6, 34.7, 29.7.

Spectroscopic data of 3-methyl-3-(phenyldisulfanyl)butan-1-ol (2ie): Column chromatography (SiO₂, hexane/ethyl acetate=100/0 to 7/1, v/v) afforded the desired product (201 mg, 88%) as a colorless oil. IR (neat, cm⁻¹) 3347, 3058, 2959, 1578, 1475, 1438, 739, 688. ¹H NMR (500 MHz, CDCl₃, 25 °C, δ): 7.60-7.54 (m, 2H), 7.30 (t, J = 7.8 Hz, 2H), 7.20 (t, J = 7.3 Hz, 1H), 3.69 (t, J = 7.0 Hz, 2H), 1.86 (t, J = 7.0 Hz, 2H), 1.30 (s, 6H). ¹³C{¹H} NMR (126 MHz, CDCl₃, 25 °C, δ): 138.6, 129.0, 127.7, 126.8, 59.9, 51.3, 43.6, 28.3. Anal. Calcd for C₁₁H₁₆OS₂: C, 57.85; H, 7.06. Found: C, 57.67; H, 7.22.

Spectroscopic data of 4-(tert-butyldisulfanyl)-1-chlorobenzene (2jc):¹⁸ Column chromatography (SiO₂, hexane/ethyl acetate=100/0 to 4/1, v/v) afforded the desired product (197 mg, 85%) as a colorless oil. ¹H NMR (500 MHz, CDCl₃, 25 °C, δ): 7.48 (d, J = 9.0 Hz, 2H), 7.25 (d, J = 9.0 Hz, 2H), 1.29 (s, 9H). ¹³C{¹H} NMR (126 MHz, CDCl₃, 25 °C, δ): 137.6, 132.2, 129.0, 128.2, 49.6, 30.0.

Spectroscopic data of 4-(tert-butyldisulfanyl)-1-methoxybenzene (2ac):¹⁸ Column chromatography (SiO₂, hexane) afforded the desired product (148 mg, 65%) as a colorless oil. ¹H NMR (500 MHz, CDCl₃, 25 °C, δ): 7.48 (d, J = 8.5 Hz, 2H), 6.83 (d, J = 9.0 Hz, 2H), 3.79 (s, 3H), 1.29 (s, 9H). ¹³C{¹H} NMR (126 MHz, CDCl₃, 25 °C, δ): 159.1, 130.4, 129.9, 114.6, 55.5, 49.1, 30.1.

Spectroscopic data of 2-(cyclohexyldisulfanyl)pyridine (2bk): Column chromatography (SiO₂, hexane/ethyl acetate=100/0 to 2/1, v/v) afforded the desired product (155 mg, 69%) as a colorless oil. IR (neat, cm⁻¹) 2928, 1573, 1560, 1445, 1416,

760, 717. ^1H NMR (500 MHz, CDCl_3 , 25 °C, δ): 8.48-8.38 (m, 1H), 7.77 (d, $J = 8.0$ Hz, 1H), 7.66-7.59 (m, 1H), 7.09-7.01 (m, 1H), 2.92-2.79 (m, 1H), 2.06-1.98 (m, 2H), 1.83-1.69 (m, 2H), 1.66-1.50 (m, 1H), 1.49-1.15 (m, 5H). $^{13}\text{C}\{^1\text{H}\}$ NMR (126 MHz, CDCl_3 , 25 °C, δ): 161.6, 149.4, 137.0, 120.4, 119.5, 50.1, 32.8, 26.2, 25.6. HRMS (ESI-TOF) m/z : $[\text{M}+\text{H}]^+$ calcd for $\text{C}_{12}\text{H}_{16}\text{NS}_2$, 226.0719; found, 226.0717.

Spectroscopic data of 4-(cyclohexyldisulfanyl)pyridine (2dk):^{16c} Column chromatography (alumina, hexane/chloroform=2/3 to 0/100, v/v) afforded the desired product (196 mg, 87%) as a colorless oil. ^1H NMR (500 MHz, CDCl_3 , 25 °C, δ): 8.48-8.42 (m, 2H), 7.48-7.43 (m, 2H), 2.86-2.77 (m, 1H), 2.04-1.97 (m, 2H), 1.82-1.74 (m, 2H), 1.65-1.56 (m, 1H), 1.45-1.16 (m, 5H). $^{13}\text{C}\{^1\text{H}\}$ NMR (126 MHz, CDCl_3 , 25 °C, δ): 150.2, 149.5, 120.0, 50.3, 32.8, 26.1, 25.5.

Spectroscopic data of 2-(octyldisulfanyl)pyridine (2bl):¹⁸ Column chromatography (alumina, hexane/ethyl acetate=100/0 to 3/1, v/v) afforded the desired product (178 mg, 70%) as a colorless oil. ^1H NMR (500 MHz, CDCl_3 , 25 °C, δ): 8.48-8.43 (m, 1H), 7.73 (d, $J = 8.0$ Hz, 1H), 7.67-7.60 (m, 1H), 7.10-7.04 (m, 1H), 2.79 (t, $J = 7.5$ Hz, 2H), 1.76-1.63 (m, 2H), 1.43-1.33 (m, 2H), 1.33-1.19 (m, 8H), 0.87 (t, $J = 6.8$ Hz, 3H). $^{13}\text{C}\{^1\text{H}\}$ NMR (126 MHz, CDCl_3 , 25 °C, δ): 160.9, 149.7, 137.0, 120.6, 119.6, 39.2, 31.9, 29.3, 29.1, 28.6, 22.7, 14.2.

Spectroscopic data of 1-(tert-butyl)disulfanyloctane (2lc): Column chromatography (SiO_2 , hexane/ethyl acetate=100/0 to 1/1, v/v) afforded the desired product (158 mg, 67%) as a colorless oil. IR (neat, cm^{-1}) 2957, 2925, 2855, 1456, 1362. ^1H NMR (500 MHz,

CDCl₃, 25 °C, δ): 2.70 (t, $J = 7.5$ Hz, 2H), 1.68-1.60 (m, 2H), 1.42-1.20 (m, 19H), 0.88 (t, $J = 7.0$ Hz, 3H). ¹³C{¹H} NMR (126 MHz, CDCl₃, 25 °C, δ): 47.8, 41.2, 32.0, 30.1, 29.5, 29.3, 28.7, 22.8, 14.2. Anal. Calcd for C₁₂H₂₆S₂: C, 61.47; H, 11.18. Found: C, 61.53; H, 11.02.

Spectroscopic data of 6-(*tert*-butyldisulfanyl)hexan-1-ol (2mc): Column chromatography (SiO₂, hexane/ethyl acetate=100/0 to 1/1, v/v) afforded the desired product (162 mg, 70%) as a colorless oil. IR (neat, cm⁻¹) 3334, 2929, 726. ¹H NMR (500 MHz, CDCl₃, 25 °C, δ): 3.64 (t, $J = 6.5$ Hz, 2H), 2.71 (t, $J = 7.3$ Hz, 2H), 1.72-1.63 (m, 2H), 1.62-1.54 (m, 2H), 1.48 (br s, 1H), 1.46-1.34 (m, 4H), 1.33 (s, 9H). ¹³C{¹H} NMR (126 MHz, CDCl₃, 25 °C, δ): 63.0, 47.8, 40.9, 32.7, 30.1, 29.4, 28.4, 25.5. Anal. Calcd for C₁₀H₂₂OS₂: C, 54.01; H, 9.97. Found: C, 53.94; H, 10.09.

Spectroscopic data of 3-(*tert*-butyldisulfanyl)propan-1-ol (2nc): Column chromatography (SiO₂, hexane/ethyl acetate=100/0 to 3/1, v/v) afforded the desired product (119 mg, 66%) as a colorless oil. IR (neat, cm⁻¹) 3334, 2959. ¹H NMR (500 MHz, CDCl₃, 25 °C, δ): 3.75 (t, $J = 6.3$ Hz, 2H), 2.82 (t, $J = 7.0$ Hz, 2H), 1.93 (tt, $J = 7.0, 6.3$ Hz, 2H), 1.63 (br s, 1H), 1.34 (s, 9H). ¹³C{¹H} NMR (126 MHz, CDCl₃, 25 °C, δ): 61.2, 48.0, 37.2, 32.1, 30.1. Anal. Calcd for C₇H₁₆OS₂: C, 46.63; H, 8.94. Found: C, 46.38; H, 9.08.

Spectroscopic data of methyl 3-((4-hydroxy-2-methylbutan-2-yl)disulfanyl)propanoate (2oe): Column chromatography (SiO₂, hexane/ethyl acetate=100/0 to 3/1, v/v) afforded the desired product (174 mg, 76%) as a colorless oil.

IR (neat, cm^{-1}) 3422, 2956, 1738. ^1H NMR (500 MHz, CDCl_3 , 25 $^\circ\text{C}$, δ): 3.78 (t, $J = 7.0$ Hz, 2H), 3.71 (s, 3H), 2.94 (t, $J = 7.3$ Hz, 2H), 2.72 (t, $J = 7.3$ Hz, 2H), 1.90 (t, $J = 7.0$ Hz, 2H), 1.75 (br s, 1H), 1.34 (s, 6H). $^{13}\text{C}\{^1\text{H}\}$ NMR (126 MHz, CDCl_3 , 25 $^\circ\text{C}$, δ): 172.4, 59.9, 52.0, 50.0, 43.6, 34.8, 34.2, 28.3. Anal. Calcd for $\text{C}_9\text{H}_{18}\text{O}_3\text{S}_2$: C, 45.35; H, 7.61. Found: C, 45.16; H, 7.84.

Spectroscopic data of 3-(octyldisulfanyl)-3-methylbutan-1-ol (2le): Column chromatography (SiO_2 , hexane/ethyl acetate=100/0 to 1/1, v/v) afforded the desired product (169 mg, 65%) as a colorless oil. IR (neat, cm^{-1}) 3335, 2925. ^1H NMR (500 MHz, CDCl_3 , 25 $^\circ\text{C}$, δ): 3.79 (t, $J = 7.0$ Hz, 2H), 2.71 (t, $J = 7.5$ Hz, 2H), 1.90 (t, $J = 6.8$ Hz, 2H), 1.68-1.57 (m, 3H), 1.40-1.21 (m, 16H), 0.88 (t, $J = 6.8$ Hz, 3H). $^{13}\text{C}\{^1\text{H}\}$ NMR (126 MHz, CDCl_3 , 25 $^\circ\text{C}$, δ): 60.0, 49.7, 43.6, 40.9, 31.9, 29.5, 29.3, 28.7, 28.3, 22.8, 14.2. Anal. Calcd for $\text{C}_{13}\text{H}_{28}\text{OS}_2$: C, 59.04; H, 10.67. Found: C, 58.87; H, 11.01.

Spectroscopic data of methyl 3-(tert-butyldisulfaneyl)propanoate (2oc):^{16b} Column chromatography (SiO_2 , hexane/dichloromethane=4/1 to 1/1, v/v) afforded the desired product (127 mg, 60%) as a colorless oil. ^1H NMR (500 MHz, CDCl_3 , 25 $^\circ\text{C}$, δ): 3.70 (s, 3H), 2.93 (t, $J = 7.3$ Hz, 2H), 2.72 (t, $J = 7.3$ Hz, 2H), 1.34 (s, 9H). $^{13}\text{C}\{^1\text{H}\}$ NMR (126 MHz, CDCl_3 , 25 $^\circ\text{C}$, δ): 172.3, 51.9, 48.0, 34.9, 34.1, 30.0.

Spectroscopic data of 3-(cyclohexyldisulfanyl)-3-methylbutan-1-ol (2ek): Column chromatography (SiO_2 , hexane/ethyl acetate=100/0 to 7/3, v/v) afforded the desired product (158 mg, 67%) as a colorless oil. IR (neat, cm^{-1}) 3347, 2929, 2852, 1447. ^1H NMR (500 MHz, CDCl_3 , 25 $^\circ\text{C}$, δ): 3.79 (t, $J = 7.0$ Hz, 2H), 2.73-2.68 (m, 1H), 2.11-2.03

(m, 2H), 1.89 (t, $J = 7.0$ Hz, 2H), 1.82-1.73 (m, 2H), 1.64-1.58 (m, 1H), 1.52 (br s, 1H), 1.35-1.18 (m, 11H). $^{13}\text{C}\{^1\text{H}\}$ NMR (126 MHz, CDCl_3 , 25 °C, δ): 60.0, 50.3, 49.3, 43.7, 33.0, 28.3, 26.1, 25.8. Anal. Calcd for $\text{C}_{11}\text{H}_{22}\text{OS}_2$: C, 56.36; H, 9.46. Found: C, 56.04; H, 9.57.

Measurements of Nanosecond Laser Flash Spectroscopy. The transient absorption spectra of **F1** in the presence of **11** were measured under nitrogen atmosphere using the following system. A solution of **F1** (0.12 mM) and **11** (13 mM) in MeOH/ H_2O /pyridine (9:1:0.05, v/v, 3 mL) was set in a sealed quartz cell (10 x 10 x 40 mm³) after removing O_2 by freeze-pump-thaw cycle. The sample solution was irradiated by a laser pulse at 355 nm with 6 ns duration of a Nd:YAG laser (GCR150, Spectra Physics). The repetition rate of the laser pulses was 10 Hz. A Xe flash lamp with 2 μs duration (L4633, Hamamatsu Photonics) was used as the probe light source. The probe light transmitted through the laser-irradiated part of the sample solution was conducted into a monochromator (Kymera-193i, Andor Technology) through glass fiber and was captured by an intensified charge-coupled device detector (ICCD; DH334T, Andor Technology). The width of the ICCD gate was set at 100 ns. A digital pulse-delay generator (DG535, Stanford Research Systems) was used to synchronize the laser, the flash lamp, and the ICCD gate and adjust the delay time between the laser pulse and the ICCD gate. The difference absorption spectra shown in Figure 2 were obtained by subtracting an absorption spectrum collected without laser excitation from absorption spectra collected after laser excitation.

2-6 References and Notes

- [1] Briggs, W. R.; Christie, J. M. *Trends Plant Sci* **2002**, *7*, 204-210. (b) Kagawa, T. *J Plant Res* **2003**, *116*, 77-82. (c) Christie, J. M. *Annu. Rev. Plant Biol.* **2007**, *58*, 21-45.
- [2] Christie, J. M.; Salomon, M.; Nozue, K.; Wada, M.; Briggs, W. R. *Proc. Natl. Acad. Sci. U. S. A.* **1999**, *96*, 8779-8783.
- [3] (a) Swartz, T. E.; Corchnoy, S. B.; Christie, J. M.; Lewis, J. W.; Szundi, I.; Briggs, W. R.; Bogomolni, R. A. *J. Biol. Chem.* **2001**, *276*, 36493-36500. (b) Schleicher, E.; Kowalczyk, R. M.; Kay, C. W.; Hegemann, P.; Bacher, A.; Fischer, M.; Bittl, R.; Richter, G.; Weber, S. *J. Am. Chem. Soc.* **2004**, *126*, 11067-11076. (c) Chang, X. P.; Gao, Y. J.; Fang, W. H.; Cui, G.; Thiel, W. *Angew. Chem. Int. Ed.* **2017**, *56*, 9341-9345.
- [4] (a) Murahashi, S. I.; Oda, T.; Masui, Y. *J. Am. Chem. Soc.* **1989**, *111*, 5002-5003. (b) Imada, Y.; Iida, H.; Ono, S.; Murahashi, S. *J. Am. Chem. Soc.* **2003**, *125*, 2868-2869. (c) Imada, Y.; Iida, H.; Naota, T. *J. Am. Chem. Soc.* **2005**, *127*, 14544-14545. (d) Murray, A. T.; Matton, P.; Fairhurst, N. W.; John, M. P.; Carbery, D. R. *Org. Lett.* **2012**, *14*, 3656-3659. (e) Ishikawa, T.; Kimura, M.; Kumoi, T.; Iida, H. *ACS Catal.* **2017**, *7*, 4986-4989. (f) Okai, H.; Tanimoto, K.; Ohkado, R.; Iida, H. *Org. Lett.* **2020**, *22*, 8002-8006.
- [5] (a) Murahashi, S. I. *Angew. Chem. Int. Ed.* **1995**, *34*, 2443-2465. (b) Cibulka, R. *Eur. J. Org. Chem.* **2015**, *2015*, 915-932. (c) Iida, H.; Imada, Y.; Murahashi, S. I. *Org. Biomol. Chem.* **2015**, *13*, 7599-7613.
- [6] (a) Fukuzumi, S.; Kuroda, S.; Tanaka, T. *J. Am. Chem. Soc.* **1985**, *107*, 3020-3027. (b) Cibulka, R.; Vasold, R.; König, B. *Chem. –Eur. J.* **2004**, *10*, 6224-6231. (c)

- Muhldorf, B.; Wolf, R. *Angew. Chem. Int. Ed.* **2016**, *55*, 427-430. (d) Metternich, J. B.; Gilmour, R. *J. Am. Chem. Soc.* **2016**, *138*, 1040-1045. (e) Zelenka, J.; Cibulka, R.; Roithova, J. *Angew. Chem. Int. Ed.* **2019**, *58*, 15412-15420.
- [7] König, B.; Kümmel, S.; Svobodová, E.; Cibulka, R. *Phys. Sci. Rev.* **2018**, *3*.
- [8] Loechler, E. L.; Hollocher, T. C. *J. Am. Chem. Soc.* **1980**, *102*, 7312-7321.
- [9] (a) Lee, M. H.; Yang, Z.; Lim, C. W.; Lee, Y. H.; Dongbang, S.; Kang, C.; Kim, J. S. *Chem. Rev.* **2013**, *113*, 5071-5109. (b) Fass, D.; Thorpe, C. *Chem. Rev.* **2018**, *118*, 1169-1198. (c) Narayan, M.; Welker, E.; Wedemeyer, W. J.; Scheraga, H. A. *Acc. Chem. Res.* **2000**, *33*, 805-812.
- [10] (a) Jiang, C. S.; Muller, W. E.; Schroder, H. C.; Guo, Y. W. *Chem. Rev.* **2012**, *112*, 2179-2207. (b) Nielsen, D. S.; Shepherd, N. E.; Xu, W.; Lucke, A. J.; Stoermer, M. J.; Fairlie, D. P. *Chem. Rev.* **2017**, *117*, 8094-8128.
- [11] (a) Gronbeck, H.; Curioni, A.; Andreoni, W. *J. Am. Chem. Soc.* **2000**, *122*, 3839-3842. (b) Cui, H. K.; Guo, Y.; He, Y.; Wang, F. L.; Chang, H. N.; Wang, Y. J.; Wu, F. M.; Tian, C. L.; Liu, L. *Angew. Chem. Int. Ed.* **2013**, *52*, 9558-9562.
- [12] (a) Chankhamjon, P.; Boettger-Schmidt, D.; Scherlach, K.; Urbansky, B.; Lackner, G.; Kalb, D.; Dahse, H. M.; Hoffmeister, D.; Hertweck, C. *Angew. Chem. Int. Ed.* **2014**, *53*, 13409-13413. (b) Block, E.; Ahmad, S.; Jain, M. K.; Crecely, R. W.; Apitz-Castro, R.; Cruz, M. R. *J. Am. Chem. Soc.* **2002**, *106*, 8295-8296. (c) Silva, F.; Khokhar, S. S.; Williams, D. M.; Saunders, R.; Evans, G. J. S.; Graz, M.; Wirth, T. *Angew. Chem. Int. Ed.* **2018**, *57*, 12290-12293. (d) Lindquist, N.; Fenical, W. *Tetrahedron Lett.* **1990**, *31*, 2389-2392. (e) Scharf, D. H.; Remme, N.; Habel, A.; Chankhamjon, P.; Scherlach, K.; Heinekamp, T.; Hortschansky, P.; Brakhage, A. A.; Hertweck, C. *J. Am. Chem. Soc.* **2011**, *133*, 12322-12325. (f) Fujiwara, M.; Watanabe,

- H.; Matsui, K. *J. Biochem.* **1954**, *41*, 29-39. (g) Block, E.; Ahmad, S.; Catalfamo, J. L.; Jain, M. K.; Apitz-Castro, R. *J. Am. Chem. Soc.* **2002**, *108*, 7045-7055.
- [13] (a) Musiejuk, M.; Witt, D. *Org. Prep. Proced. Int.* **2015**, *47*, 95-131. (b) Swan, J. M. *Nature* **1957**, *180*, 643-645. (c) Sivaramakrishnan, S.; Keerthi, K.; Gates, K. S. *J. Am. Chem. Soc.* **2005**, *127*, 10830-10831. (d) Bottecchia, C.; Erdmann, N.; Tijssen, P. M.; Milroy, L. G.; Brunsveld, L.; Hessel, V.; Noël, T. *ChemSusChem* **2016**, *9*, 1781-1785. (e) Dethe, D. H.; Srivastava, A.; Dherange, B. D.; Kumar, B. V. *Adv. Synth. Catal.* **2018**, *360*, 3020-3025. (f) Xiao, X.; Xue, J.; Jiang, X. *Nat Commun* **2018**, *9*, 2191.
- [14] (a) Barton, D. H. R.; Hesse, R. H.; Osullivan, A. C.; Pechet, M. M. *J. Org. Chem.* **1991**, *56*, 6697-6702. (b) Ohtani, M.; Narisada, M. *J. Org. Chem.* **1991**, *56*, 5475-5478. (c) Brzezinska, E.; Ternay, A. L. *J. Org. Chem.* **1994**, *59*, 8239-8244. (d) Hiver, P.; Dicko, A.; Paquer, D. *Tetrahedron Lett.* **1994**, *35*, 9569-9572. (e) Klose, J.; Reese, C. B.; Song, Q. L. *Tetrahedron* **1997**, *53*, 14411-14416. (f) Bao, M.; Shimizu, M. *Tetrahedron* **2003**, *59*, 9655-9659. (g) Gamblin, D. P.; Garnier, P.; van Kasteren, S.; Oldham, N. J.; Fairbanks, A. J.; Davis, B. G. *Angew. Chem. Int. Ed.* **2004**, *43*, 828-833. (h) Harusawa, S.; Yoshida, K.; Kojima, C.; Araki, L.; Kurihara, T. *Tetrahedron* **2004**, *60*, 11911-11922. (i) Hunter, R.; Cairra, M.; Stellenboom, N. *J. Org. Chem.* **2006**, *71*, 8268-8271. (j) Keshari, T.; Kapoor, R.; Yadav, L. D. S. *Synlett* **2016**, *27*, 1878-1882.
- [15] (a) Do, Q. T.; Elothmani, D.; LeGuillanton, G.; Simonet, J. *Tetrahedron Lett.* **1997**, *38*, 3383-3384. (b) Arisawa, M.; Yamaguchi, M. *J. Am. Chem. Soc.* **2003**, *125*, 6624-6625. (c) Tanaka, K.; Ajiki, K. *Tetrahedron Lett.* **2004**, *45*, 5677-5679. (d) Han, M.; Lee, J. T.; Hahn, H. G. *Tetrahedron Lett.* **2011**, *52*, 236-239. (e) Boyd, D. R.; Sharma, N. D.; Shepherd, S. D.; Allenmark, S. G.; Allen, C. C. R. *RSC Adv.* **2014**, *4*, 27607-

27619. (f) Musiejuk, M.; Klucznik, T.; Rachon, J.; Witt, D. *RSC Adv.* **2015**, *5*, 31347-31351. (g) Viswanatharaju Rudraraju, K.; Parsons, Z. D.; Lewis, C. D.; Gates, K. S. *J. Org. Chem.* **2017**, *82*, 776-780.
- [16] (a) Dou, Y. C.; Huang, X.; Wang, H.; Yang, L. T.; Li, H.; Yuan, B. X.; Yang, G. Y. *Green Chem.* **2017**, *19*, 2491-2495. (b) Qiu, X.; Yang, X. X.; Zhang, Y. Q.; Song, S.; Jiao, N. *Org. Chem. Front.* **2019**, *6*, 2220-2225. (c) Song, L. J.; Li, W. H.; Duan, W. X.; An, J. C.; Tang, S. Y.; Li, L. J.; Yang, G. y. *Green Chem.* **2019**, *21*, 1432-1438.
- [17] (a) Brodersen, N.; Arbuzova, A.; Herrmann, A.; Egger, H.; Liebscher, J. *Tetrahedron* **2011**, *67*, 7763-7774. (b) Iwasa, E.; Hamashima, Y.; Fujishiro, S.; Hashizume, D.; Sodeoka, M. *Tetrahedron* **2011**, *67*, 6587-6599. (c) Vandavasi, J. K.; Hu, W. P.; Chen, C. Y.; Wang, J. J. *Tetrahedron* **2011**, *67*, 8895-8901. (d) Miller, S. E.; Kallenbach, N. R.; Arora, P. S. *Tetrahedron* **2012**, *68*, 4434-4437. (e) Smith, R.; Zeng, X. J.; Muller-Bunz, H.; Zhu, X. M. *Tetrahedron Lett.* **2013**, *54*, 5348-5350. (f) Yuan, J. W.; Liu, C.; Lei, A. W. *Org. Chem. Front.* **2015**, *2*, 677-680.
- [18] Huang, P.; Wang, P.; Tang, S.; Fu, Z.; Lei, A. *Angew. Chem. Int. Ed.* **2018**, *57*, 8115-8119.
- [19] In general, the thiols display slightly different reactivity toward the oxidation in the order of: ArSH > primary AlkSH > tertiary AlkSH. See refs 16b and 18.
- [20] Kottke, T.; Heberle, J.; Hehn, D.; Dick, B.; Hegemann, P. *Biophys. J.* **2003**, *84*, 1192-1201.
- [21] (a) Gelalcha, F. G. *Chem. Rev.* **2007**, *107*, 3338-3361. (b) Holtmann, D.; Hollmann, F. *Chembiochem* **2016**, *17*, 1391-1398.
- [22] The other attempts for the detection of FISR using NMR and mass measurements failed due to its unstable character.

Chapter 2

- [23] (a) Grande, H. J.; Van Schagen, C. G.; Jarbandhan, T.; Müller, F. *Helv. Chim. Acta* **1977**, *60*, 348-366. (b) Van Schagen, C. G.; Müller, F. *Helv. Chim. Acta* **1980**, *63*, 2187-2201.

Chapter 3

Flavin photocatalyzed S-N bond formation by dehydrogenative coupling of thiols and amines

3-1 Abstract

3-2 Introduction

3-3 Results and Discussion

3-4 Conclusion

3-5 Experimental Section

3-6 References and Notes

3-1 Abstract

A novel photoreaction process that uses riboflavin derivatives as organophotocatalysts to enable aerobic oxidative multistep S–S, S–N, and S–O bond formation between thiols and amines is described herein. The reaction was performed under mild, metal-free conditions using air (1 atm) as an environmentally benign oxidant to produce sulfinamides and sulfonamides.

3-2 Introduction

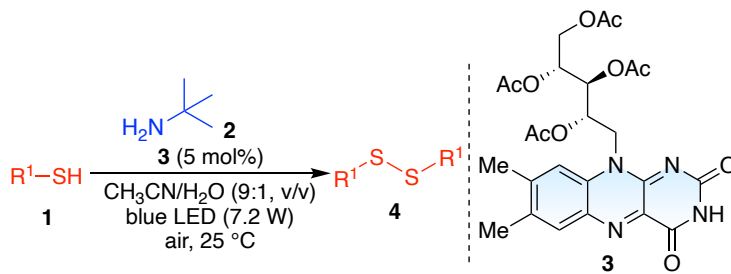
Riboflavin and its derivatives are naturally occurring organic molecules that function as unique redox organocatalysts that promote a variety of oxidations, making them attractive tools for the development of environmentally friendly and sustainable transformations.^{1,2} Recently, there has been significant interest in photocatalytic oxidation, which is a nonthermal process. Riboflavin and its analogs have been reported to efficiently oxidize toluenes,³ alcohols,⁴ amines,⁵ and other compounds⁶ under visible-light irradiation to give the corresponding products.⁷ In addition, riboflavin is known to serve as a functional core of blue-light sensitive photoreceptor called phototropin in higher plants, which regulates blue-light responses including a stem bending toward light.⁸ The author has recently established a method to mimic this photoreaction process of phototropin and succeeded in the synthesis of unsymmetrical disulfides by aerobic photooxidative heterocoupling of two different thiols using a simple riboflavin derivative as a catalyst.⁹ The selective formation of S–S bond occurred efficiently under visible-light irradiation with the consumption of O₂ (air, 1 atm), which has been recognized as an ideal oxidant with environmental and economic benefits. Given the usefulness of disulfides as synthetic intermediates,¹⁰ this system has potential for application in multistep reactions, where in situ-generated disulfides and flavin-catalyzed reactions can further promote bond-forming reactions between sulfur and other atoms.

Sulfinamides and sulfonamides are widely used in pharmaceuticals, agrochemicals, and other functional molecules due to their attractive biological activity and chemical stability.¹¹ The conventional method of generating sulfinamides and sulfonamides involves the reaction of sulfinyl or sulfonyl chlorides with amine nucleophiles.¹² However, these chlorides are harmful and require pre-functionalization using chlorinating reagents

or oxidants. On the other hand, the dehydrogenative coupling of thiols and amines is promising for atom- and step-economical synthesis, allowing the efficient production of the desired products from readily available starting materials. Thus, various approaches have been reported, including the use of transition metal catalysts,¹³ iodine and oxidants,¹⁴ and electrochemical methods.¹⁵ In this context, the author presents a novel photocatalytic approach using riboflavin derivatives for aerobic oxidative S–N bond formation between thiols and amines, yielding sulfinamides and sulfonamides. In this system, the riboflavin-based photocatalyst not only facilitated the synthesis of disulfides through the aerobic oxidation of thiols but also catalyzed the subsequent formation of S–N and S–O bonds. Despite the development of various oxidative reactions using flavin photocatalysts, to the best of the author's knowledge, there have been no reports of successful S–N bond formation between thiols and amines.

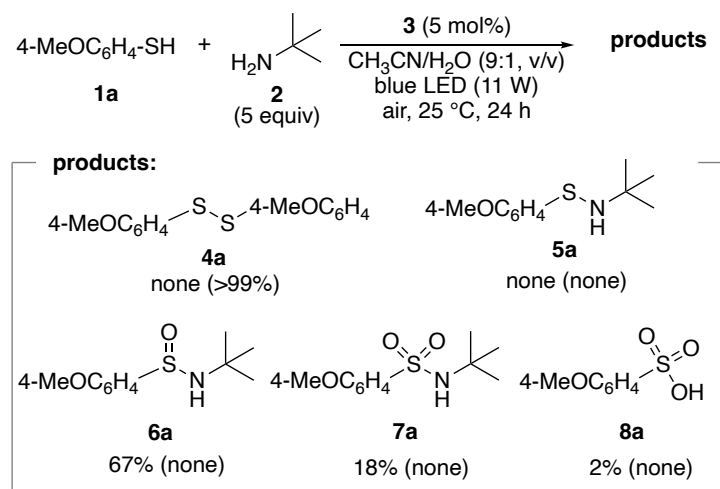
3-3 Results and Discussion

First, 4-methoxybenzenethiol (**1a**) was oxidized in the presence of 5 equiv of *tert*-butylamine (**2**) using riboflavin tetraacetate (**3**) as a photocatalyst in CH₃CN/H₂O (9:1, v/v) in air (1 atm, balloon) under blue light irradiation at 25 °C (Table 1). As a result, the corresponding disulfide **4a** was obtained in only 5 min (entry 1). When **2** was added, the reaction barely occurred and the yield of **4a** was 9% (entry 2). The addition of primary amines promoted the conversion of **1a**. Other thiols, such as unsubstituted benzenethiol (**1b**), electron-withdrawing 4-chlorobenzenethiol (**1c**), and 1-octanethiol (**1d**) were also smoothly transformed into the corresponding disulfides in 67–94% yield over 5–60 min (entries 3–5). In contrast, the oxidations of **1b** and **1d** were inhibited under dark conditions, affording the corresponding disulfides in 24% and 5% yields, respectively (entries 6 and 7). Flavin photocatalysis significantly enhanced the oxidation of thiols, although the oxidation proceeded slightly under dark conditions. Notably, when the reaction time was increased to 6 h, disulfide **4a** was further converted (entry 8). After reacting **1a** and **2** for 24 h, the corresponding sulfinamide **6a** and sulfonamide **7a** were obtained in 67% and 18% yields, respectively, which could have been formed by the oxidative S–N bond formation of **4a** and **2** (Scheme 1). The corresponding sulfenamide **5a** and sulfonic acid **8a** were hardly formed, with yields of 0% and 2%, respectively. However, without visible light irradiation, only disulfide **4a** was obtained, with no further conversion to **5a–8a**. This suggests that light irradiation is essential for the oxidative formation of the S–N bond (Scheme 1).

Table 1. Aerobic oxidative synthesis of disulfides from thiols in the presence of amine.^a


entry	1	2 (equiv)	time (min)	conv. of 1 (%)	yield of 4 (%)
1	4-MeOC ₆ H ₄ SH (1a)	5	5	>99	>99
2	1a	–	5	37	9
3	PhSH (1b)	5	5	>99	94
4	4-ClC ₆ H ₄ SH (1c)	5	5	>99	88
5	C ₈ H ₁₇ SH (1d)	5	60	>99	67
6 ^b	1b	5	5	>99	24
7 ^b	1d	5	60	43	5
8	1a	5	360	>99	0

^aConditions: **1** (0.025 M), **2** (0.125 M), **3** (5 mol%), and CH₃CN/H₂O (9:1, v/v) with blue LED (7.2 W) in air (1 atm, balloon) at 25 °C. The yield was determined by GC and ¹H NMR using tetraethylene glycol dimethyl ether and 1,1,2,2-tetrachloroethane as internal standards. ^bUnder dark conditions.



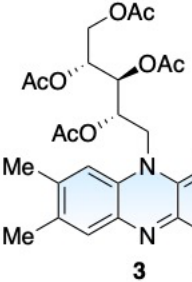
Scheme 1. Aerobic oxidative transformation of **1a** and **2** to **4a–8a** using flavin photocatalyst under blue LED irradiation for 24 h. The values within parentheses are the results obtained when the reaction was performed without light irradiation for 6 h.

The catalytic activities of the flavin compounds in the oxidative multistep reaction of **1a** in the presence of **2** were investigated using neutral flavins (Table 2). When isoalloxazines **3** and **9** and alloxazine **10** with various substituents were used, the conversion of **1a** proceeded efficiently over 6 h and showed high catalytic activity (entries 1–7). The relatively electron-rich isoalloxazines **3** and **9a**, as well as the electron-rich alloxazine **10a**, further promoted the oxidative conversion of **4a** to **6a** and **7a** rather than to the corresponding compounds **9b**, **9c**, **10b**, and **10c**, which have relatively electron-deficient-conjugated systems. Among the flavin catalysts tested, riboflavin tetraacetate (**3**), which can be easily prepared from inexpensive riboflavin (vitamin B₂) by a single-step acetylation,¹⁶ showed the best catalytic activity in the present oxidative reaction, with a total yield of 81% for **6a** and **7a** (entry 1). However, when eosin Y (**11**), a commonly used photocatalyst, was used in this photoreaction, no conversion to **5a–7a** was observed even though **4a** was formed (entry 8). This difference in the catalytic activity may be


attributed to the difference in the reduction potentials in the excited states of **3** ($E^*_{\text{red}} = 1.67 \text{ V vs. SCE}$)¹⁷ and **11** ($E^*_{\text{red}} = 0.83 \text{ V vs. SCE}$).¹⁸

Table 2. Effect of photocatalysts on the aerobic oxidative reaction of **1a** and **2**.^a


$$\mathbf{1a} + \mathbf{2} \xrightarrow[\text{air, 25 } ^\circ\text{C, 6 h}]{\text{catalyst (5 mol\%)} \\ \text{CH}_3\text{CN/H}_2\text{O (9:1, v/v)} \\ \text{blue LED (7.2 W)}} \mathbf{4a} + \mathbf{5a} + \mathbf{6a} + \mathbf{7a} + \mathbf{8a}$$



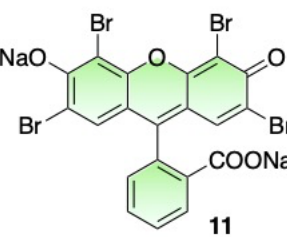
3



$R^3, R^7, R^8 = \text{Me}$ **9a**
 $R^3 = \text{Me}, R^7, R^8 = \text{H}$ **9b**
 $R^3 = \text{Me}, R^7 = \text{CF}_3, R^8 = \text{H}$ **9c**



$R^7, R^8 = \text{Me}$ **10a**
 $R^7, R^8 = \text{H}$ **10b**
 $R^7 = \text{H}, R^8 = \text{CF}_3$ **10c**



11

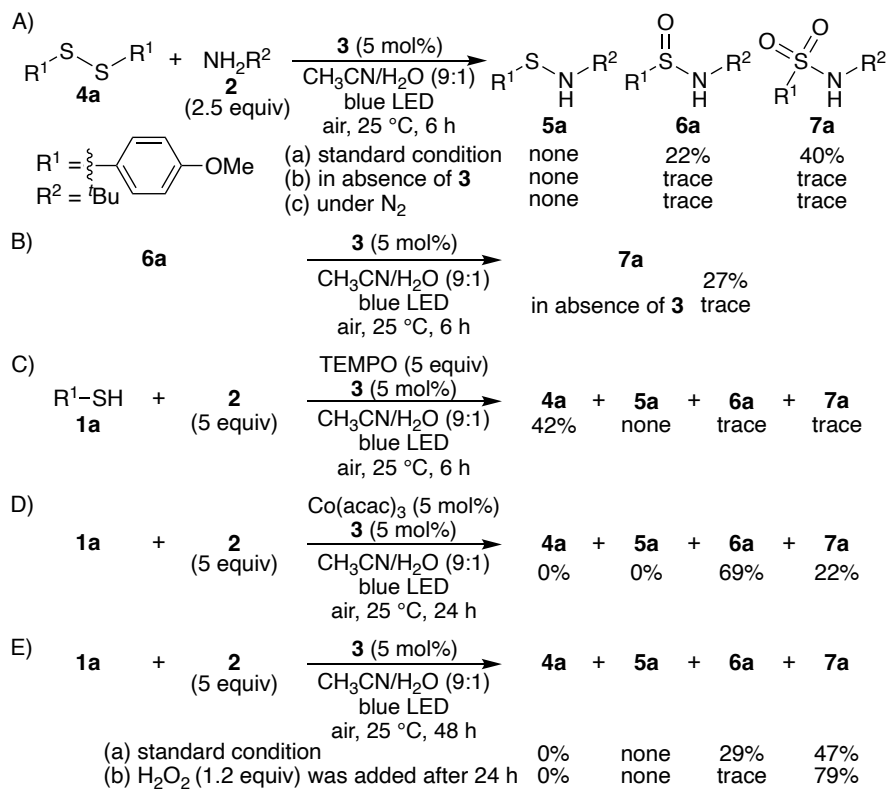
entry	catalyst	conv. of 1a (%)	yield of 4a (%)	total yield of 6a and 7a (%)
1	3	>99	0	81
2	9a	>99	0	76
3	9b	>99	6	48
4	9c	>99	77	8
5 ^b	10a	>99	0	76
6 ^b	10b	>99	3	41
7 ^b	10c	>99	0	64
8 ^c	11	>99	87	1

^aConditions: **1a** (0.025 M), **2** (0.125 M), catalyst (5 mol%), and CH₃CN/H₂O (9:1, v/v) with a blue LED (7.2 W) in air (1 atm, balloon) at 25 °C for 6 h. The yield was determined by GC using tetraethylene glycol dimethyl ether as an internal standard. ^bPurple LED was used. ^cGreen LED was used.

Several control experiments were performed to elucidate the reaction mechanism. First, the reaction was performed under standard conditions using disulfide **4a** as the starting material to validate whether **4a** produced early in the reaction acted as a reaction

intermediate for conversion to **6a** and **7a** (Scheme 2Aa). The results showed that **4a** was transformed into desired sulfinamide **6a** and sulfonamide **7a** in 22% and 40% yields, respectively. This suggests that oxidative S–N bond formation occurs after the S–S bond formation in thiols. Without the flavin catalyst or under nitrogen conditions, no products **5a–7a** were obtained via S–N bond formation (Schemes 2Ab and c). In previously reported cases, the coupling of thiols and amines proceeded to generate sulfenamides via the nucleophilic attack of amines on disulfides formed in situ.^{15,19} However, in this reaction system, no formation of sulfenamides **5** could be detected, while disulfides **4** were formed. It was suggested that sulfinamides **6** were formed directly from disulfides **4** and not via formation of **5**. In contrast, **6a** was oxygenated to sulfonamide **7a** under standard conditions, although **7a** was not produced without flavin catalyst **3**. The reactions of **4a** and **6a** to **6a** and **7a** occurred without reducing reagents (Schemes 2Aa and B), indicating that the flavin catalyst acted as a photosensitizer and facilitated radical-mediated processes. The addition of the radical inhibitor 2,2,6,6-tetramethylpiperidine 1-oxyl (TEMPO) to this reaction system afforded **4a** in 42% yield, but inhibited the formation of **6a** and **7a** (Scheme 2C). The S–S bond formation in **4a** from **1a** proceeds nonradically. In contrast, the subsequent oxidative S–N bond formation to **6a** and **7a** is thought to have proceeded via a radical process. To confirm the effect of singlet oxygen on this reaction, Co(acac)₃, a singlet oxygen quencher, was added to the reaction system (Scheme 2D).²⁰ Since the yields of **6a** and **7a** with and without Co(acac)₃ were almost the same (Schemes 1 and 2D), it is unlikely that singlet oxygen is involved in this reaction. The author also performed an experiment in which the blue light source was turned on and off during the reaction of **1a** and **2** (Figure 1). The yields of **6a** and **7a** increased only upon irradiation with visible light, and the reaction did not proceed without irradiation,

indicating that this reaction did not involve a radical chain process.



Scheme 2. Control experiments.

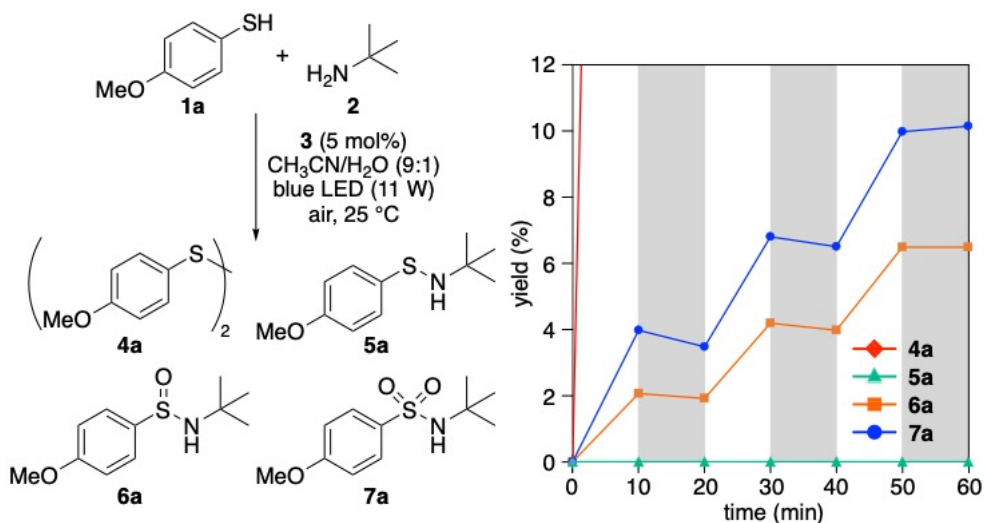
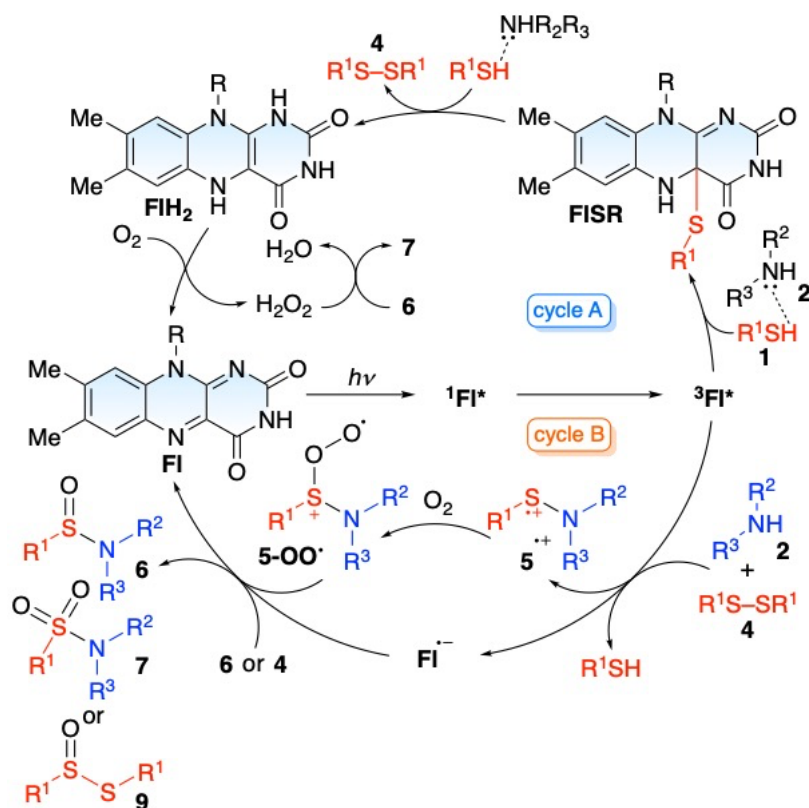


Figure 1. Switching light on/off experiment of the reaction of **1a** and **2**. From the on state, the blue LED was turned on and off every 10 min. The gray areas indicate the time when the light was turned off.

A possible reaction mechanism based on several experimental results and previous studies is shown in Scheme 3. **FI** is excited by visible-light irradiation to produce $^3\text{FI}^*$ via $^1\text{FI}^*$. The produced $^3\text{FI}^*$ then reacts with thiol **1** to form flavin-thiol adducts (**FISR**) as shown in cycle A.⁹ With the help of basic amine **2**, thiol **1** is nucleophilically activated to promote the nucleophilic attack on **FISR**, smoothly producing disulfide **4** and reduced flavin (**FIH₂**). The produced **FIH₂** reacts with O₂, reverting to the initial **FI** and generating H₂O₂ in the process.²¹ Additionally, $^3\text{FI}^*$ undergoes a reaction with **2** and **4** to produce the radical cation intermediate **5⁺**, which promptly reacts with O₂ to generate the active intermediate **5-OO[•]** (cycle B).^{20,22} The *in-situ* formed **5-OO[•]** is converted to the desired **6** by the transfer of an oxygen atom to **6** or **4**, yielding **7** or **9**. The **FI⁻** formed from $^3\text{FI}^*$ was transformed into the initial **FI** probably via electron transfer to the radical cations generated during the reaction of **5-OO[•]** with **6** or **4**. To determine whether the H₂O₂ produced in cycle A was involved in oxygenation, 1.2 equiv of H₂O₂ was added to the

reaction solution, which was obtained by reacting **1a** and **2** for 24 h under standard conditions (Scheme 2E). The results showed that **6a** and **7a** were produced in 29% and 47% yields, respectively, in the absence of H₂O₂, whereas the addition of H₂O₂ enhanced the oxygenation of **6a** and gave **7a** in 79% yield. This suggests that the H₂O₂ generated in this reaction was involved in the oxygenation of **6** to **7**. The addition of H₂O₂ was beneficial for the chemoselective synthesis of sulfonamides. Therefore, in this system, the combination of O₂ and visible-light irradiation facilitates the multi-step synthesis of sulfinamides and sulfonamides from thiols and amines. This was attributed to the multifunctional roles of the flavin catalyst in S–S, S–N, and S–O bond formation.



Scheme 3. Proposed catalytic cycle for S-S, S-N, S-O bond formation.

3-4 Conclusion

In conclusion, the author developed a novel approach for the synthesis of sulfinamides and sulfonamides through S–N bond formation by coupling thiols with amines using flavin photocatalysts. In the presence of amines, the photocatalytic oxidation of thiols to disulfides by flavins is enhanced. The flavin catalyst also promotes the formation of S–N and S–O bonds (oxygenation) under air and visible-light irradiation. In this reaction, the flavin catalyst was used for two cycles. At this stage, only the knowledge that a new catalytic reaction proceeded using a flavin photocatalyst was obtained. Further investigation and improvement of the selectivity for sulfinamides and sulfonamides, substrate scope, and catalyst design will provide practical organic synthesis methods.

3-5 Experimental Section

General

The NMR spectra were measured using JEOL JNM-L400 and JNM ECX-500 spectrometers (JEOL, Akishima, Japan) operating at 400 and 500 MHz, respectively, for ^1H and 100 and 126 MHz, respectively, for ^{13}C using tetramethylsilane (TMS) or a solvent residual peak as the internal standard. The GC measurements were performed on a Shimadzu GC-2014 gas chromatograph (Shimadzu, Kyoto, Japan) equipped with a flame ionization detector (FID) using a Supelco Equity-5 (30 m x 0.25 mm) column.

Materials

Riboflavin tetraacetate (**3**),¹⁶ 10-(2-hydroxyethyl)-3,7,8-trimethylisoalloxazine (**9a**),²³ 10-(2-hydroxyethyl)-3-methylisoalloxazine (**9b**),²⁴ 10-(2-hydroxyethyl)-3-methyl-7-trifluoromethylisoalloxazine (**9c**),²⁵ 7,8-dimethyl-1,3-dimethylalloxazine (**10a**),²⁶ 1,3-dimethylalloxazine (**10b**),²⁷ and 8-trifluoromethyl-1,3-dimethylalloxazine (**10c**),²⁷ were synthesized according to the previously reported methods. Other starting materials were purchased from Sigma-Aldrich (St. Louis, USA), FUJIFILM Wako Pure Chemical Corporation (Osaka, Japan), Nacalai tesque (Kyoto, Japan), and Tokyo Kasei (TCI, Tokyo, Japan) and were used as received.

Experimental Procedures

Typical procedure for catalytic aerobic oxidation of 1a with 2. A mixture of 4-methoxybenzenethiol (**1a**, 140 mg, 1.0 mmol), tert-butylamine (**2**, 5.1 mmol), **3** (27.2 mg, 0.050 mmol), CH_3CN (36 mL) and H_2O (4.0 mL) was stirred and irradiated (blue LED, 11 W) under air at 25 °C for 24 h. After the solvent was removed by evaporation, the

yields of the products **4a-8a** were determined to be 0% (**4a**), 0% (**5a**), 67% (**6a**), 18% (**7a**), and 2% (**8a**) yields, respectively, by the ¹H NMR measurement using 1,1,2,2-tetrachloroethane as an internal standard. These results are summarized in Scheme 1. The residue was purified by column chromatography (SiO₂, hexane/ethyl acetate = 4/1 to 1/2, v/v) to give **6a** (136 mg, 60%) as a pale yellow solid and **7a** (49.2 mg, 20%) as a pale yellow solid.

Spectroscopic data of *N*-(4-methoxyphenylsulfinyl)-*N*-(*tert*-butyl)amine (6a**)^{13a}:**

Column chromatography (SiO₂, hexane/ethyl acetate=4/1 to 1/2, v/v) afforded the desired product (136 mg, 60%) as a pale yellow solid. ¹H NMR (500 MHz, CDCl₃, 25 °C, δ): 7.57 (dt, *J* = 8.9, 2.5 Hz, 2H), 6.95 (dt, *J* = 9.0, 2.5 Hz, 2H), 3.96 (br s, 1H), 3.82 (s, 3H), 1.40 (s, 9H). ¹³C{¹H} NMR (126 MHz, CDCl₃, 25 °C, δ): 161.7, 138.0, 127.4, 114.2, 55.6, 54.2, 31.2.

Spectroscopic data of *N*-(4-methoxyphenylsulfonyl)-*N*-(*tert*-butyl)amine (7a**)^{13a}:**

Column chromatography (SiO₂, hexane/ethyl acetate=4/1 to 1/2, v/v) afforded the desired product (49.2 mg, 20%) as a pale yellow solid. ¹H NMR (500 MHz, CDCl₃, 25 °C, δ): 7.83 (dt, *J* = 8.9, 2.5 Hz, 2H), 6.95(dt, *J* = 9.0, 2.6 Hz, 2H), 4.86 (br s, 1H), 3.87 (s, 3H), 1.21 (s, 9H). ¹³C{¹H} NMR (126 MHz, CDCl₃, 25 °C, δ): 162.5, 135.2, 129.2, 114.1, 55.7, 54.5, 30.2.

3-6 References and Notes

- [1] (a) Murahashi, S.; Oda, T.; Masui, Y. *J. Am. Chem. Soc.* **1989**, *111*, 5002-5003. (b) Imada, Y.; Iida, H.; Ono, S.; Murahashi, S.-I. *J. Am. Chem. Soc.* **2003**, *125*, 2868-2869. (c) Imada, Y.; Iida, H.; Murahashi, S.-I.; Naota, T. *Angew. Chem. Int. Ed.* **2005**, *44*, 1704-1706. (d) Murray, A. T.; Matton, P.; Fairhurst, N. W. G.; John, M. P.; Carbery, D. R. *Org. Lett.* **2012**, *14*, 3656-3659. (e) Ishikawa, T.; Kimura, M.; Kumoi, T.; Iida, H. *ACS Catal.* **2017**, *7*, 4986-4989. (f) Tanimoto, K.; Okai, H.; Oka, M.; Ohkado, R.; Iida, H. *Org. Lett.* **2021**, *23*, 2084-2088.
- [2] (a) Murahashi, S. I. *Angew. Chem. Int. Ed.* **1995**, *34*, 2443-2465. (b) Cibulka, R. *Eur. J. Org. Chem.* **2015**, *2015*, 915-932. (c) Iida, H.; Imada, Y.; Murahashi, S. I. *Org. Biomol. Chem.* **2015**, *13*, 7599-7613.
- [3] (a) Lechner, R.; Kümmel, S.; König, B. *Photochem. Photobiol. Sci.* **2010**, *9*, 1367-1377. (b) Muhldorf, B.; Wolf, R. *Angew. Chem. Int. Ed.* **2016**, *55*, 427-430. (c) Zelenka, J.; Svobodova, E.; Tarabek, J.; Hoskovcova, I.; Boguschova, V.; Bailly, S.; Sikorski, M.; Roithova, J.; Cibulka, R. *Org. Lett.* **2019**, *21*, 114-119.
- [4] (a) Fukuzumi, S.; Kuroda, S.; Tanaka, T. *J. Am. Chem. Soc.* **1985**, *107*, 3020-3027. (b) Cibulka, R.; Vasold, R.; König, B. *Chem. –Eur. J.* **2004**, *10*, 6223-6231. (c) Schmaderer, H.; Hilgers, P.; Lechner, R.; König, B. *Adv. Synth. Catal.* **2009**, *351*, 163-174. (d) Feldmeier, C.; Bartling, H.; Magerl, K.; Gschwind, R. M. *Angew. Chem. Int. Ed.* **2015**, *54*, 1347-1351.
- [5] König, B.; Lechner, R. *Synthesis* **2010**, *2010*, 1712-1718.
- [6] (a) Metternich, J. B.; Gilmour, R. *J. Am. Chem. Soc.* **2016**, *138*, 1040-1045. (b) Ramirez, N. P.; König, B.; Gonzalez-Gomez, J. C. *Org. Lett.* **2019**, *21*, 1368-1373. (c) Knowles, O. J.; Johannissen, L. O.; Crisenza, G. E. M.; Hay, S.; Leys, D.; Procter,

- D. J. *Angew. Chem. Int. Ed.* **2022**, *61*, e202212158. (d) Shiogai, Y.; Oka, M.; Iida, H. *Org. Biomol. Chem.* **2023**, *21*, 2081-2085.
- [7] (a) König, B.; Kümmel, S.; Svobodová, E.; Cibulka, R. *Phys. Sci. Rev.* **2018**, *3*. (b) Cibulka, R.; Fraaije, M. W. *Flavin-Based Catalysis: Principles and Applications*; Wiley, 2021. (c) Srivastava, V.; Singh, P. K.; Srivastava, A.; Singh, P. P. *RSC Adv.* **2021**, *11*, 14251-14259.
- [8] (a) Briggs, W. R.; Christie, J. M. *Trends Plant Sci* **2002**, *7*, 204-210. (b) Christie, J. M. *Annu. Rev. Plant Biol.* **2007**, *58*, 21-45.
- [9] Oka, M.; Katsube, D.; Tsuji, T.; Iida, H. *Org. Lett.* **2020**, *22*, 9244-9248.
- [10] Pramanik, M.; Choudhuri, K.; Mal, P. *Org. Biomol. Chem.* **2020**, *18*, 8771-8792.
- [11] (a) Drews, J. *Science* **2000**, *287*, 1960-1964. (b) Devendar, P.; Yang, G.-F. *Top. Curr. Chem.* **2017**, *375*, 82. (c) Scott, K. A.; Njardarson, J. T. *Top. Curr. Chem.* **2018**, *376*, 5. (d) Lücking, U. *Org. Chem. Front.* **2019**, *6*, 1319-1324.
- [12] Mondal, S.; Malakar, S. *Tetrahedron* **2020**, *76*, 131662.
- [13] (a) Taniguchi, N. *Eur. J. Org. Chem.* **2010**, *2010*, 2670-2673. (b) Taniguchi, N. *Eur. J. Org. Chem.* **2016**, *2016*, 2157-2162. (c) Chatterjee, S.; Makai, S.; Morandi, B. *Angew. Chem. Int. Ed.* **2021**, *60*, 758-765.
- [14] Feng, J.-B.; Wu, X.-F. *Org. Biomol. Chem.* **2016**, *14*, 6951-6954.
- [15] Laudadio, G.; Barmoutsis, E.; Schotten, C.; Struik, L.; Govaerts, S.; Browne, D. L.; Noel, T. *J. Am. Chem. Soc.* **2019**, *141*, 5664-5668.
- [16] Takeda, A.; Okai, H.; Watabe, K.; Iida, H. *J. Org. Chem.* **2022**, *87*, 10372-10376.
- [17] Mühldorf, B.; Wolf, R. *Chem. Commun.* **2015**, *51*, 8425-8428.
- [18] Neumann, M.; Földner, S.; König, B.; Zeitler, K. *Angew. Chem. Int. Ed.* **2011**, *50*, 951-954.

- [19] (a) Dou, Y.; Huang, X.; Wang, H.; Yang, L.; Li, H.; Yuan, B.; Yang, G. *Green Chem.* **2017**, *19*, 2491-2495. (b) Cao, Y.; Abdolmohammadi, S.; Ahmadi, R.; Issakhov, A.; Ebadi, A. G.; Vessally, E. *RSC Adv.* **2021**, *11*, 32394-32407.
- [20] Neveselý, T.; Svobodová, E.; Chudoba, J.; Sikorski, M.; Cibulka, R. *Adv. Synth. Catal.* **2016**, *358*, 1654-1663.
- [21] Kemal, C.; Chan, T. W.; Bruice, T. C. *J. Am. Chem. Soc.* **1977**, *99*, 7272-7286.
- [22] Dad'ova, J.; Svobodova, E.; Sikorski, M.; Konig, B.; Cibulka, R. *Chemcatchem* **2012**, *4*, 620-623.
- [23] Sakai, T.; Kumoi, T.; Ishikawa, T.; Nitta, T.; Iida, H. *Org. Biomol. Chem.* **2018**, *16*, 3999-4007.
- [24] Zelenka, J.; Hartman, T.; Klimova, K.; Hampl, F.; Cibulka, R. *Chemcatchem* **2014**, *6*, 2843-2846.
- [25] Li, W.-S.; Zhang, N.; Sayre, L. M. *Tetrahedron* **2001**, *57*, 4507-4522.
- [26] Chen, S.; Hossain, M. S.; Foss, F. W., Jr. *Org. Lett.* **2012**, *14*, 2806-2809.
- Ménová, P.; Dvořáková, H.; Eigner, V.; Ludvík, J.; Cibulka, R. *Adv. Synth. Catal.* **2013**, *355*, 3451-3462.

Chapter 4

Aerobic oxidative homo-coupling of thiols by flavin-iodine organocatalysis

- 4-1 Abstract
- 4-2 Introduction
- 4-3 Results and Discussion
- 4-4 Conclusion
- 4-5 Experimental Section
- 4-6 References and Notes

4-1 Abstract

Using the flavin-iodine coupled catalyst system, the aerobic oxidative homocoupling of thiols proceeded under mild metal-free conditions and efficiently produced the desired disulfides. The biomimetic flavin catalyst activated O₂ at room temperature through electron transfer from the iodine catalyst.

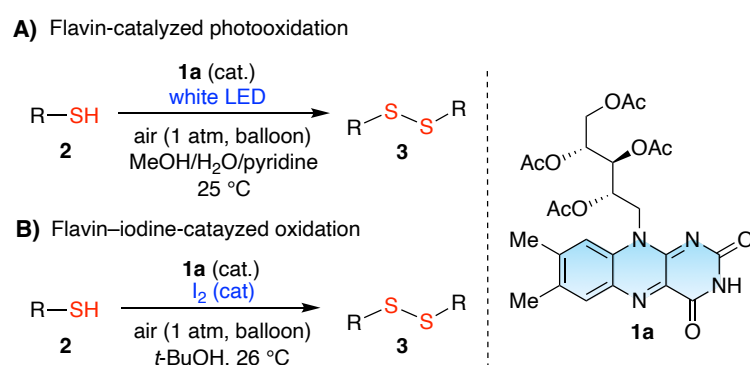
4-2 Introduction

In organic synthesis, it is important to establish catalytic systems that allow efficient aerobic oxidation to proceed under environmentally friendly conditions.¹ Since O₂ is abundant in the air and atom economy, much effort has been focused on developing catalytic reactions using O₂ as an oxidant. However, the activation of O₂ generally requires harsh conditions such as high temperatures or pressures, transition metal catalysts, and the addition of reagents that generate large amounts of waste. Therefore, developing a green approach using O₂ as the terminal oxidant is desirable via activation under mild conditions.

Flavin catalysts are organocatalysts developed to mimic the function of the oxygenase “flavin monooxygenase”² and have attracted much attention as redox catalysts³ and photocatalysts⁴ that are capable of activating O₂ under mild conditions.⁵ Recently, inspired by the multiple catalytic systems of enzymes, the author’s laboratory has developed a novel approach for environmentally benign aerobic oxidative transformations catalyzed by the coupling of flavin and iodine.⁶ This dual catalytic system is capable not only of C–S, and C–N bond formations, as observed in the sulfenylation⁷ and azolation of indoles,⁸ but also in the heteroaromatic ring formations by multistep aerobic oxidations.⁹ In this flavin-iodine-catalyzed system, thiols are transformed into disulfides, but the generated disulfides are used as intermediates in the C–S bond formation reaction and are immediately consumed.^{7a} Consequently, the flavin–iodine catalyzed system is expected to facilitate aerobic thiol oxidation under mild conditions efficiently. Nevertheless, this system has not been practically applied in the synthesis of disulfides.

Disulfides are important compounds commonly used as starting materials in organic

synthesis¹⁰ and also essential in biochemistry¹¹ and materials chemistry.¹² In the homo- and cross-coupling of thiols,¹³ the oxidation of simple thiols using O₂ as an oxidant is the most ideal atom-economical and environmentally friendly approach.^{13b,14} In addition, the author recently reported the aerobic oxidative homo- and cross-coupling of thiols driven by visible light and O₂, using riboflavin tetraacetate (**1a**), obtained in a simple step from low-cost and commercial riboflavin (vitamin B₂), as a photoorganocatalyst (Scheme 1A).¹⁵ Herein, the author reports an aerobic oxidative homo-coupling of thiols catalyzed by the coupling of **1a** and iodine. This allowed the disulfides to be efficiently obtained under mild metal-free conditions without light irradiation (Scheme 1B).



Scheme 1. Riboflavin-catalyzed aerobic oxidation of thiols using (A) photocatalysis with **1a** and (B) coupled catalysis with **1a** and iodine.

4-3 Results and Discussion

First, the catalytic activity of flavin in the oxidation of 1-octanethiol (**2a**) was investigated to optimize the reaction conditions. The reaction was performed in MeOH in air (1 atm, balloon) at 26 °C for 4 h (Table 1). Various neutral flavins (**1** and **4**)¹⁶ and cationic flavinium salts (**5–7**)^{17,18} were used as the catalysts (Figure 1, 5 mol%). The results showed that, in the presence of I₂ (5 mol%), neutral flavin **1a**¹⁶ efficiently promoted the oxidation of **2a**, yielding the desired disulfide **3a** in 86% yield (entry 1, Table 1). Riboflavin tetrabutyrate (**1b**), a commercially available riboflavin derivative, showed comparable catalytic activity, whereas nonprotected riboflavin (**1c**) showed less progress in the reaction because of its lower solubility (entries 2 and 3). Alloxazine **4**, which contains an electron-deficient CF₃ group, has often been used in the photocatalytic dehydrogenation of alcohols¹⁹, but the yield of **3a** was only 14% (entry 4). Cationic flavinium salts **5–7**, which are known organocatalysts for efficient oxygenations^{5a}, did not afford **3a** in high yields (entries 5–7). The effects of iodine sources and solvents were also studied, and it was shown that simple I₂ and the protic solvent *t*-BuOH were the best (Table 2).

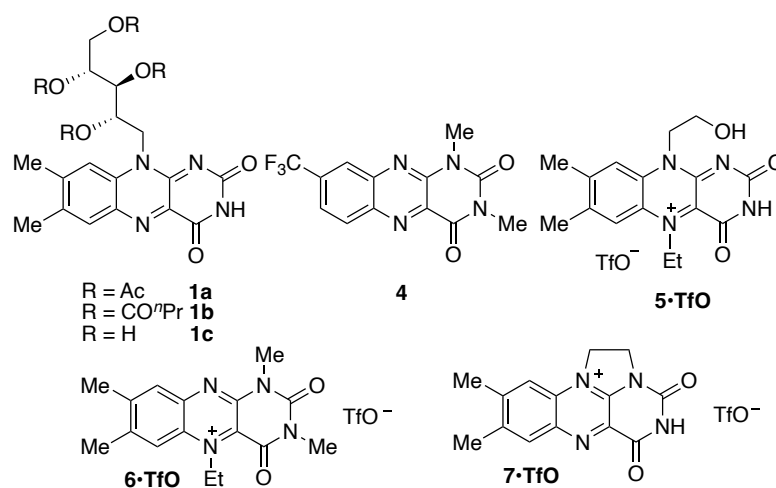


Figure 1. Structure of flavin derivatives.

Table 1. Effect of flavin and flavinium catalysts on the oxidation of **2a**.^a

entry	flavin	I ₂ (mol%)	yield (%)
1	1a	5	86
2	1b	5	82
3	1c	5	23
4	4	5	14
5	5·TfO	5	24
6	6·TfO	5	72
7	7·TfO	5	20
8	–	5	10
9	1a	–	2
10 ^b	1a	5	17

^aConditions: **2a** (0.5 M), flavin (5 mol%), I₂ (5 mol%) and MeOH under air (1 atm, balloon) at ca. 26 °C for 4 h. The yield was determined by GC using biphenyl as an internal standard. ^bUnder N₂. Average of two runs.

Table 2. Screening of iodine sources and solvents.^a

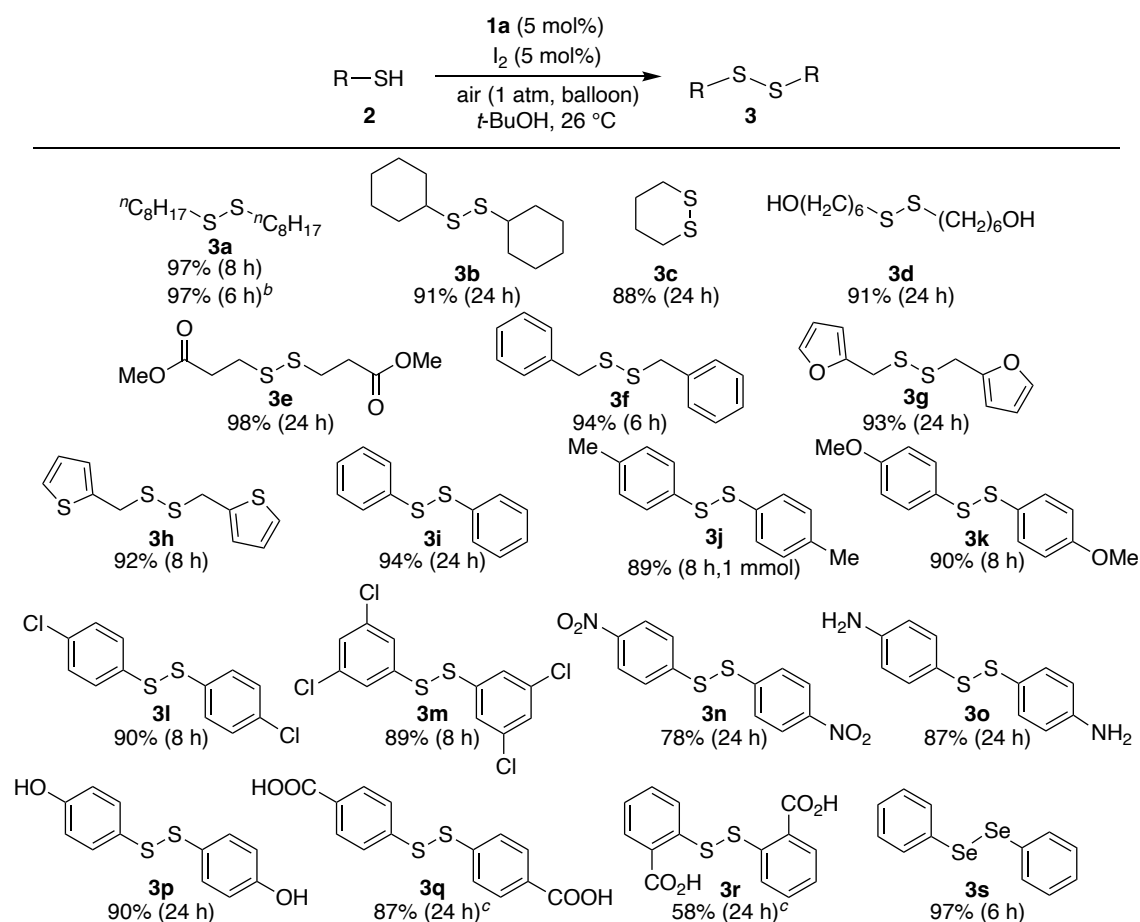
$$\begin{array}{ccc}
 \text{}^n\text{C}_8\text{H}_{17}\text{SH} & \xrightarrow[\text{air (1 atm, balloon)}]{\text{1 a (5 mol\%)} \\ \text{iodine (cat.)}} & \text{}^n\text{C}_8\text{H}_{17}\text{-S-S-}\text{}^n\text{C}_8\text{H}_{17} \\
 \text{2 a} & \text{solvent, 26 }^\circ\text{C, 4 h} & \text{3 a}
 \end{array}$$

entry	iodine (mol%)	solvent	yield (%)
1	I ₂ (5)	MeOH	86
2	NH ₄ I (10)	MeOH	1
3	KI (10)	MeOH	2
4	HI (10)	MeOH	29
5	TBAI (10)	MeOH	2
6	I ₂ (5)	CH ₃ CN	65
7	I ₂ (5)	pyridine	81
8	I ₂ (5)	CHCl ₃	32
9	I ₂ (5)	AcOEt	52
10	I ₂ (5)	<i>t</i> -BuOH	91

^aConditions: **2a** (0.5 M), **1a** (5 mol%), iodine source (5 or 10 mol%), and solvent under air (1 atm, balloon) at 26 °C for 4 h. The yield was determined by GC, using biphenyl as an internal standard.

Next, the substrate scope of the oxidative homocoupling of thiols was investigated under the optimized reaction conditions (Table 3). The reactions of primary alkanethiol **2a** and secondary alkanethiol **2b** afforded the desired disulfides **3a** and **3b** in high yields of 97% and 91%, respectively. 1,4-Butanedithiol (**2c**) underwent intermolecular cyclization to afford cyclic disulfide **3c**. The oxidation of alkanethiols bearing hydroxyl and ester groups proceeded smoothly (**3d** and **3e**). Arylmercaptans with phenyl, furyl, and thiophenyl groups (**2f–h**) were also converted into the corresponding disulfides **3f–h** in 92%–94% yields. Arenethiols containing electron-donating or electron-withdrawing groups **2i–m** afforded the corresponding disulfides **3i–m** in high yields, whereas **2n** was converted to **3n** in a relatively low yield owing to its low solubility. As previously reported,

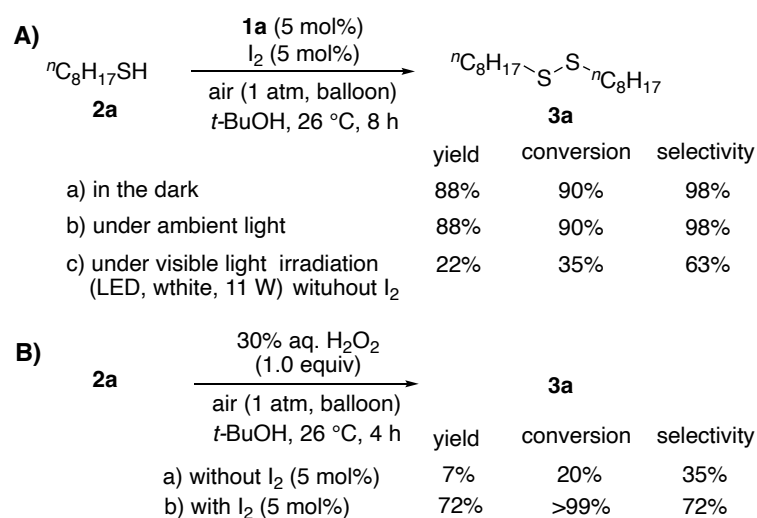
examples of the flavin-catalyzed photooxidation of thiols required the addition of a base (Scheme 1A), and its application to acidic substrates was difficult.¹⁵ However, this catalytic reaction yielded the desired disulfides in high yields not only from thiols bearing basic amino groups (**2o**) but also from thiols with acidic hydroxy and carboxyl groups (**2p-r**), indicating that a variety of functional groups are acceptable. Furthermore, diselenide **3s** was obtained in 97% yield, even from benzeneselenol (**2s**). This demonstrates the potential of this method, which is applicable to other chalcogen compounds in addition to thiols.

Table 3. Aerobic oxidation of thiols by flavin-iodine catalysis.^a

^aConditions: **2** (0.5 M), **1a** (5 mol%), I₂ (5 mol%) and *t*-BuOH under air (1 atm, balloon) at 26 °C. ^bWith **1b** as the catalyst. ^cIsolated as the corresponding methyl ester after esterification with (trimethylsilyl)diazomethane.

Control experiments were performed to elucidate the reaction mechanism. When the reaction was performed without flavin **1a**, I₂ or under nitrogen, the homocoupling of **2a** hardly proceeded, indicating that flavin, iodine, and O₂ were required (Table 1, entries 8-10). The author then studied the effect of light irradiation on this catalytic reaction and found no difference between the reactions performed in the dark and under ambient light (Scheme 2Aa,b), while reactions without I₂ and under white LED irradiation resulted in

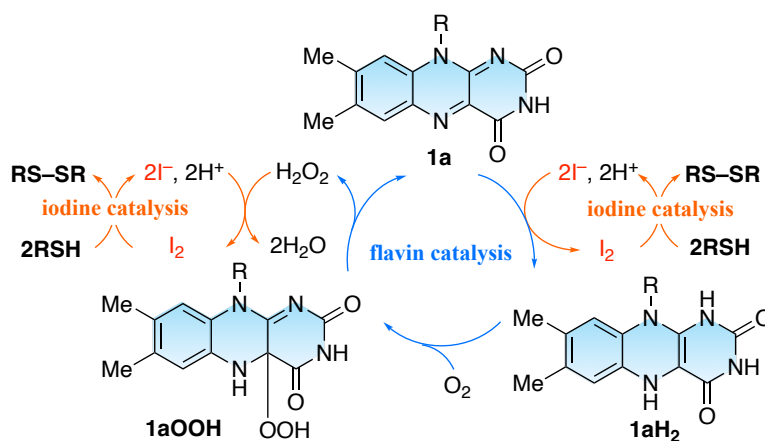
lower yields and selectivities than those without visible light irradiation (Scheme 2Ac). Unlike the previously reported photocatalytic reaction of **1a**, which involved an aerobic oxidative homocoupling reaction of thiols promoted by the addition of a base¹⁵, this reaction proceeded efficiently under neutral conditions, suggesting that the reaction was non-photocatalytic.



Scheme 2. Control experiments to determine the effect of (A) light irradiation and (B) H₂O₂ generated in situ.

Based on these experimental results and previously reported literature, the proposed reaction mechanism for the flavin-iodine-catalyzed aerobic oxidative homocoupling of thiols is shown in Scheme 3. Thiols reacted with I₂ and are oxidized to disulfides by forming a sulfenyl iodide (RS-I) to give I⁻.^{20,21} The cationic flavinium salt with relatively higher oxidizing power can directly convert thiols to disulfides,^{7a} while the neutral flavin **1a** did not proceed to oxidation of thiols under conditions without I₂ (Table 1, entry 9).²² In this catalytic system, the neutral flavin **1a** acts as a redox catalyst, oxidizing I⁻ to regenerate I₂, which itself is reduced to reduced flavin **1aH₂**.⁶ The produced **1aH₂**

activates O_2 , producing H_2O_2 through the hydroperoxyflavin **1aOOH**, and the flavin returns to the initial **1a**.²³ To further investigate the role of the generated H_2O_2 , the oxidation of **2a** was performed using H_2O_2 as an oxidant. Without I_2 , **1a** was directly oxidized **2a** in a low yield of 7% and selectivity of 35% (Scheme 2Ba). By contrast, **2a** was smoothly oxidized to **3a** when a catalytic amount of I_2 was added (Scheme 2Bb). This suggests that the H_2O_2 produced in the catalytic cycle of flavin is also involved in the oxidation of I^- , providing I_2 . Therefore, this reaction system is driven by O_2 in the atmosphere and emits only environmentally friendly H_2O as a byproduct, resulting in the development of a green and efficient oxidation system.



Scheme 3. Proposed mechanism of this catalytic system.

4-4 Conclusion

In conclusion, the combination of I₂ and a neutral flavin catalyst such as **1a**, which can be easily prepared, allows for the efficient synthesis of disulfides through the aerobic oxidative homocoupling of thiols. I₂ was involved in the oxidation of thiols, and the resulting I⁻ was catalytically regenerated to I₂ by flavins through the activation of O₂. Although the previously reported photooxidation of thiols using **1a** as a photocatalyst requires visible-light irradiation and the addition of a base, the flavin-iodine catalyst system not only allows the oxidation of thiols to proceed without visible-light irradiation but also does not affect the acidity of the reaction system. Thus, this method can be applied to various thiols, including basic amino and acidic carboxyl groups. Furthermore, because this simple and efficient methodology can be applied to the oxidation of selenium and thiols, it can be used for the multistep and multicomponent synthesis of chalcogen-containing compounds, which are important in biological and medicinal chemistry.

4-5 Experimental Section

General

The NMR spectra were measured using JEOL JNM-L400 and JNM ECX-500 spectrometers (JEOL, Akishima, Japan) operating at 400 and 500 MHz, respectively, for ^1H and 100 and 126 MHz, respectively, for ^{13}C using tetramethylsilane (TMS) or a solvent residual peak as the internal standard. The GC measurements were performed on a Shimadzu GC-2014 gas chromatograph (Shimadzu, Kyoto, Japan) equipped with a flame ionization detector (FID) using a Supelco Equity-5 (30 m x 0.25 mm) column.

Materials. All starting materials were purchased from Sigma-Aldrich, Fujifilm Wako Pure Chemical Corporation, or Tokyo Chemical Industry and used as received. Riboflavin tetraacetate (**1a**),¹⁶ 1,3-dimethyl-8-trifluoromethylalloxazine (**4**),¹⁷ 5-ethyl-10-(2-hydroxyethyl)-7,8-dimethylisoalloxazinium triflate (**5•TfO**),¹⁸ 5-ethyl-1,3,7,8-tetramethylalloxazinium triflate (**6•TfO**),¹⁸ and 1,10-ethylene-7,8-dimethylisoalloxazinium triflate (**7•TfO**)¹⁸ were prepared according to previously reported methods.

Typical Procedure for the Catalytic Aerobic Oxidation of 2a. A mixture of **2a** (73.1 mg, 0.50 mmol), **1a** (13.6 mg, 0.025 mmol), I_2 (6.35 mg, 0.025 mmol), and *t*-BuOH (1.0 mL) was stirred at 26 °C (water bath) for 8 h under air (1 atm, balloon) in the dark. The solvent was removed using evaporation and the residue was purified via column chromatography (SiO_2 , chloroform) to obtain **3a** (70.7 mg, 97%) as a colorless oil; the results have been summarized in Table 3.

Spectroscopic data of 1,2-dioctyldisulfane (3a):^{14c} Column chromatography (SiO₂, chloroform) afforded the desired product (70.7 mg, 97%) as a colorless oil. ¹H NMR (500 MHz, CDCl₃, 25 °C, δ): 2.68 (t, J = 7.4 Hz, 4H), 1.67 (quin, J = 7.4 Hz, 4H), 1.41-1.33 (m, 4H), 1.32-1.20 (m, 16H), 0.88 (t, J = 6.9 Hz, 6H). ¹³C{¹H} NMR (126 MHz, CDCl₃, 25 °C, δ): 39.3, 31.8, 29.3, 28.6, 22.7, 14.1.

Spectroscopic data of 1,2-dicyclohexyldisulfane (3b):^{14d} Column chromatography (SiO₂, chloroform) afforded the desired product (52.2 mg, 91%) as a colorless oil. ¹H NMR (500 MHz, CDCl₃, 25 °C, δ): 2.72-2.64 (m, 2H), 2.08-2.01 (m, 4H), 1.82-1.73 (m, 4H), 1.65-1.58 (m, 2H), 1.37-1.18 (m, 10H). ¹³C{¹H} NMR (126 MHz, CDCl₃, 25 °C, δ): 50.1, 33.0, 26.2, 25.8.

Spectroscopic data of 1,2-dithiane (3c):²⁴ Column chromatography (SiO₂, chloroform) afforded the desired product (93 mg, 88%) as a colorless oil. ¹H NMR (500 MHz, CDCl₃, 25 °C, δ): 2.85 (s, 4H), 1.97 (s, 4H). ¹³C{¹H} NMR (126 MHz, CDCl₃, 25 °C, δ): 33.5, 27.9.

Spectroscopic data of 6,6'-disulfanediybis(hexan-1-ol) (3d):²⁵ Column chromatography (SiO₂, hexane/ethyl acetate = 1/1, v/v) afforded the desired product (60.9 mg, 91%) as a colorless oil. ¹H NMR (500 MHz, CDCl₃, 25 °C, δ): 3.65 (t, J = 6.5 Hz, 4H), 2.69 (t, J = 7.3 Hz, 4H), 1.75-1.65 (m, 6H), 1.58 (quin, J = 6.9 Hz, 4H), 1.45-1.35 (m, 8H). ¹³C{¹H} NMR (126 MHz, CDCl₃, 25 °C, δ): 62.9, 39.1, 32.7, 29.2, 28.4, 25.5.

Spectroscopic data of dimethyl 3,3'-disulfanediylpropionate (3e):^{14c} Column chromatography (SiO₂, chloroform) afforded the desired product (58.3 mg, 98%) as a colorless oil. ¹H NMR (500 MHz, CDCl₃, 25 °C, δ): 3.71 (s, 6H), 2.93 (t, J = 7.0 Hz, 4H), 2.75 (t, J = 7.0 Hz, 4H). ¹³C{¹H} NMR (126 MHz, CDCl₃, 25 °C, δ): 172.2, 52.0, 34.0, 33.2.

Spectroscopic data of 1,2-dibenzylidysulfane (3f):^{14d} Column chromatography (SiO₂, chloroform) afforded the desired product (58.8 mg, 94%) as a colorless oil. ¹H NMR (500 MHz, CDCl₃, 25 °C, δ): 7.34-7.21 (m, 10H), 3.60 (s, 4H). ¹³C{¹H} NMR (126 MHz, CDCl₃, 25 °C, δ): 137.5, 129.6, 128.6, 127.6, 43.4.

Spectroscopic data of 1,2-bis(furan-2-ylmethyl)disulfane (3g):²⁶ Column chromatography (SiO₂, chloroform) afforded the desired product (53.5 mg, 93%) as a white solid. ¹H NMR (500 MHz, CDCl₃, 25 °C, δ): 7.38 (d, J = 1.7 Hz, 2H), 6.33 (dd, J = 3.1, 1.9 Hz, 2H), 6.22 (d, J = 3.2 Hz, 2H), 3.69 (s, 4H). ¹³C{¹H} NMR (126 MHz, CDCl₃, 25 °C, δ): 150.3, 142.6, 110.9, 109.1, 35.8.

Spectroscopic data of 1,2-bis(thiophen-2-ylmethyl)disulfane (3h):²⁷ Column chromatography (SiO₂, chloroform) afforded the desired product (59.9 mg, 92%) as a colorless oil. ¹H NMR (500 MHz, CDCl₃, 25 °C, δ): 7.24-7.22 (m, 2H), 6.95-6.92 (m, 4H), 3.86 (s, 4H). ¹³C{¹H} NMR (126 MHz, CDCl₃, 25 °C, δ): 139.9, 127.3, 127.1, 125.8, 37.8.

Spectroscopic data of 1,2-dibenzenedisulfane (3i):²⁸ Column chromatography (SiO₂, chloroform) afforded the desired product (105 mg, 94%) as a pale yellow solid. ¹H NMR (500 MHz, CDCl₃, 25 °C, δ): 7.50 (d, J = 8.3 Hz, 4H), 7.33-7.27 (m, 4H), 7.22 (t, J = 7.8 Hz, 2H), ¹³C{¹H} NMR (126 MHz, CDCl₃, 25 °C, δ): 137.2, 129.2, 127.7, 127.3.

Spectroscopic data of 1,2-di-p-tolyldisulfane (3j):^{14d} Column chromatography (SiO₂, chloroform) afforded the desired product (229 mg, 89%) as a white solid. ¹H NMR (500 MHz, CDCl₃, 25 °C, δ): 7.38 (d, J = 8.1 Hz, 4H), 7.10 (d, J = 7.9 Hz, 4H), 2.31 (s, 6H). ¹³C{¹H} NMR (126 MHz, CDCl₃, 25 °C, δ): 137.6, 134.0, 129.9, 128.7, 21.2.

Spectroscopic data of 1,2-bis(4-methoxyphenyl)disulfane (3k):^{14d} Column chromatography (SiO₂, chloroform) afforded the desired product (131 mg, 90%) as a white solid. ¹H NMR (500 MHz, CDCl₃, 25 °C, δ): 7.39 (d, J = 8.8 Hz, 4H), 6.83 (d, J = 8.8 Hz, 4H), 3.80 (s, 6H). ¹³C{¹H} NMR (126 MHz, CDCl₃, 25 °C, δ): 160.1, 132.8, 128.6, 114.8, 55.5.

Spectroscopic data of 1,2-bis(4-chlorophenyl)disulfane (3l):^{14d} Column chromatography (SiO₂, chloroform) afforded the desired product (130 mg, 90%) as a white solid. ¹H NMR (500 MHz, CDCl₃, 25 °C, δ): 7.40 (d, J = 8.1 Hz, 4H), 7.28 (d, J = 8.1 Hz, 4H). ¹³C{¹H} NMR (126 MHz, CDCl₃, 25 °C, δ): 135.3, 133.8, 129.51, 129.46.

Spectroscopic data of 1,2-bis(3,5-dichlorophenyl)disulfane (3m):²⁹ Column chromatography (SiO₂, chloroform) afforded the desired product (130 mg, 90%) as a white solid. ¹H NMR (500 MHz, CDCl₃, 25 °C, δ): 7.34 (d, J = 1.8 Hz, 4H), 7.24 (t, J =

1.7 Hz, 2H). $^{13}\text{C}\{^1\text{H}\}$ NMR (126 MHz, CDCl_3 , 25 °C, δ): 139.4, 136.0, 127.9, 125.1.

Spectroscopic data of 1,2-bis(4-nitrophenyl)disulfane (3n):^{14d} Column chromatography (SiO_2 , hexane/ethyl acetate = 4/1 to 1/1, v/v) afforded the desired product (121 mg, 80%) as a white solid. ^1H NMR (500 MHz, CDCl_3 , 25 °C, δ): 8.20 (d, J = 8.8 Hz, 4H), 7.62 (d, J = 8.8 Hz, 4H). $^{13}\text{C}\{^1\text{H}\}$ NMR (126 MHz, CDCl_3 , 25 °C, δ): 147.1, 144.2, 126.5, 124.6.

Spectroscopic data of 1,2-bis(4-aminophenyl)disulfane (3o):^{14d} Column chromatography (SiO_2 , chloroform) afforded the desired product (108 mg, 78%) as a pale yellow solid. ^1H NMR (500 MHz, CDCl_3 , 25 °C, δ): 7.25 (d, J = 8.6 Hz, 4H), 6.58 (d, J = 8.7 Hz, 4H), 3.77 (s, 4H). $^{13}\text{C}\{^1\text{H}\}$ NMR (126 MHz, CDCl_3 , 25 °C, δ): 147.2, 134.1, 125.9, 115.5.

Spectroscopic data of 1,2-bis(4-hydroxyphenyl)disulfane (3p):^{14d} Column chromatography (SiO_2 , hexane/ethyl acetate = 4/1 to 1/1, v/v) afforded the desired product (110 mg, 90%) as a white solid. ^1H NMR (500 MHz, CDCl_3 , 25 °C, δ): 9.82 (s, 2H), 7.27 (d, J = 8.6 Hz, 4H), 6.76 (d, J = 8.7 Hz, 4H). $^{13}\text{C}\{^1\text{H}\}$ NMR (126 MHz, CDCl_3 , 25 °C, δ): 158.3, 133.0, 125.1, 116.3.

Spectroscopic data of dimethyl 4,4'-disulfanediyldibenzoate (3q):^{14d} Column chromatography (SiO_2 , hexane/ethyl acetate = 9/1 to 3/1, v/v) afforded the desired product (72.4 mg, 87%) as a white solid. ^1H NMR (500 MHz, CDCl_3 , 25 °C, δ): 7.96 (d, J = 8.6 Hz, 4H), 7.52 (d, J = 8.6 Hz, 4H), 3.89 (s, 6H). $^{13}\text{C}\{^1\text{H}\}$ NMR (126 MHz, CDCl_3 ,

25 °C, δ): 166.4, 142.2, 130.4, 128.9, 126.1, 52.3.

Spectroscopic data of dimethyl 2,2'-disulfanediylldibenzoate (3r):^{14d} Column chromatography (SiO₂, hexane/ethyl acetate = 9/1, v/v) afforded the desired product (48.2 mg, 58%) as a white solid. ¹H NMR (500 MHz, CDCl₃, 25 °C, δ): 8.06 (dd, J = 7.8, 1.4 Hz, 2H), 7.76 (dd, J = 8.1, 0.91 Hz, 2H), 7.43-7.37 (m, 2H), 7.26-7.20 (m, 2H), 3.99 (s, 6H). ¹³C{¹H} NMR (126 MHz, CDCl₃, 25 °C, δ): 167.0, 140.4, 133.2, 131.6, 127.4, 125.9, 125.6, 52.5.

Spectroscopic data of 1,2-diphenyldiselenide (3s):³⁰ Column chromatography (SiO₂, chloroform) afforded the desired product (74.2 mg, 97%) as a yellow solid. ¹H NMR (500 MHz, CDCl₃, 25 °C, δ): 7.62-7.57 (m, 4H), 7.30-7.21 (m, 6H). ¹³C{¹H} NMR (126 MHz, CDCl₃, 25 °C, δ): 131.6, 131.1, 129.3, 127.9.

4-6 References and Notes

- [1] Hill, C. L. *Nature* **1999**, *401*, 436. (b) Simándi, L. I. *Advances in Catalytic Activation of Dioxygen by Metal Complexes*; Kluwer Academic, 2002. (c) *Green Oxidation in Organic Synthesis*; Wiley, 2019.
- [2] (a) Bruice, T. C. *Acc. Chem. Res.* **1980**, *13*, 256. (b) Murahashi, S. I.; Oda, T.; Masui, Y. *J. Am. Chem. Soc.* **1989**, *111*, 5002. (c) Murahashi, S. I. *Angew. Chem. Int. Ed.* **1995**, *34*, 2443.
- [3] (a) Imada, Y.; Iida, H.; Ono, S.; Murahashi, S. *J. Am. Chem. Soc.* **2003**, *125*, 2868-2869. (b) Imada, Y.; Iida, H.; Murahashi, S.-I.; Naota, T. *Angew. Chem. Int. Ed.* **2005**, *44*, 1704-1706. (c) Chen, S.; Foss, F. W., Jr. *Org. Lett.* **2012**, *14*, 5150-5153. (d) Kotoucova, H.; Strnadova, I.; Kovandova, M.; Chudoba, J.; Dvorakova, H.; Cibulka, R. *Org. Biomol. Chem.* **2014**, *12*, 2137-2142. (e) Murahashi, S.-I.; Zhang, D.; Iida, H.; Miyawaki, T.; Uenaka, M.; Murano, K.; Meguro, K. *Chem. Commun.* **2014**, *50*, 10295-10298.
- [4] (a) Metternich, J. B.; Gilmour, R. *J. Am. Chem. Soc.* **2016**, *138*, 1040-1045. (b) Ramirez, N. P.; Konig, B.; Gonzalez-Gomez, J. C. *Org. Lett.* **2019**, *21*, 1368-1373. (c) Zelenka, J.; Cibulka, R.; Roithová, J. *Angew. Chem. Int. Ed.* **2019**, *58*, 15412-15420.
- [5] (a) Iida, H.; Imada, Y.; Murahashi, S. I. *Org. Biomol. Chem.* **2015**, *13*, 7599-7613. (b) Cibulka, R. *Eur. J. Org. Chem.* **2015**, *2015*, 915-932. (c) König, B.; Kümmel, S.; Svobodová, E.; Cibulka, R. *Phys. Sci. Rev.* **2018**, *3*.
- [6] Ishikawa, T.; Kimura, M.; Kumoi, T.; Iida, H. *ACS Catal.* **2017**, *7*, 4986-4989.
- [7] (a) Ohkado, R.; Ishikawa, T.; Iida, H. *Green Chem.* **2018**, *20*, 984-988. (b) Iida, H.; Demizu, R.; Ohkado, R. *J. Org. Chem.* **2018**, *83*, 12291. (c) Tanimoto, K.; Ohkado,

- R.; Iida, H. *J. Org. Chem.* **2019**, *84*, 14980. (d) Jiang, X.; Shen, Z.; Zheng, C.; Fang, L.; Chen, K.; Yu, C. *Tetrahedron Lett.* **2020**, *61*, 152141.
- [8] Tanimoto, K.; Okai, H.; Oka, M.; Ohkado, R.; Iida, H. *Org. Lett.* **2021**, *23*, 2084-2088.
- [9] Okai, H.; Tanimoto, K.; Ohkado, R.; Iida, H. *Org. Lett.* **2020**, *22*, 8002-8006.
- [10] Pramanik, M.; Choudhuri, K.; Mal, P. *Org. Biomol. Chem.* **2020**, *18*, 8771-8792.
- [11] (a) Narayan, M.; Welker, E.; Wedemeyer, W. J.; Scheraga, H. A. *Acc. Chem. Res.* **2000**, *33*, 805-812. (b) Lee, M. H.; Yang, Z.; Lim, C. W.; Lee, Y. H.; Dongbang, S.; Kang, C.; Kim, J. S. *Chem. Rev.* **2013**, *113*, 5071-5109. (c) Nielsen, D. S.; Shepherd, N. E.; Xu, W.; Lucke, A. J.; Stoermer, M. J.; Fairlie, D. P. *Chem. Rev.* **2017**, *117*, 8094-8128. (d) Fass, D.; Thorpe, C. *Chem. Rev.* **2018**, *118*, 1169-1198.
- [12] (a) Gronbeck, H.; Curioni, A.; Andreoni, W. *J. Am. Chem. Soc.* **2000**, *122*, 3839-3842. (b) Cui, H.-K.; Guo, Y.; He, Y.; Wang, F.-L.; Chang, H.-N.; Wang, Y.-J.; Wu, F.-M.; Tian, C.-L.; Liu, L. *Angew. Chem. Int. Ed.* **2013**, *52*, 9558-9562.
- [13] (a) Witt, D. *Synthesis-stuttgart* **2008**, *2008*, 2491-2509. (b) Mandal, B.; Basu, B. *RSC Adv.* **2014**, *4*.
- [14] (a) Abdel-Mohsen, H. T.; Sudheendran, K.; Conrad, J.; Beifuss, U. *Green Chem.* **2013**, *15*, 1490-1495. (b) Dou, Y.; Huang, X.; Wang, H.; Yang, L.; Li, H.; Yuan, B.; Yang, G. *Green Chem.* **2017**, *19*, 2491-2495. (c) Qiu, X.; Yang, X. X.; Zhang, Y. Q.; Song, S.; Jiao, N. *Org. Chem. Front.* **2019**, *6*, 2220-2225. (d) Song, L. J.; Li, W. H.; Duan, W. X.; An, J. C.; Tang, S. Y.; Li, L. J.; Yang, G. *Green Chem.* **2019**, *21*, 1432-1438.
- [15] Oka, M.; Katsube, D.; Tsuji, T.; Iida, H. *Org. Lett.* **2020**, *22*, 9244-9248.
- [16] Müller, F. [147] Synthesis of 2-substituted riboflavin analogs. In *Vitamins and*

- Coenzymes*, Methods in Enzymology, Vol. 18; Academic Press, 1971; pp 453-458.
- [17] Ménová, P.; Dvořáková, H.; Eigner, V.; Ludvík, J.; Cibulka, R. *Adv. Synth. Catal.* **2013**, *355*, 3451-3462.
- [18] Sakai, T.; Kumoi, T.; Ishikawa, T.; Nitta, T.; Iida, H. *Org. Biomol. Chem.* **2018**, *16*, 3999-4007.
- [19] Tolba, A. H.; Vávra, F.; Chudoba, J.; Cibulka, R. *Eur. J. Org. Chem.* **2020**, *2020*, 1579-1585.
- [20] Goto, K.; Holler, M. *Chem. Commun.* **1998**, 1915-1916.
- [21] Bettanin, L.; Saba, S.; Galetto, F. Z.; Mike, G. A.; Rafique, J.; Braga, A. L. *Tetrahedron Lett.* **2017**, *58*, 4713-4716.
- [22] (a) Loechler, E. L.; Hollocher, T. C. *J. Am. Chem. Soc.* **1975**, *97*, 3235-3237. (b) Loechler, E. L.; Hollocher, T. C. *J. Am. Chem. Soc.* **1980**, *102*, 7312-7321.
- [23] Kemal, C.; Chan, T. W.; Bruice, T. C. *J. Am. Chem. Soc.* **1977**, *99*, 7272-7286.
- [24] Abul-Futouh, H.; Almazahreh, L. R.; Harb, M. K.; Görls, H.; El-khateeb, M.; Weigand, W. *Inorg. Chem.* **2017**, *56*, 10437-10451.
- [25] Rattanangkool, E.; Krailat, W.; Vilaivan, T.; Phuwapraisirisan, P.; Sukwattanasinitt, M.; Wacharasindhu, S. *Eur. J. Org. Chem.* **2014**, *2014*, 4795-4804.
- [26] Talla, A.; Driessen, B.; Straathof, N. J. W.; Milroy, L.-G.; Brunsveld, L.; Hessel, V.; Noël, T. *Adv. Synth. Catal.* **2015**, *357*, 2180-2186.
- [27] He, W.; Ding, Y.; Tu, J.; Que, C.; Yang, Z.; Xu, J. *Org. Biomol. Chem.* **2018**, *16*, 1659-1666.
- [28] Abbasi, M.; Nowrouzi, N.; Mousavi, S. *ChemistrySelect* **2019**, *4*, 12227-12231.
- [29] Kim, J.; Kang, B.; Hong, S. H. *ACS Catal.* **2020**, *10*, 6013-6022.
- [30] Singh, D.; Deobald, A. M.; Camargo, L. R. S.; Tabarelli, G.; Rodrigues, O. E. D.;

Braga, A. L. *Org. Lett.* **2010**, *12*, 3288-3291.

Chapter 5

Colorimetric chiral sensing using flavin/melamine supramolecular organogels

- 5-1 Abstract
- 5-2 Introduction
- 5-3 Results and Discussion
- 5-4 Conclusion
- 5-5 Experimental Section
- 5-6 References and Notes

5-1 Abstract

In this study, chiral supramolecular organogels were formed via a hierarchical self-assembly of optically active riboflavin derivatives protected by carbamoyl groups and melamine derivatives. The supramolecular chirality exhibited by the helical stacking of riboflavin/melamine complexes, along with the redox and photocatalytic activities of riboflavin enable the application of supramolecular gels as chiral sensors that respond to phototropic stimuli. The chirality of chiral alcohols was successfully distinguished via a visible change from yellow to green in the gel.

5-2 Introduction

Helical supramolecular structures with controlled helix sense, formed by the self-assembly of small molecules, have garnered considerable attention in recent years.¹ This approach involves integrating small organic molecules, which possess inherent functionalities such as catalysis and optical properties, into a controlled right- or left-handed helical array. This method holds promise for the development of novel chiral materials exhibiting attractive functions. Owing to their induced and amplified supramolecular chirality, these helical supramolecules have potential applications in chiral sensing and optical resolution,² enantioselective catalysis,³ circularly polarized luminescence,⁴ and chiral optics and electronics.⁵ Although various successful examples of artificial helical polymers have been reported,^{1c,6} examples of supramolecular systems are limited. Furthermore, arranging the desired functional molecules in a helical configuration is challenging.

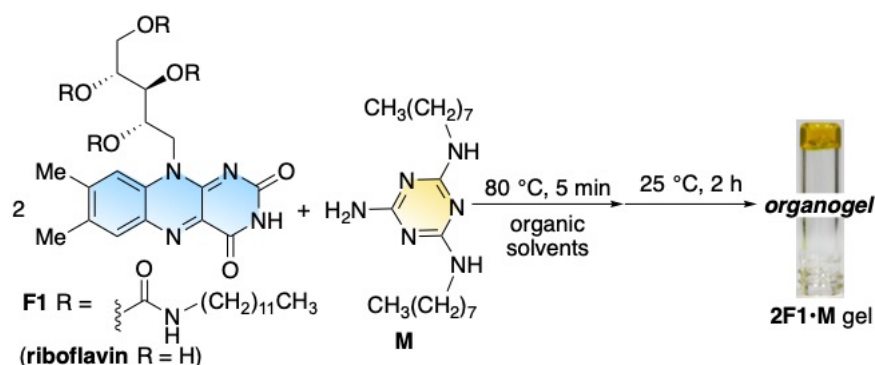
Riboflavin (widely known as vitamin B₂) and its derivatives, which are ubiquitous in nature, are involved in many biochemical processes by binding to proteins as cofactors.⁷ For example, light responses such as stem bending toward light, which is characteristic of higher plants, are attributed to the function of riboflavin in phototropin (a blue light receptor protein).⁸ It also serves as an active site for flavin-containing monooxygenase, which is essential for detoxification of xenobiotics.⁹ Riboflavin is composed of a planar π -conjugated isoalloxazine ring and an optically active ribityl group, and it has a variety of properties including photosensitivity, redox activity, and catalytic activity.¹⁰ The well-regulated chiral environment and non-covalent interactions of the surrounding proteins are responsible for the sophisticated biological functions of flavoproteins and flavoenzymes. Artificial supramolecules based on riboflavin are expected to be used as

unique chiral materials with biomimetic or novel artificial properties, owing to their diverse biological systems.⁷⁻⁹ Such findings are important for elucidating the biological functions of flavoenzymes and flavoproteins. Although remarkable advances have been made in the design of various functional supramolecular systems using vitamin B₁₂ analogs such as porphyrins,¹¹ there has been almost no development of riboflavin-containing supramolecules with chiral functions involving chiral recognition ability and asymmetric catalysis.¹²

In this study, chiral supramolecular gels based on riboflavin and melamine were prepared. The gel can be used for visible colorimetric chiral sensing of chiral compounds because of the helical chirality induced by self-assembly. Photocatalysis of riboflavin induces an enantioselective color change in the gel under visible-light irradiation, causing chiral sensing. Although several methods such as chiral high-performance liquid chromatography (HPLC) and gas chromatography (GC) have been developed over the past few decades to accurately obtain chiral information, the development of simpler methods that can easily visualize chiral discrimination remains a challenge.¹³ Enantioselective sensors have also been realized through the use of various chiral materials, like polymers,¹⁴ supramolecules,¹⁵ organometallic frameworks,¹⁶ and carbon nanotubes or graphene.¹⁷ Methods based on changes in absorbance of chiral chromogenic units are promising in facilitating chiral sensing.¹⁸

5-3 Results and Discussion

Carbamoylated riboflavin **F1**, where the optically active ribityl group of riboflavin (vitamin B₂) is protected with a carbamate group, and achiral N,N'-dioctylmelamine (**M**), where two amino groups of melamine are octylated, were mixed at a 2:1 molar ratio in 1,2-dichloroethane (DCE) to prepare supramolecular organogels (Table 1). The gels were obtained by heating the mixture at 80 °C for 5 min to facilitate complete dissolution. Subsequently, the mixture was allowed to stand at 25 °C for 5 min (Table 1: entry 15). When the rheological properties of the obtained gels were measured, they generally exhibited a viscoelastic behavior. Specifically, the storage modulus (G') was greater than the loss modulus (G'') (Figure 1).¹⁹

Table 1. Effect of solvents in the gelation of **F1** and **M**.^a

entry	gelator	solvent	phase
1	F1 + M	toluene	G (0.70 mM) ^b
2	F1 + M	Et ₂ O	G ^c
3	F1 + M	1,4-dioxane	S
4	F1 + M	THF	S
5	F1 + M	DMF	S
6	F1 + M	DMSO	G ^d
7	F1 + M	CCl ₄	PG
8	F1 + M	Cl ₂ C=CCl ₂	PG
9	F1 + M	chlorobenzene	G (0.70 mM) ^b
10	F1 + M	<i>o</i> -dichlorobenzene	G (0.95 mM) ^b
11	F1 + M	CHCl ₃	S
12	F1 + M	CH ₂ Cl ₂	PG
13	F1 + M	CHCl ₂ CHCl ₂ (TCE)	S
14	F1 + M	ClCH ₂ CH ₂ Cl (DCE)	G (0.55 mM) ^b
15	F1 + M	DCE	G (5 min)

^aA mixture of **F1** (10 mM) and **M** (5.0 mM) in various solvent (100 μL) was heated at 80 $^\circ\text{C}$ for 5 min and allowed to stand at ca. 25 $^\circ\text{C}$ for 2 h. G: gel; P: precipitate; S: solution; PG: partial gel. ^bCritical gelation concentration. ^c**F1** and **M** were partially dissolved. ^dTurbid gel.

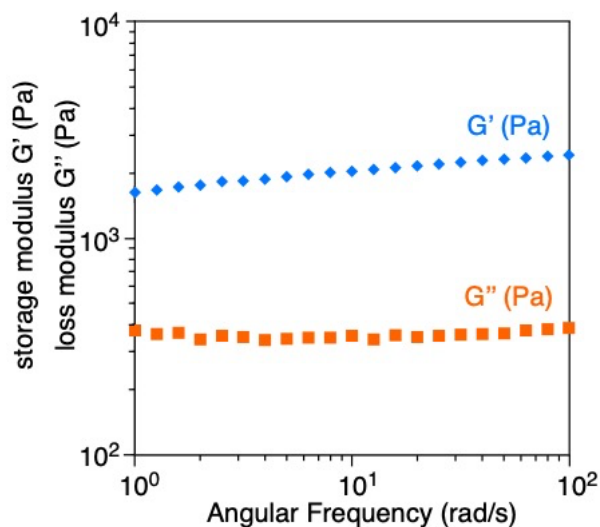


Figure 1. Angular frequency sweep measurements of the gels formed from solutions of **F1** and **M** (10 and 5.0 mM, respectively) in DCE (298 K; strain: 1%). Blue rhombus: storage modulus (G'). Orange square: loss modulus (G'').

Figures 2 and 3 show the morphologies of the supramolecular gels observed using scanning electron microscopy (SEM), scanning transmission electron microscopy (STEM), and atomic force microscopy (AFM). The SEM and STEM images of the diluted gel revealed a three-dimensional (3D) network structure containing linearly extending fibers, which is common in helical macro molecules and supramolecules (Figures 2).^{1c,6b} AFM results showed that fibers with an average height of 1.2 ± 0.2 nm were observed on the mica substrate (Figure 3). The magnified SEM images suggest that the fibrils have a one-handed-biased helical structure, which is probably right-handed (Figures 2).

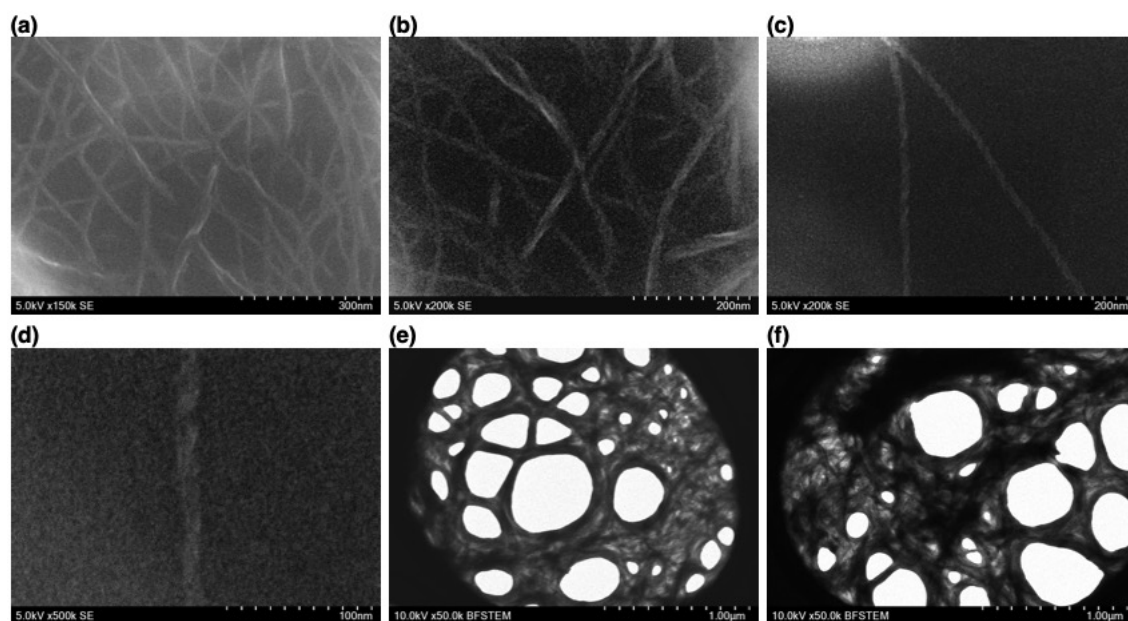


Figure 2. (a–d) SEM and (e and f) STEM images of **2F1•M** gel in DCE (5.0 mM).

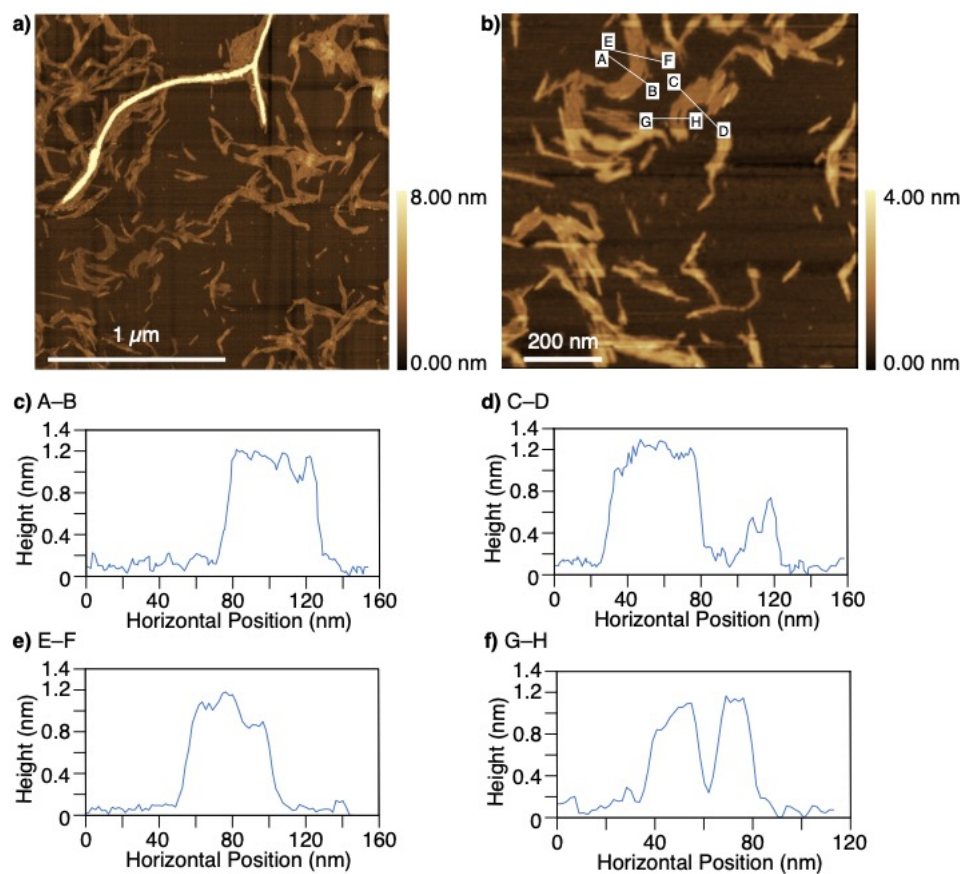


Figure 3. (a and b) AFM images of the dried **2F1•M** gel and (c–f) representative corresponding height profiles of the nanofibers.

Various spectroscopic measurements were performed to determine the supramolecular structures of the **F1** and **M** gels. ^1H NMR measurements of **F1**, **M**, and mixtures of **F1** and **M** in CDCl_3 were carried out at 25 °C. CDCl_3 , which is less prone to gelation, was used because rapid gelation can cause anisotropic effects and NMR signal loss during measurement (Table 1). The combination of **F1** and **M** shifted the signals of the N^3H proton (H^a) of **F1** and H^b proton of **M** toward lower magnetic fields (Figure 4A). This suggested that hydrogen bonds were formed between **F1** and **M**. ^1H NMR measurements were performed by changing the mixing ratio of **F1** and **M** in CDCl_3 , and a job plot analysis showed that two molecules of **F1** and one molecule of **M** formed a complex via hydrogen bonding at three points (Figure 4B).^{20,21} The hydrogen bonding of **F1** and **M** at three points confirmed by IR measurements and ^1H NMR. A shift of the N^3H proton to lower magnetic fields after gelation was also observed in the temperature-dependent ^1H NMR spectra of $2\text{F1}\cdot\text{M}$ gels in toluene- d_8 (Figure 5). The $2\text{F1}\cdot\text{M}$ gel formed in toluene- d_8 dissolved into solution when the temperature was raised to 80 °C. A temperature-dependent ^1H NMR spectra revealed that the H^a proton in **F1** shifted to a lower magnetic field upon broadening. In the IR spectra, the peaks related to the N-H and C=O vibrations of **F1** shifted to lower wavenumbers upon gelation (Figure 6).

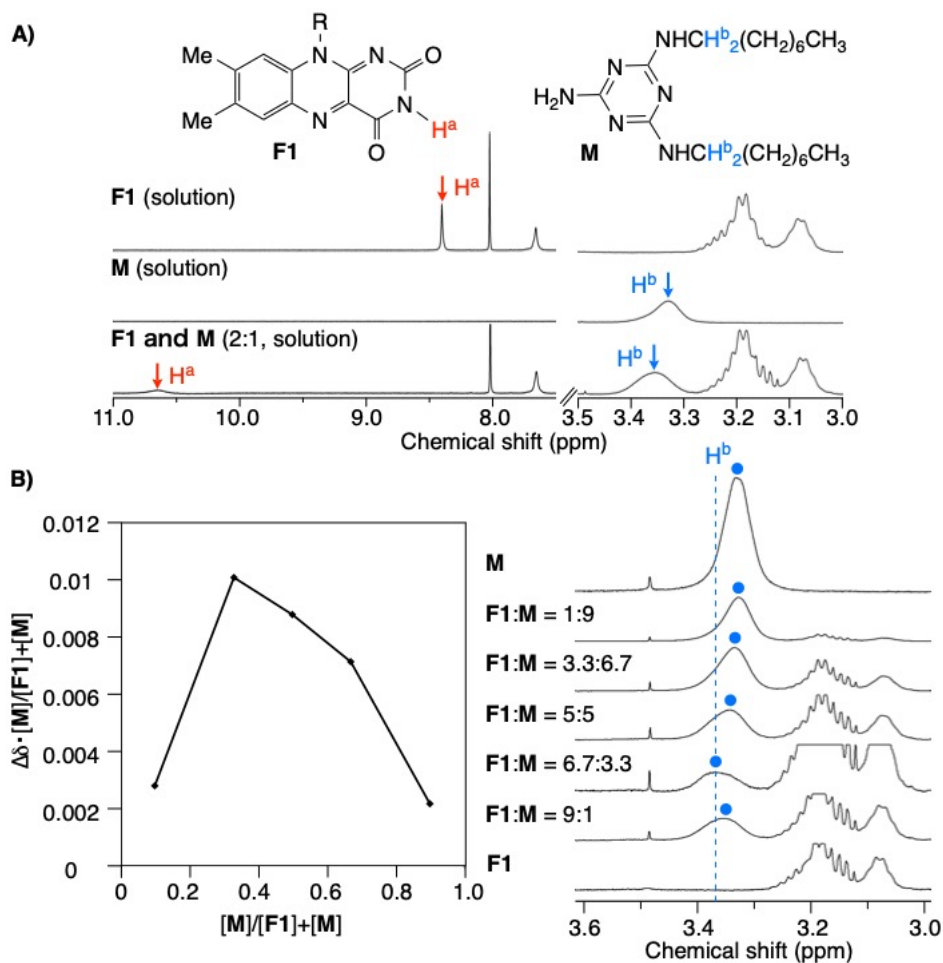


Figure 4. (A) ¹H NMR spectra of **F1** (6.7 mM), **M** (3.3 mM), and a mixture of **F1** and **M** (6.7 and 3.3 mM, respectively) in CDCl₃ at 25 °C. (B) Job plot analysis of the stoichiometry of the **F1** and **M** complex by ¹H NMR measurement of a mixture of **F1** and **M** in CDCl₃ at 25 °C. The total concentration of **F1** and **M** was 10 mM.

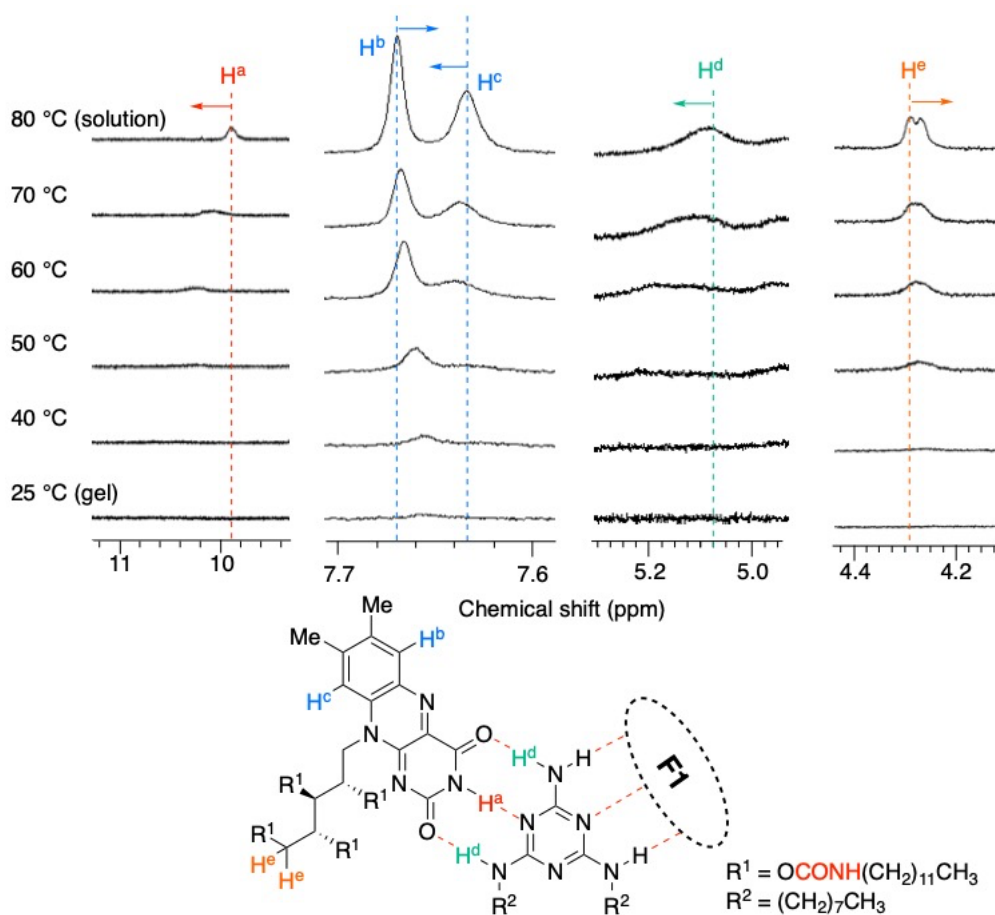


Figure 5. Temperature dependent ^1H NMR spectra of **2F1•M** organogel in toluene- d_8 (10 and 5.0 mM, respectively) at 25 °C. The organogel was allowed to stand at 25 °C for 24 h prior to the measurement, and the temperature was increased stepwise from 25 °C to 80 °C during the ^1H NMR measurement.

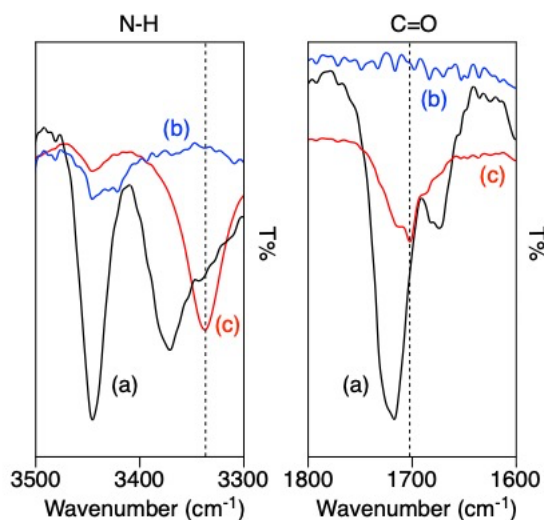


Figure 6. IR spectra of (a) **F1** solution (10 mM), (b) **M** solution (10 mM) and (c) **2F1•M** organogel (5.0 mM) in 1,1,2,2-tetrachloroethane at ca. 25 °C.

The CD and absorption spectra of the DCE solutions before and after the gelation of **F1** (10 mM) and **M** (5.0 mM) were analyzed to investigate the chiroptical properties of the supramolecular gels (Figure 7). When the absorption spectrum of the DCE solution of **F1** was measured, characteristic absorption signals due to a π -conjugated flavin chromophore appeared at about 350 and 450 nm (Figure 7Aa). The absorption spectrum of the clear yellow **2F1•M** gel showed a blue shift and hypochromic effect in the flavin chromophore region. This suggested that a supramolecular structure was formed through the π - π stacking of flavin ring with the π -conjugated plane (Figure 7Ab).²² Although the DCE solution of **F1** exhibited a weak negative Cotton effect at approximately 450 nm, a strong positive Cotton effect appeared upon gelation (Figures 7Ac and d). The CD measurements indicated that the supramolecular chirality derived from the optically active ribityl group of **F1** was expressed and amplified through the formation of **F1** and **M** associations.

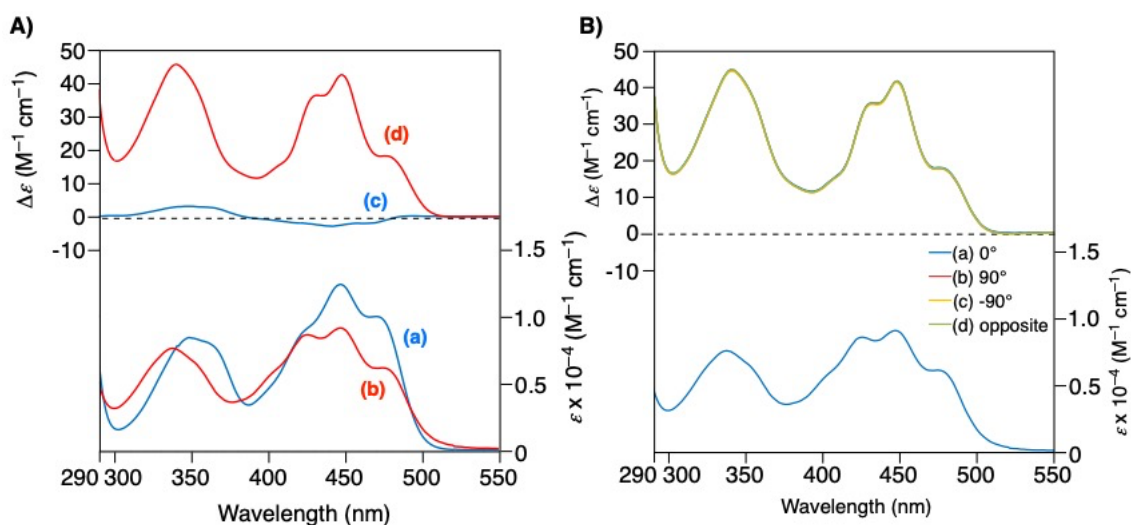
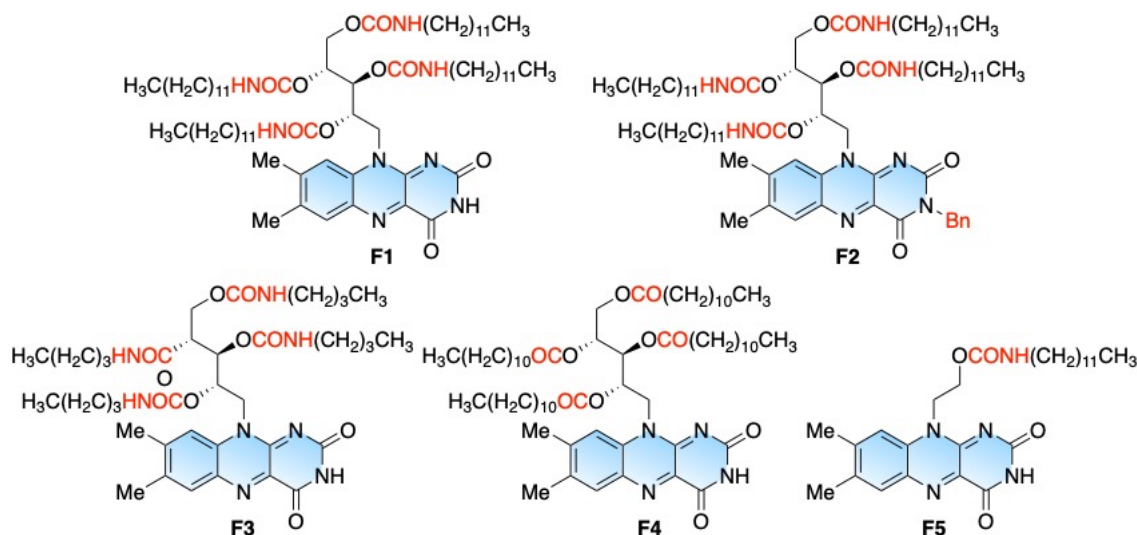


Figure 7. (A) Absorption (a, b) and circular dichroism (CD) (c, d) spectra of **F1** (0.1 mM) in DCE (a, c) and a supramolecular gel formed by **F1** and **M** (10 and 5.0 mM, respectively) in DCE (b, d). (B) CD and absorption spectra of **2F1•M** organogel in DCE (5.0 mM), measured three times by rotating a quartz cell by 90° and -90° (b, c) from the first position (a) around the axis of the incident light beam and also by setting the quartz cell in the opposite direction (d).

To investigate the substitution effect of **F1** on the gelation ability, we used **F2-F5**, an analog of **F1** as the gelator (Scheme 1). **F2** with N³ protected by a benzyl group, was synthesized to study the effect of the imide moiety of **F1**. **F2** and **M** were mixed in DCE in a 2:1 molar ratio, heated at 80 °C for 5 min (for complete dissolution), and allowed to stand at 25 °C for 7 days, but no gel was obtained (Table 2: entry 2). This suggests that the imide moiety of **F1** was involved in gel formation. In addition, **F3** and **F4** with butyl-carbamoylated and acylated ribityl groups, respectively, and **F5** with a single dodecylcarbamoylated hydroxyethyl unit, were synthesized. The DCE solutions of **F1** and **M** gelled in only 5 min, whereas the gels of **F3** and **M** took 30 min to form; **F4** and **F5** did not form gels even after 7 days (Table 2: entries 1 and 3–5). These results indicate

that the carbamoyl and long-chain dodecyl moieties modified on the ribityl group of **F1** are essential for rapid gelation.



Scheme 1. Structures of flavin derivatives.

Table 2. Gelation ability of flavin derivatives.^a

entry	gelator	solvent	phase	time
1	F1 + M	DCE	G	5 min
2	F2 + M	DCE	S	7 d
3	F3 + M	DCE	G	30 min
4	F4 + M	DCE	S	7 d
5	F5 + M	DCE	S	7 d

^aA mixture of **F** (10 mM) and **M** (5.0 mM) in various solvent (100 μ L) was heated at 80 $^{\circ}$ C for 5 min and allowed to stand at ca. 25 $^{\circ}$ C for 2 h. G: gel; S: solution.

Plausible gelation mechanisms of **F1** and **M** are shown in Figure 8. By mixing **F1** and **M** in DCE, two molecules of **F1** and one molecule of **M** formed a **2F1•M** complex via hydrogen bonding at three points between the C=O and N-H groups of the flavin ring and N and N-H groups of **M**. The conformation of **2F1•M** was deduced by density functional

theory (DFT) calculations (Figure 9). The planar $2\mathbf{F1}\cdot\mathbf{M}$ complexes with π -conjugated structures formed a one-handed excess helical stacked supramolecular aggregate (\mathbf{X}) by π - π stacking. Based on the AFM images, \mathbf{X} was predicted to have a fibrous structure with a height of approximately 1.2 nm, although the structure may have slightly changed owing to adsorption on the substrate. The supramolecular helical structure \mathbf{X} was surrounded by alkyl chains of hydrophobic dodecylcarbamate, which further aggregated to form supramolecular nanofibers (\mathbf{Y}) consisting of right-handed helices. Then, these nanofibers intertwined to form a three-dimensional network structure that immobilized a large amount of solvent, resulting in organogels.

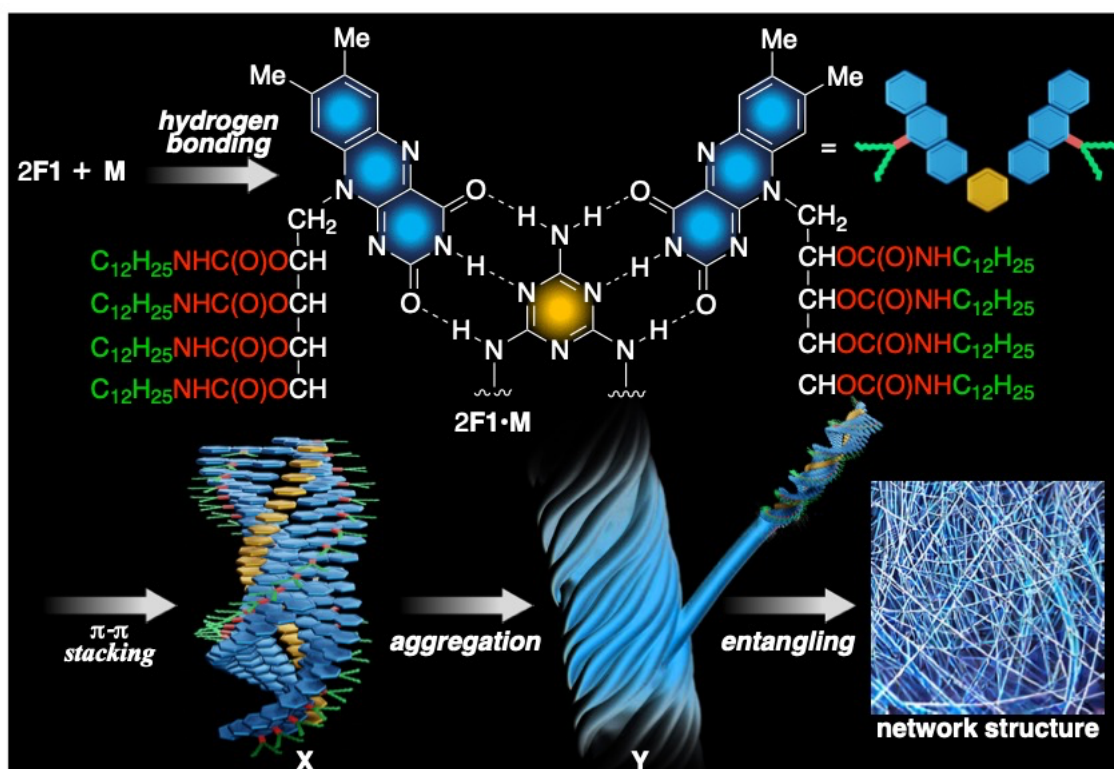
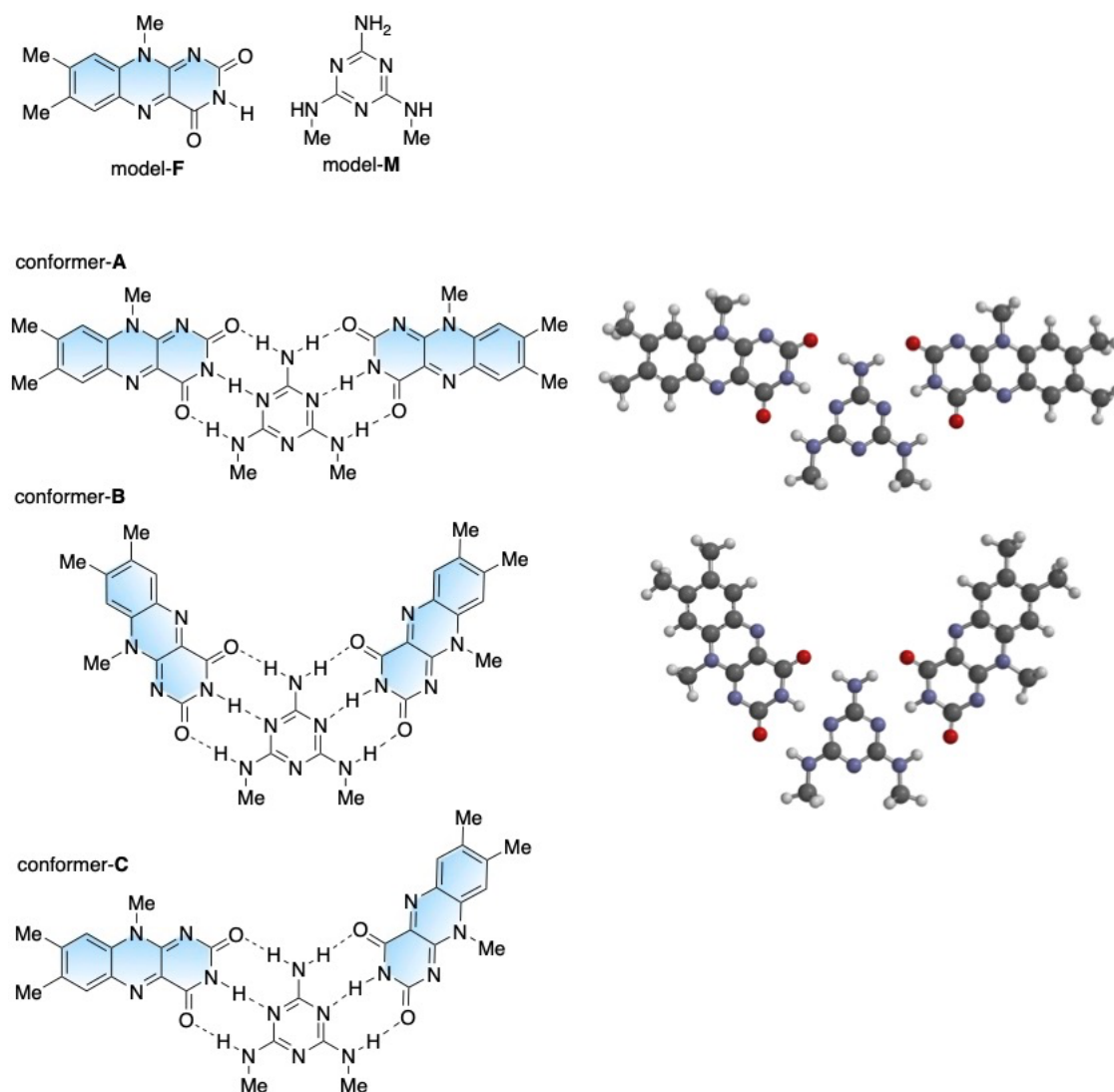


Figure 8. Proposed mechanism of gelation using F1 and M.



Conformation	Energy (hartrees)	
	B3LYP/6-31G*	M06-2X/6-311+G**
A	-2269.400586	-2269.107895
B	-2269.401138	-2269.108661
C	-2269.400889	-2269.108279

Figure 9. Energy-minimized structures calculated by Spartan'18 at the M06-2X/6-311+G** level in vacuum for four conformers for dimeric complexes of model-F and -M, formed through the hydrogen bonding of the imide unit, and calculated energies of the three conformers.

The obtained **2F1•M** supramolecular organogel was used as the chiral material. Hence, it can be adapted for colorimetric chiral sensing of optically active compounds using visual detection based on gel color changes. To detect the chirality of optically active compounds, DCE solutions of **F1** and **M** (10 and 5.0 mM, respectively) containing (2*S*,3*S*)- or (2*R*,3*R*)-diethyl tartrate (**1**; 0.10 M) were prepared. The mixture was then placed in a sample tube and capped to form a yellow gel, which was then exposed to visible light (blue LED; 7.2 W) for 4 h. After irradiation for 2 h, the gel with (2*S*,3*S*)-**1** remained yellow, whereas that with (2*R*,3*R*)-**1** changed to green (Figure 10a). Hence, the **2F1•M** gel can be used to distinguish the chirality of **1**. In addition, enantioselective colorimetric discrimination was performed using the optically active alcohols, **2** and **3** (Figures 10b and c). The results showed that (*R*)-**2**- and (2*R*,3*R*)-**3**-containing gels preferentially turned green after 2 and 1 h, respectively. The gels exhibited a greenish-yellow fluorescence resulting due to the fluorescent nature of **F1**. Chiral sensing was also possible both in the presence and absence of fluorescence (Figure 11A). Under visible-light irradiation, the fluorescence of the gel was gradually quenched, whereas that of the gel containing *R* compounds was rapidly quenched (Figure 11B). In contrast, no enantioselective color changes were observed when optically active BINOL (**4**), 1-phenylethyl alcohol (**5**), and 1-phenylethyl amine (**6**) were used as analytes (Figures 10d–g). Experimental investigations using various concentrations of **3** showed that the detection limit for **3**, which could be discriminated by the naked eye, can be estimated to be about 0.1 equiv. (0.5 mM; Figure 12). The green color of the obtained (2*R*,3*R*)-**3**-containing **2F1•M** gel was maintained for at least 72 h under N₂ atmosphere (Figure 13).

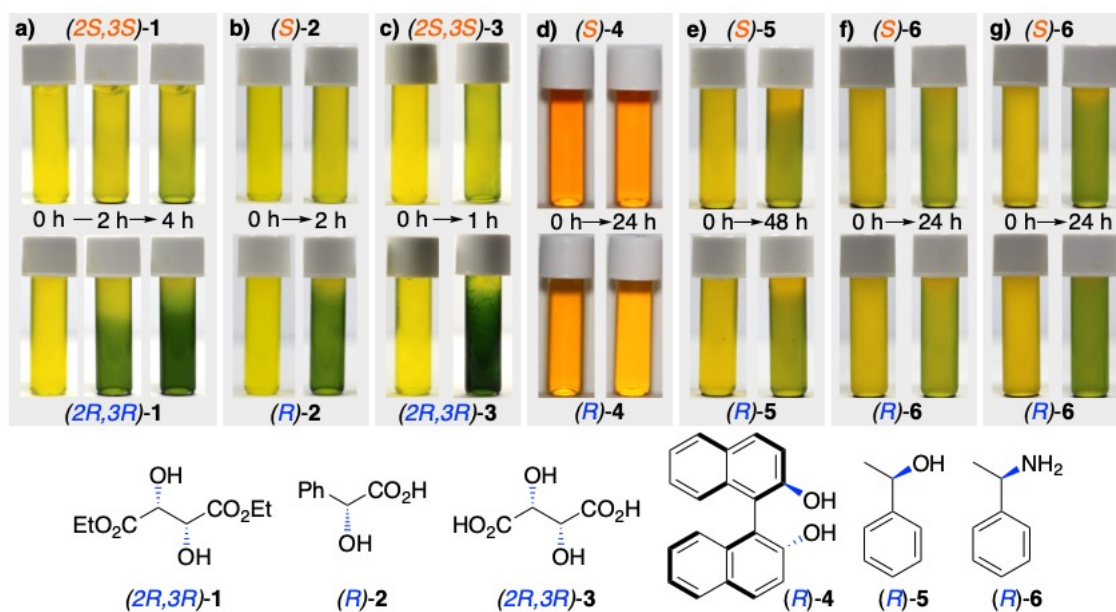


Figure 10. Images of the $2\mathbf{F1}\cdot\mathbf{M}$ gels (5.0 mM) containing optically active (a) **1** (20 equiv in DCE), (b) **2** (2.0 equiv in DCE), (c) **3** (2.0 equiv in DCE/MeOH (98:2 v/v)), (d) **4** (20 equiv in DCE), (e) **5** (40 equiv in DCE), (f) **6** (20 equiv in DCE), and (g) **6** (100 equiv in DCE) in sample tubes (0.8 mL).

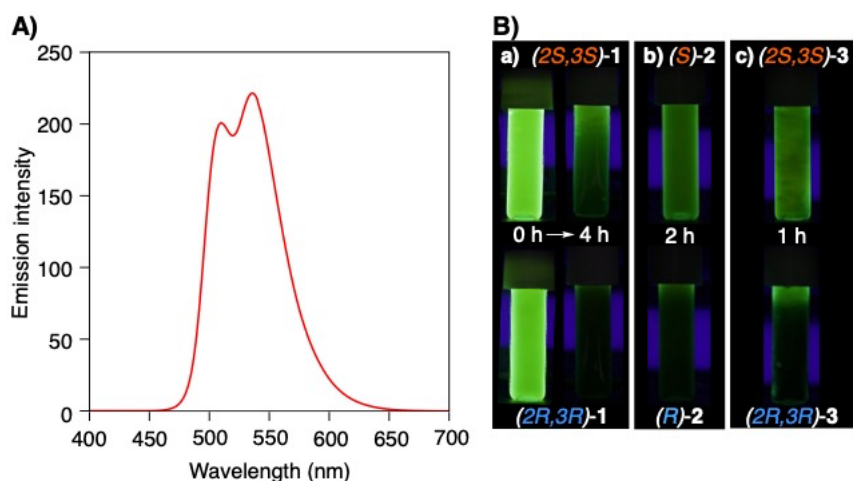


Figure 11. (A) Fluorescence spectrum (ca. 25 °C) of the organogel of **F1** and **M** in DCE (10 and 5.0 mM, respectively), formed after standing at ca. 25 °C for 24 h. Excitation wavelength was 365 nm. (B) Images of **2F1•M** gels (5.0 mM) containing optically active (a) **1** (20 equiv in DCE), (b) **2** (2.0 equiv in DCE), and (c) **3** (2.0 equiv in DCE/MeOH (98:2 v/v)) in sample tubes (0.8 mL). Fluorescence changes were observed by an UV light irradiation of 365 nm.

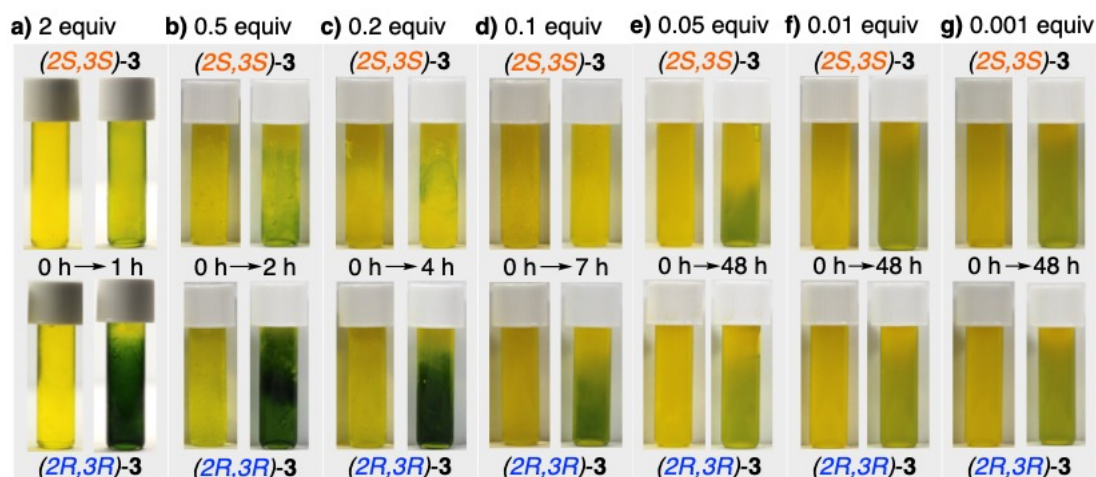


Figure 12. Photographs of sample tubes (0.8 mL) containing **2F1•M** gels (5.0 mM) with different concentrations of optically active **3** (2–0.001 equiv in DCE).

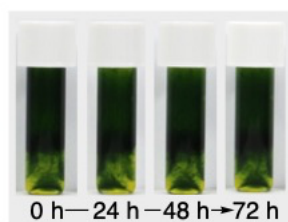


Figure 13. Images of the time-dependent change in green **2F1•M** gels (5.0 mM) containing *(2R,3R)*-**3** (1.0 equiv in DCE/MeOH (98:2 v/v)) in sample tubes (0.8 mL), after being left in a dark under N₂ atmosphere. Green gels were obtained by blue light irradiation for 4 h.

Changes were observed in the absorption spectra of **2F1•M** gels containing *(2S,3S)*- or *(2R,3R)*-**1** under blue LED irradiation (Figure 14A and B). Upon light irradiation, the characteristic absorption at about 450 nm from the π -conjugated structure of **F1** gradually decreased and a new absorption appeared around 620 nm, causing the gel to turn green. The observed absorption in the long wavelength region probably originated from the flavin radical (**F1H•**, Scheme 2).²³ The analysis of the green *(R)*-**2**-containing gel by electron spin resonance (ESR) revealed a radical signal with a *g*-value of 2.0041, suggesting the formation of **F1H•** (Figure 15a).^{23b} The change in absorption intensity at 620 nm for the **2F1•M** gels containing *(2S,3S)*- or *(2R,3R)*-**1** was plotted against time (Figure 14C). The increase in absorption intensity was not continuous; it increased rapidly after a specific induction period. The absorption of the *(2R,3R)*-**1** gel at 620 nm increased after 1 h of light exposure, but that of the *(2S,3S)*-**1** gel increased after approximately 3 h. The specific nonlinear absorption changes allow for the easy detection of the color change of the gel. Because this reaction is photoresponsive, the changed or unchanged color can be maintained even after termination of the light irradiation. The gel is a unique material that facilitates colorimetric chiral sensing under light irradiation.²⁴

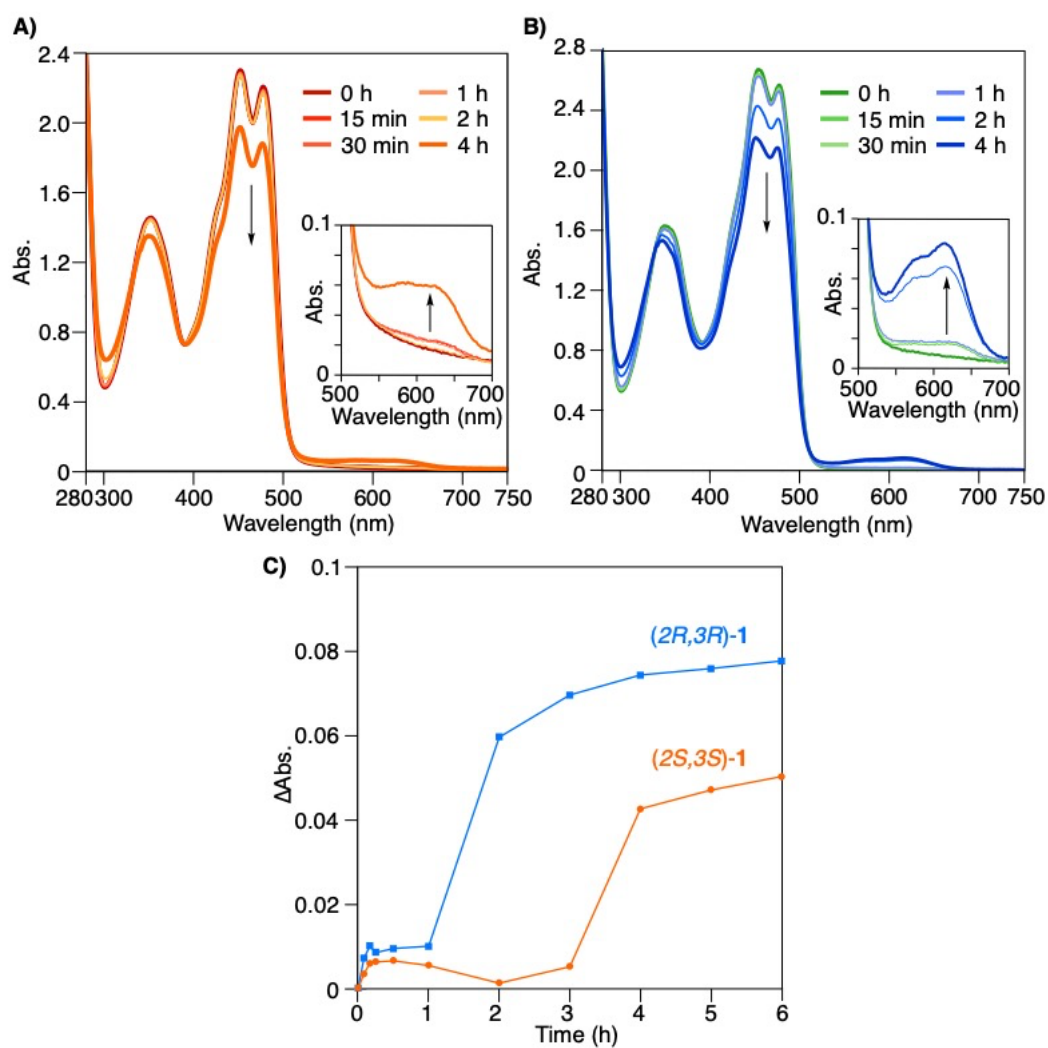
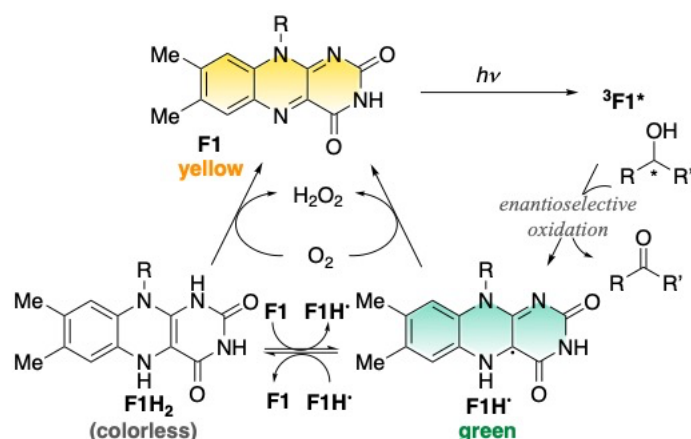


Figure 14. Absorption spectra of the **2F1•M** gel (1.0 mM) containing (A) (2*S*,3*S*)-**1** (20 equiv in DCE) and (B) (2*R*,3*R*)-**1** (20 equiv in DCE) in a 1 mm quartz cell under blue LED irradiation (7.2 W), along with an enlarged view of the longer-wavelength region (inset). (C) Change in absorption intensity of the peak at 620 nm.



Scheme 2. Proposed reaction mechanism of **F1** in the photooxidation of chiral alcohols.

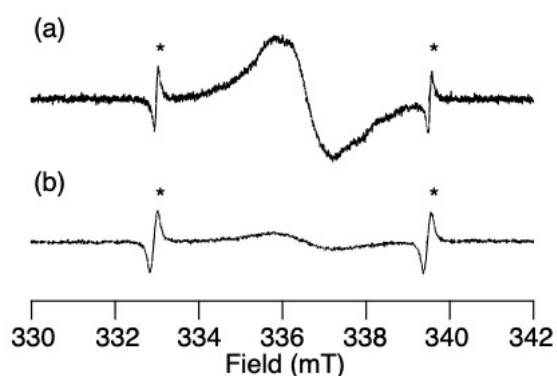


Figure 15. ESR measurements of $2\text{F1}\cdot\text{M}$ gel in the presence of $(R)\text{-2}$ after blue light irradiation for (a) 24 h and (b) 3 d under an O_2 atmosphere.

The proposed mechanism for the photoresponsive color change of supramolecular gels containing chiral alcohols is shown in Scheme 2. Riboflavin derivatives function as photocatalysts,²⁵ efficiently promoting the photooxidation of alcohols to produce aldehydes, ketones, and carboxylic acids under visible-light irradiation.^{23a,25c,26} Under blue LED irradiation, yellow **F1** gets converted into excited $^3\text{F1}^*$ with strong oxidizing power. $^3\text{F1}^*$ promotes the oxidation of alcohols to produce the corresponding ketones and

green flavin radical (**F1H**[•]).^{23a,26c} **F1H**[•] causes proportionation and disproportionation, leading to the conversion into **F1** and almost colorless **F1H**₂.^{23b,c} Under atmospheric air conditions, **F1H**[•] and **F1H**₂ react with O₂ to regenerate **F1**.^{23b,c} However, in this system, contact with O₂ was prevented because the sample tube was filled with the supramolecular gel and sealed with a screw cap. **F1H**[•] produced by the photooxidation of alcohols, initially reacted with the O₂ dissolved in the gel and converted into **F1**. As the remaining O₂ in the gel was consumed, **F1H**[•] accumulated, and the gel gradually turned green. This mechanism explains the induction period shown in Figure 14C. Therefore, if the amount of O₂ dissolved in the gel is reduced, the induction period and response time for the color change can be expected to be shorter. Because of the chiral structure of the **2F1**•**M** gel, each enantiomer exhibited a different reaction rate in the chiral gel. In general, when the colors change continuously, distinguishing the changes with the naked eye can be challenging. However, in this system, the reverse reaction of **F1H**[•] to **F1** resulted in a significant difference in the amount of **F1H**[•] present at any given time, and the gel containing the preferentially reacting enantiomer showed a significant color change, easily distinguishable with the naked eye. The structural changes before and after the color change of the **2F1**•**M** gel (5.0 mM) containing (2*R*,3*R*)-**1** (20 equiv.) were observed by transmission electron microscope (TEM). The 3D network structure consisting of nanofibrils did not change significantly after the color change due to light irradiation (Figure 16). As indicated by the change in the absorption spectra (Figure 14B), the color change appeared to result from the partial conversion of **F1** to **F1H**[•] rather than from an overall change in the higher-order structure.

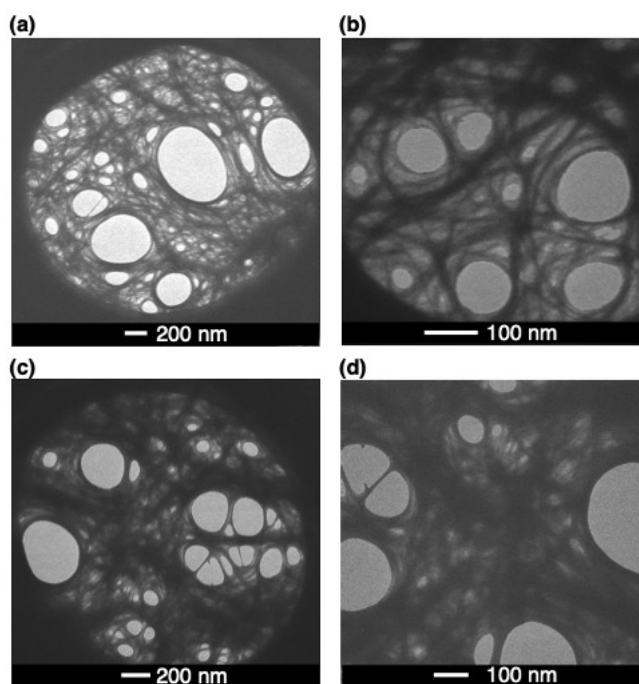


Figure 16. TEM images of the (a and b) yellow **2F1•M** gel (5.0 mM) (before light irradiation) and (c and d) green **2F1•M** gel (after 5 h light irradiation) containing (*2R,3R*)-**1** (20 equiv in DCE).

5-4 Conclusion

In conclusion, supramolecular organogels with riboflavin and melamine derivatives that exhibit supramolecular chirality owing to the hierarchical self-assembly of the riboflavin and melamine derivatives were developed. The resulting gels can be applied to the visible colorimetric chiral sensing of chiral alcohols using light responsivity. This system is expected to be useful for the development of novel bioinspired chiral supramolecules and soft materials with desirable functions.

5-5 Experimental Section

General

Melting points (M.p.) were determined on a SANSYO SMP-300 (SANSYO, Tokyo, Japan). The IR spectra were recorded on a JASCO FT/IR-660plus spectrophotometer (JASCO, Tokyo, Japan). The absorption, fluorescence, and circular dichroism (CD) spectra were measured in a 0.01, 0.02, 0.1 or 1.0 cm quartz cell using a JASCO V-560 spectrophotometer, FP-8300 spectrofluorometer, and J-720 and J-1500 spectrophotometers, respectively. The NMR spectra were measured using JEOL JNM-L400 and JNM ECX-500 spectrometers (JEOL, Tokyo, Japan) operating at 400 and 500 MHz, respectively, for ^1H and 100 and 126 MHz, respectively, for ^{13}C using tetramethylsilane (TMS) or a solvent residual peak as the internal standard. The electrospray ionization mass (ESI-MS) spectra were recorded using a Bruker microTOFII-SHIY3 mass spectrometer (Bruker, Billerica, USA). Rheological measurement was performed by a strain-controlled rheometer (TA Instruments ARES) with steel parallel-plate geometry (25 mm diameter). Scanning electron microscopy (SEM) was performed on a Hitachi High-Tech SU9000 (Hitachi High-Tech, Tokyo, Japan) with an accelerating voltage of 5 kV. Scanning transmission electron microscope (STEM) was also performed on a Hitachi High-Tech SU9000 with an accelerating voltage of 10 kV. Tapping mode atomic force microscope (AFM) was performed on Shimadzu SPM-9700 with an Al coated Si tip cantilever (2.8 N m^{-1}). The chiral HPLC analyses were performed on a JASCO PU-2080 Plus liquid chromatograph equipped with a UV-visible detector (JASCO UV-2070 Plus) and an optical rotation detector (JASCO OR-1590 Plus, Hg–Xe without filter) using COSMOSIL 5SL-II Packed Column (0.46 cm (i.d.) x 25 cm, Nacalai tesque). Electron spin resonance (ESR) spectra were recorded on

a Bruker E500 spectrometer operating at the X band and equipped with an Oxford helium cryostat.

Materials

All starting materials were purchased from Sigma-Aldrich (St. Louis, USA), FUJIFILM Wako Pure Chemical (Osaka, Japan), Nacalai tesque (Kyoto, Japan), and Tokyo Chemical Industry (Tokyo, Japan) and were used without further purification unless otherwise noted. N₂,N₄-Dioctyl-1,3,5-triazine-2,4,6-triamine (**M**)²⁷ was synthesized according to the previously reported method. Chiral reagents were also purchased from the commercial suppliers as follows: diethyl L-(+)-tartrate ((*1R,2R*)-**1**, Sigma-Aldrich, >99% ee), diethyl D-(-)-tartrate ((*1S,2S*)-**1**, Sigma-Aldrich, >99% ee), D-(-)-mandelic acid ((*R*)-**2**, TCI), L-(+)-mandelic acid ((*S*)-**2**, TCI), L-(+)-tartaric acid ((*1R,2R*)-**3**, TCI), D-(-)-tartaric acid ((*1S,2S*)-**3**, TCI).

Synthesis of Flavin Derivatives

Synthesis of F1. Dodecyl isocyanate (3.84 mL, 32.9 mmol)²⁸ was added to a suspension of riboflavin (2.00 g, 5.31 mmol) and copper(I) iodide (6.08 g, 31.9 mmol) in dry DMF (130 mL) under N₂ atmosphere. The mixture was stirred at 50 °C for 8 h, then MeOH (20 mL) was added. After the solvent was evaporated under reduced pressure, CHCl₃ (1.2 L) was added to the residue, and the solution was washed with water (300 mL x 3) and brine (300 mL x 3), dried over MgSO₄, filtrated, and evaporated to dryness to give the crude product (8.60 g) as a yellow solid. A part of residue (2.99 g) was purified by column chromatography (SiO₂, CHCl₃/ethyl acetate = 100/0 to 9/1 and CHCl₃/MeOH = 99/1 to 9/1, v/v), and reprecipitation with ethyl acetate to give **F1** (1.83 g, 81%) as a yellow solid.

Spectroscopic data of F1: Yellow solid. Mp: 220.5-221.0 °C. IR (KBr, cm^{-1}): 3343, 2921, 2852, 1699, 1584, 1545, 1466, 1260, 1150. ^1H NMR (500 MHz, CDCl_3 , 50 °C): δ 8.46 (s, 1H), 8.00 (s, 1H), 7.66 (s, 1H), 6.02 (br s, 1H), 5.71 (br s, 1H), 5.21 (br s, 5H), 4.78 (br s, 2H), 4.40 (br d, $J = 10.0$ Hz, 1H), 4.12 (br d, $J = 10.0$ Hz, 1H), 3.30-3.02 (br m, 6H), 2.75 (br s, 2H), 2.53 (s, 3H), 2.42 (s, 3H), 1.62-0.95 (m, 80H), 0.93-0.81 (m, 12H). $^{13}\text{C}\{^1\text{H}\}$ NMR (126 MHz, CDCl_3 , 50 °C): δ 159.5, 156.0, 155.7, 155.5, 155.3, 155.1, 150.9, 147.8, 136.7, 136.2, 135.0, 132.8, 131.9, 116.2, 71.1, 70.9, 63.3, 46.0, 41.5, 41.2, 41.0, 32.0, 30.0, 29.9, 29.7, 29.6, 29.44, 29.38, 29.3, 27.0, 26.9, 26.6, 22.7, 21.4, 19.4, 14.1. HRMS (ESI⁺): m/z calcd for $\text{C}_{69}\text{H}_{120}\text{N}_8\text{O}_{10}\text{Na}$ ($\text{M}+\text{Na}^+$), 1243.9020; found, 1243.8976. The purity of the obtained **F1** was also confirmed by HPLC analysis.

Synthesis of F2. A mixture of **F1** (303 mg, 0.248 mmol), benzyl bromide (83.5 mg, 0.488 mmol), and K_2CO_3 (135 mg, 0.979 mmol) in dry DMF (7.4 mL) was stirred at ca. 25 °C for 3 h under N_2 atmosphere, and water (200 mL) was added to the reaction mixture. After standing overnight, the yellow precipitate was collected by filtration, washed with water (20 mL x 3), and dissolved in CHCl_3 (50 mL), and the solution was dried over MgSO_4 . After the solvent was removed by evaporation, the residue was purified by column chromatography (SiO_2 , $\text{CHCl}_3/\text{hexane} = 1/10$ to $\text{CHCl}_3/\text{MeOH} = 20/1$, v/v) to give **F2** (263 mg, 81%) as a yellow solid.

Spectroscopic data of F2: Yellow solid. Mp: 208.9-209.9 °C. IR (KBr, cm^{-1}): 3335, 2922, 2851, 1700, 1583, 1547, 1466, 1265, 1149, 766. ^1H NMR (500 MHz, CDCl_3 , 50 °C): δ 7.98 (s, 1H), 7.61 (s, 1H), 7.57 (d, $J = 5.0$ Hz, 2H), 7.29-7.18 (m, 3H), 6.15 (br s, 1H), 5.72 (br s, 1H), 5.36-4.90 (m, 7H), 4.62 (br s, 2H), 4.39 (br d, $J = 10.0$ Hz, 1H), 4.13 (br d, $J = 10.0$ Hz, 1H), 3.30-2.98 (m, 6H), 2.70 (br s, 2H), 2.51 (s, 3H), 2.40 (s, 3H), 1.60-

0.96 (m, 80H), 0.94-0.81 (m, 12H). $^{13}\text{C}\{^1\text{H}\}$ NMR (126 MHz, CDCl_3 , 50 °C): δ 160.2, 156.3, 156.1, 155.8, 155.3, 149.6, 147.4, 137.5, 136.5, 136.3, 135.4, 133.1, 132.1, 129.9, 128.6, 127.9, 116.3, 71.5, 71.3, 63.7, 45.9, 45.5, 41.8, 41.5, 41.3, 32.3, 30.3, 30.2, 30.0, 29.9, 29.8, 29.7, 29.6, 27.3, 27.19, 27.17, 26.9, 23.0, 21.7, 19.6, 14.4. HRMS (ESI+): m/z calcd for $\text{C}_{79}\text{H}_{126}\text{N}_8\text{O}_{10}\text{Na}$ ($\text{M}+\text{Na}^+$), 1333.9489; found, 1333.9458.

Synthesis of F3. Butyl isocyanate (1.80 mL, 16.0 mmol) was added to a suspension of riboflavin (1.08 g, 2.87 mmol) and copper(I) iodide (3.08 g, 16.2 mmol) in dry DMF (150 mL) under N_2 atmosphere. The mixture was stirred at 70 °C for 6 h, then MeOH (10 mL) was added. After the solvent was evaporated under reduced pressure, CHCl_3 (500 mL) was added to the residue, and the solution was washed with water (400 mL x 4) and brine (400 mL), dried over MgSO_4 , filtrated, and evaporated to dryness to give the crude product (2.32 g) as a yellow solid. A part of residue (1.99 g) was purified by column chromatography (SiO_2 , CHCl_3 /ethyl acetate = 100/0 to 9/1 and CHCl_3 /MeOH = 99/1 to 9/1, v/v) and reprecipitation with diethyl ether to give **F3** (791 mg, 42%) as a yellow solid.

Spectroscopic data of F3: Yellow solid. Mp: 229.8-231.4 °C. IR (KBr, cm^{-1}): 3342, 3053, 2933, 2872, 1700, 1543, 1463, 1250, 1149. ^1H NMR (500 MHz, $\text{DMSO}-d_6$, 50 °C): δ 11.3 (s, 1H), 7.86 (s, 1H), 7.71 (br s, 1H), 7.45-6.70 (br m, 4H), 5.46 (br s, 1H), 5.38-4.40 (br m, 4H), 4.31 (br s, 1H), 4.08 (br s, 1H), 3.05-2.90 (br m, 6H), 2.56 (s, 2H), 2.50 (s, 3H, overlapped with $\text{DMSO}-d_5$), 2.38 (s, 3H), 1.45-1.20 (m, 12H), 1.05-0.65 (m, 16H). $^{13}\text{C}\{^1\text{H}\}$ NMR (126 MHz, $\text{DMSO}-d_6$, 50 °C): δ 159.7, 155.8, 155.6, 155.3, 155.1, 154.7, 150.5, 146.6, 136.5, 135.7, 133.9, 131.4, 131.1, 116.5, 72.3, 70.7, 69.0, 62.2, 45.1, 31.4, 31.0, 20.7, 20.5, 19.4 19.34, 19.26, 18.9, 18.7, 13.6, 13.4. HRMS (ESI+): m/z calcd for $\text{C}_{37}\text{H}_{56}\text{N}_8\text{O}_{10}\text{Na}$ ($\text{M}+\text{Na}^+$), 795.4012; found, 795.3982.

Synthesis of F4. A mixture of riboflavin (500 mg, 1.33 mmol), 4-dimethylamino pyridine (8.15 mg, 0.0667 mmol), and lauric anhydride (3.05 g, 7.97 mmol) in dichloromethane/pyridine (1/1 v/v, 13.3 mL) was stirred under reflux for 24 h. An additional lauric anhydride (1.01 g, 2.64 mmol) was added to the reaction mixture, and the mixture was then stirred for additional 24 h. After an addition of CHCl_3 (100 mL), the mixture was washed with water (100 mL x 3), dried over MgSO_4 , filtrated, and evaporated to dryness. The residue was roughly purified by column chromatography (SiO_2 , $\text{CHCl}_3/\text{MeOH} = 100/0$ to $24/1$, v/v), and the obtained crude mixture was then purified by column chromatography (SiO_2 , hexane/ethyl acetate = $100/0$ to $3/2$, v/v) to give **F4** (1.01 g, 69%) as a yellow solid.

Spectroscopic data of F4: yellow solid. Mp: 199.5-200.1 °C. IR (KBr, cm^{-1}): 3432, 3168, 3114, 3042, 2956, 2923, 2852, 1746, 1662, 1577, 1537, 1507, 1159. ^1H NMR (500 MHz, CDCl_3 , 50 °C, δ): 8.26 (s, 1H), 8.02 (s, 1H), 7.56 (s, 1H), 5.69 (d, $J = 10.0$ Hz, 1H), 5.51-5.36 (m, 2H), 5.29-4.73 (br s, 2H), 4.46 (dd, $J = 2.8, 12.2$ Hz, 1H), 4.20 (dd, $J = 6.2, 12.2$ Hz, 1H), 2.63-2.50 (m, 4H), 2.49-2.37 (m, 6H), 2.36-2.22 (m, 2H), 2.12-1.98 (m, 1H), 1.97-1.80 (m, 1H), 1.75-1.54 (m, 6H), 1.44-1.04 (m, 64H), 1.02-0.93 (m, 2H), 0.88 (t, $J = 7.5$ Hz, 12H). ^{13}C $\{^1\text{H}\}$ NMR (125 MHz, CDCl_3 , 50 °C, δ): 173.4, 173.1, 172.6, 172.5, 159.3, 154.3, 151.0, 147.9, 136.8, 136.4, 134.8, 133.2, 131.5, 115.9, 70.7, 69.3, 62.0, 45.1, 34.4, 34.3, 34.2, 33.9, 32.1, 29.8, 29.7, 29.51, 29.46, 29.30, 29.25, 29.1, 25.04, 24.98, 24.5, 22.8, 21.4, 19.4, 14.2. HRMS (ESI+): m/z calcd for $\text{C}_{65}\text{H}_{108}\text{N}_4\text{O}_{10}\text{Na}$ ($\text{M}+\text{Na}^+$), 1127.7958; found, 1127.7977.

Synthesis of F5. A mixture of 10-(2-hydroxyethyl)-7,8-dimethylisoalloxazine (1.00 g, 3.49 mmol)²⁹, copper(I) iodide (1.01 g, 5.30 mmol) and dodecyl isocyanate (2.53 mL,

10.6 mmol)²⁸ in dry DMF (77 mL) was stirred under N₂ atmosphere at 70 °C for 7 h. MeOH (10 mL) was added and stirred for 15 min. After the solvent was evaporated under reduced pressure, CHCl₃ (300 mL) was added to the residue, and the solution was washed with water (200 mL x 2) and brine (200 mL x 3), dried over MgSO₄, filtrated, and evaporated to dryness. The residue was purified by column chromatography (SiO₂, CHCl₃/ethyl acetate=49/1 to 9/1 and CHCl₃/MeOH=99/1 to 19/1, v/v) to give **F5** (112 mg, 6.4%) as a yellow solid.

Spectroscopic data of F5: Yellow solid. Mp: 254.8-255.6 °C. IR (KBr, cm⁻¹): 3247, 3049, 2924, 1718, 1543. ¹H NMR (500 MHz, CF₃COOD, 25 °C, δ): 8.21 (br s, 1H), 8.17 (br s, 1H), 5.28 (br s, 2H), 4.80 (br s, 2H), 2.97 (br s, 2H), 2.69 (s, 3H), 2.55 (s, 3H), 1.36-0.98 (m, 20H), 0.75 (br t, *J* = 6.25 Hz, 3H). ¹³C{¹H} NMR (126 MHz, CF₃COOD, 25 °C, δ): 161.6, 159.9, 151.7, 147.7, 143.7, 141.9, 134.7, 132.6, 131.0, 127.6, 118.6, 63.2, 50.5, 43.5, 33.7, 31.3, 31.24, 31.15, 31.1, 31.0, 30.9, 28.2, 24.2, 23.1, 20.4, 14.5. HRMS (ESI+): *m/z* calcd for C₂₇H₃₉N₅O₄Na (M+Na⁺), 520.2894; found, 520.2905.

Gelation Ability of F1 and M in Various Solvents. A mixture of **F1** (10 mM) and **M** (5.0 mM) in various solvent (100 μL) was heated at 80 °C for 5 min and allowed to stand at ca. 25 °C for 2 h. The gelation was confirmed by the inverse flow method (Table 1 and 2).

Analysis of Rheological Property. The measurement of the rheological property was conducted using the organogel that was formed as follows: by heating at 80 °C (oil bath) for 5 min, **F1** (12.2 mg, 0.0100 mmol) and **M** (1.75 mg, 0.00500 mmol) were completely dissolved in distilled 1,2-dichloroethane (DCE, 1.0 mL) and were stood at room

temperature for 24 h to obtain the organogel. The plot of the shear storage moduli (G') and the shear loss moduli (G'') of the gel versus the angular frequency revealed the G' value was higher than the G'' value over a range of angular frequency from 1 to 100 rad/s, indicated the viscoelastic nature that is typically observed for the supramolecular gels (Figure 1).

SEM and STEM Measurements. By heating at 80 °C (oil bath) for 5 min, **F1** (6.11 mg, 0.00500 mmol, 10 mM) and **M** (0.876 mg, 0.00250 mmol, 5.0 mM) were completely dissolved in distilled DCE (500 μ L). The temperature was gradually decreased from 80 °C to 25 °C over a period of 5.5 h, and then allowed to stand at 25 °C for an additional 18.5 h to obtain the gel. The gel was diluted with DCE and cast on a mica substrate, after which the sample was dried under a vacuum. The sample for SEM analysis was prepared by casting the supramolecular gels onto cover glasses and drying them under a vacuum. The sample for STEM analysis was prepared by casting the supramolecular gels onto copper microgrids (200 mesh, JEOL, NO. 780111613) and drying them under a vacuum.

AFM Measurement. By heating at 80 °C (oil bath) for 5 min, **F1** (2.44 mg, 0.00200 mmol, 10 mM) and **M** (0.350 mg, 0.00100 mmol, 5.0 mM) were completely dissolved in distilled DCE (200 μ L). The temperature was gradually decreased from 80 °C to 25 °C over a period of 5.5 h, and then allowed to stand at 25 °C for an additional 18.5 h to obtain the gel. The gel was diluted with DCE and cast on a mica substrate, after which the sample dried under vacuum. The AFM images showed that the nanofibers partially aligned in parallel on the substrate and appeared to form the single layer of the two-dimensional crystals (Figure 3).

Measurement of Chiroptical Property. By heating at 80 °C (oil bath) for 5 min, **F1** (12.2 mg, 0.0100 mmol) and **M** (1.75 mg, 0.00500 mmol) were completely dissolved in distilled DCE (1.0 mL). A portion of the obtained 1,2-dichloroethane solution was added to a 0.01 cm quartz cell. The temperature was gradually decreased from 80 °C to 25 °C over a period of 5.5 h (10 °C / h), and then allowed to stand at 25 °C for an additional 18.5 h to obtain the gel. The absorption and CD spectra of the obtained organogel were measured at ca. 25 °C (Figure 7). To confirm the presence of artifacts arising from the scattering and linear dichroism, the CD spectra were measured three times by rotating the sample quartz cell around the axis of the incident light beam and also by inverting the quartz cell (Figure 7B). The observed CD signals were constant throughout the rotation angles (in contrast to linear dichroism). Therefore, the observed CD signals were predominantly attributed to the genuine CD signals.^{12c,30}

DFT Calculation of 2F1•M Complex. The **2F1•M** complex can theoretically adopt three conformations (A, B, and C, Figure 9). The ¹H NMR measurement of **2F1•M** showed that both **F1** molecules were in the same environment, indicating the C₂ symmetry of **2F1•M**. Therefore, the possibility of conformer C was ruled out. To compare the stability between the conformers A and B, the molecular modeling and density functional theory (DFT) calculations were performed by Spartan '18 software (Wavefunction, I. I., CA).³¹ The simplified **F** and **M** compounds were used as the model compounds. The possible conformations (conformers A and B) for the **2F1•M** complex were constructed and fully optimized using the DFT calculations with the B3LYP functional and 6-31G* basis sets in Spartan '18 software. The geometries were further refined by the DFT calculations using the M06-2X functional with 6-311+G** basis sets. The energy-minimized

structures of the conformers A and B are shown in Figure 9. Based on the calculation, conformer A was found to be more stable than conformer B. Although the energy difference between the two conformers is small (2.0 kJ/mol) and the possibility of a stability reversal cannot be ruled out depending on the higher-order structure of the aggregate. However, because it was difficult to obtain concrete data on the precise higher-order structure, this manuscript assumes that the **2F1•M** complex adopts the conformation of A, as determined by the DFT calculation.

Table 3 Cartesian coordinates of conformer A optimized by B3LYP/6-31G*.

Atom	x	y	z
H	9.8944	2.4504	0.1051
C	9.4774	2.6054	1.0944
C	8.4587	3.0266	3.6514
C	8.1229	2.3224	1.3402
C	10.3075	3.0883	2.1024
C	9.793	3.308	3.4113
C	7.6048	2.5358	2.6437
H	8.0211	3.1745	4.6354
C	11.7558	3.3757	1.7953
H	12.4251	2.7711	2.4203
H	12.0068	4.4254	1.9923
H	11.9931	3.1646	0.7492
C	10.678	3.8347	4.5148
H	10.1193	3.9341	5.4491
H	11.093	4.8204	4.2678
H	11.5304	3.1708	4.7048
N	7.2686	1.8433	0.3586
N	6.2958	2.2789	2.9566
C	5.5186	1.8294	2.0167
C	5.9388	1.5777	0.6407
C	4.084	1.5413	2.3397
N	5.1636	1.1328	-0.3092
N	3.355	1.078	1.276
H	2.3434	0.8596	1.4436
C	3.8342	0.8668	-0.0294
O	3.071	0.4529	-0.8923
O	3.6146	1.7091	3.4597
C	7.7652	1.6142	-1.003
H	6.9343	1.2393	-1.5957
H	8.5745	0.878	-0.9857
H	8.1354	2.5532	-1.4259
H	-7.4963	-3.1311	-6.1561
C	-7.8764	-3.0408	-5.1453
C	-8.9104	-2.8274	-2.5671
C	-7.0207	-2.6497	-4.1021
C	-9.2199	-3.3181	-4.9088
C	-9.7557	-3.2119	-3.5934
C	-7.549	-2.5411	-2.7887
H	-9.2708	-2.73	-1.5471
C	-10.106	-3.7306	-6.0579
H	-10.9383	-3.0279	-6.1906

H	-10.5524	-4.7181	-5.885
H	-9.5493	-3.7737	-6.9983
C	-11.2104	-3.508	-3.3206
H	-11.4466	-3.3625	-2.2628
H	-11.4716	-4.5416	-3.5811
H	-11.8743	-2.8568	-3.9034
N	-5.6785	-2.3629	-4.3018
N	-6.7763	-2.1589	-1.7239
C	-5.5234	-1.8921	-1.9415
C	-4.8703	-1.9741	-3.2459
C	-4.6661	-1.4605	-0.7915
N	-3.6122	-1.7118	-3.4699
N	-3.3625	-1.2089	-1.1312
C	-2.8045	-1.3186	-2.4173
O	-1.6183	-1.0674	-2.5845
O	-5.1041	-1.3426	0.3481
C	-5.0944	-2.4636	-5.6442
H	-4.0437	-2.1949	-5.5655
H	-5.6071	-1.7773	-6.3248
H	-5.1923	-3.4877	-6.0161
H	-2.721	-0.886	-0.3672
C	-0.0387	0.6414	3.0091
N	-1.6161	-0.2697	1.0263
N	-1.322	0.3865	3.3162
N	0.5296	0.4782	1.7907
C	-0.3078	0.0195	0.8307
C	-2.0609	-0.0657	2.2892
N	0.7544	1.1016	3.9993
N	0.1944	-0.162	-0.4
N	-3.3599	-0.339	2.5336
H	1.7294	1.294	3.7821
H	-0.4074	-0.4822	-1.1544
H	1.1717	0.0487	-0.5869
H	-3.9263	-0.696	1.767
C	0.2863	1.3093	5.3544
H	-0.5449	2.0228	5.3883
H	1.1188	1.7044	5.9416
H	-0.0605	0.3744	5.8117
C	-3.9717	-0.17	3.835
H	-5.0226	-0.4593	3.7528
H	-3.9135	0.8709	4.1751
H	-3.4877	-0.7941	4.5961

Table 4 Cartesian coordinates of conformer A optimized by M06-2X/6-311+G**.

Atom	x	y	z
H	9.8584	2.4458	0.0978
C	9.444	2.6007	1.0852
C	8.4365	3.0176	3.6408
C	8.0919	2.3234	1.3378
C	10.2716	3.0744	2.0898
C	9.7648	3.2908	3.3966
C	7.5848	2.5349	2.6338
H	7.9999	3.1642	4.6226
C	11.7186	3.357	1.7943
H	12.3701	2.7365	2.4174
H	11.9648	4.4003	2.0117
H	11.9554	3.1594	0.7484
C	10.6636	3.8065	4.4879
H	10.1179	3.8968	5.4265
H	11.07	4.79	4.2357
H	11.5124	3.1371	4.6513
N	7.2369	1.8474	0.3594
N	6.2738	2.2803	2.9459
C	5.5045	1.8329	2.0185
C	5.9216	1.5751	0.6404
C	4.0684	1.5481	2.3454
N	5.1485	1.1227	-0.2963
N	3.3461	1.0745	1.2908
H	2.3359	0.8583	1.4521
C	3.8249	0.8534	-0.0086
O	3.0632	0.4323	-0.8506
O	3.6033	1.7242	3.451
C	7.7382	1.6308	-0.9977
H	6.9123	1.278	-1.6062
H	8.5335	0.8842	-0.9791
H	8.1221	2.5704	-1.397
H	-7.4647	-3.1118	-6.1386
C	-7.8485	-3.0273	-5.1306
C	-8.8892	-2.8259	-2.562
C	-7.0024	-2.6389	-4.0819
C	-9.1848	-3.3068	-4.8978
C	-9.7233	-3.2081	-3.5893
C	-7.5329	-2.5364	-2.7817
H	-9.2512	-2.7333	-1.5439
C	-10.0727	-3.7158	-6.0406
H	-10.9055	-3.0163	-6.1548

H	-10.5061	-4.704	-5.8641
H	-9.5208	-3.7466	-6.9796
C	-11.1746	-3.5144	-3.3363
H	-11.4165	-3.3907	-2.2812
H	-11.4185	-4.5408	-3.6226
H	-11.826	-2.8533	-3.9141
N	-5.6634	-2.3508	-4.2784
N	-6.7592	-2.1546	-1.7155
C	-5.5192	-1.8899	-1.9282
C	-4.861	-1.9689	-3.2327
C	-4.6632	-1.4595	-0.774
N	-3.6092	-1.7084	-3.4491
N	-3.3664	-1.2077	-1.1119
C	-2.8077	-1.3187	-2.3935
O	-1.6329	-1.0681	-2.5445
O	-5.0966	-1.346	0.3517
C	-5.0898	-2.4511	-5.6207
H	-4.0404	-2.1823	-5.5558
H	-5.6108	-1.7656	-6.2919
H	-5.1916	-3.4749	-5.985
H	-2.7213	-0.8884	-0.354
C	-0.035	0.6432	2.9899
N	-1.6041	-0.2725	1.018
N	-1.3123	0.3879	3.2956
N	0.5308	0.4757	1.7778
C	-0.3017	0.0136	0.8244
C	-2.0478	-0.065	2.2737
N	0.7493	1.1069	3.9764
N	0.2001	-0.1722	-0.4003
N	-3.3403	-0.333	2.5227
H	1.7211	1.3046	3.7664
H	-0.3999	-0.4986	-1.1501
H	1.1751	0.0323	-0.5848
H	-3.9132	-0.69	1.7654
C	0.2617	1.3134	5.3228
H	-0.5589	2.0339	5.3383
H	1.0872	1.6941	5.9229
H	-0.1014	0.3798	5.7591
C	-3.9303	-0.1568	3.8322
H	-4.9766	-0.4518	3.7721
H	-3.8673	0.8836	4.1554
H	-3.4239	-0.7716	4.579

Table 5 Cartesian coordinates of conformer B optimized by B3LYP/6-31G*.

Atom	x	y	z
H	9.4706	1.2387	2.1589
C	8.8118	1.2346	1.2986
C	7.164	1.2328	-0.9467
C	7.4313	1.0425	1.4713
C	9.3605	1.4241	0.033
C	8.5239	1.4244	-1.1195
C	6.5918	1.0416	0.327
H	6.4847	1.2237	-1.7939
C	10.8483	1.6279	-0.1075
H	11.0777	2.5839	-0.5962
H	11.3023	0.8428	-0.7258
H	11.3473	1.6203	0.8659
C	9.1039	1.6302	-2.4978
H	8.3247	1.5722	-3.2625
H	9.8639	0.8753	-2.7354
H	9.5909	2.6095	-2.5895
N	6.852	0.8547	2.7175
N	5.2374	0.8581	0.4197
C	4.7219	0.6867	1.6003
C	5.4854	0.6755	2.8454
C	3.2424	0.4803	1.7211
N	4.9735	0.5114	4.0347
N	2.8066	0.3163	3.0125
H	1.7785	0.1694	3.1538
C	3.6085	0.3307	4.1641
O	3.0894	0.1825	5.2655
O	2.4973	0.4602	0.7501
C	7.6873	0.844	3.9242
H	7.0313	0.6818	4.7765
H	8.2046	1.8032	4.0273
H	8.4234	0.0369	3.8581
H	-8.2889	-1.1073	-5.1043
C	-7.2327	-0.9256	-5.264
C	-4.5281	-0.4635	-5.7393
C	-6.3613	-0.8162	-4.1676
C	-6.7663	-0.8058	-6.5706
C	-5.3847	-0.5698	-6.8214
C	-4.9829	-0.581	-4.411
H	-3.4662	-0.2835	-5.8775
C	-7.7375	-0.9264	-7.7183
H	-7.4687	-1.7545	-8.3867

H	-7.7443	-0.0172	-8.3324
H	-8.757	-1.1006	-7.3627
C	-4.8619	-0.4375	-8.231
H	-3.7811	-0.2681	-8.2312
H	-5.3313	0.4011	-8.7622
H	-5.0589	-1.3395	-8.825
N	-6.7908	-0.9291	-2.8537
N	-4.0744	-0.4641	-3.3926
C	-4.5053	-0.5745	-2.1717
C	-5.8972	-0.8167	-1.8019
C	-3.5254	-0.4498	-1.0449
N	-6.3363	-0.93	-0.578
N	-4.0876	-0.585	0.1999
C	-5.4442	-0.8187	0.473
O	-5.819	-0.9211	1.6367
O	-2.3321	-0.2455	-1.2287
C	-8.2073	-1.1748	-2.5589
H	-8.3142	-1.2167	-1.4774
H	-8.5203	-2.1238	-3.0032
H	-8.8172	-0.363	-2.9647
H	-3.4442	-0.5107	1.0248
C	-0.6261	-0.2634	4.6182
N	-2.2748	-0.3901	2.4915
N	-1.929	-0.4745	4.8661
N	-0.0723	-0.1017	3.3915
C	-0.9463	-0.1724	2.3613
C	-2.7039	-0.5319	3.7696
N	0.2069	-0.2066	5.6768
N	-0.4593	-0.0142	1.1185
N	-4.0225	-0.7478	3.9519
H	1.1974	-0.054	5.4972
H	-1.0773	-0.0825	0.3143
H	0.534	0.1444	0.9752
H	-4.619	-0.7901	3.1279
C	-0.2421	-0.3569	7.0453
H	-0.9542	0.4281	7.3266
H	0.6345	-0.2912	7.6951
H	-0.7339	-1.3235	7.2052
C	-4.6211	-0.9093	5.2606
H	-5.6887	-1.1009	5.1208
H	-4.4978	-0.0098	5.8762
H	-4.1743	-1.7485	5.8062

Table 6 Cartesian coordinates of conformer B optimized by M06-2X/6-311+G**.

Atom	x	y	z
H	9.4411	1.2732	2.1703
C	8.7855	1.2519	1.31
C	7.1502	1.2038	-0.9367
C	7.4075	1.05	1.475
C	9.3308	1.4268	0.0485
C	8.5026	1.4046	-1.1029
C	6.5817	1.0251	0.3348
H	6.4736	1.1775	-1.7839
C	10.811	1.6432	-0.1028
H	11.016	2.6031	-0.5852
H	11.2547	0.8672	-0.7326
H	11.3153	1.6303	0.8634
C	9.0943	1.5965	-2.4735
H	8.3197	1.5461	-3.2381
H	9.8402	0.8284	-2.6949
H	9.5925	2.5662	-2.5582
N	6.8279	0.8747	2.7196
N	5.2276	0.8304	0.4293
C	4.7168	0.6704	1.5983
C	5.4759	0.6813	2.8491
C	3.2375	0.4549	1.7163
N	4.9617	0.5237	4.03
N	2.8031	0.2988	3.0021
H	1.778	0.1504	3.1439
C	3.5998	0.3296	4.1523
O	3.0755	0.1832	5.2365
O	2.5039	0.4233	0.7551
C	7.6654	0.8998	3.9186
H	7.0202	0.7543	4.7788
H	8.1712	1.8638	3.9899
H	8.4032	0.098	3.8648
H	-8.2768	-1.0945	-5.0746
C	-7.2225	-0.9167	-5.2394
C	-4.5239	-0.4636	-5.7236
C	-6.3451	-0.8053	-4.1511
C	-6.7584	-0.8029	-6.5397
C	-5.3827	-0.5708	-6.7949
C	-4.9782	-0.5772	-4.3995
H	-3.463	-0.288	-5.8639
C	-7.7193	-0.9304	-7.6892
H	-7.446	-1.7713	-8.3324

H	-7.7042	-0.0324	-8.3125
H	-8.7387	-1.0863	-7.3377
C	-4.8793	-0.4459	-8.2075
H	-3.8017	-0.2859	-8.2201
H	-5.3532	0.3928	-8.7247
H	-5.0962	-1.3474	-8.7866
N	-6.7731	-0.9109	-2.8388
N	-4.0687	-0.4628	-3.3799
C	-4.4946	-0.568	-2.1712
C	-5.8892	-0.8005	-1.7956
C	-3.5106	-0.4476	-1.0452
N	-6.3219	-0.9044	-0.5766
N	-4.0722	-0.5725	0.1941
C	-5.4272	-0.791	0.4686
O	-5.7887	-0.8761	1.624
O	-2.3299	-0.2573	-1.227
C	-8.1897	-1.1422	-2.5554
H	-8.3125	-1.1795	-1.4785
H	-8.5014	-2.0881	-3.0001
H	-8.7819	-0.3259	-2.9712
H	-3.4304	-0.5005	1.0166
C	-0.6146	-0.2781	4.589
N	-2.2549	-0.393	2.4701
N	-1.9133	-0.4855	4.8334
N	-0.0618	-0.1181	3.3678
C	-0.9313	-0.185	2.343
C	-2.685	-0.5348	3.7416
N	0.2072	-0.2264	5.6479
N	-0.4441	-0.0323	1.1042
N	-3.9966	-0.7446	3.9284
H	1.1977	-0.0791	5.4822
H	-1.0603	-0.0995	0.3038
H	0.5472	0.1191	0.9626
H	-4.5997	-0.7788	3.1128
C	-0.2698	-0.3864	7.0047
H	-0.9909	0.3925	7.2633
H	0.5885	-0.3196	7.6718
H	-0.7581	-1.3543	7.1383
C	-4.574	-0.9102	5.2446
H	-5.6415	-1.0892	5.1215
H	-4.4247	-0.0179	5.8574
H	-4.1227	-1.7567	5.7672

Colorimetric Chiral Sensing. By heating at 80 °C (oil bath) for 5 min, **F1** (12.2 mg, 0.0100 mmol), **M** (1.75 mg, 0.00500 mmol), and (*2R,3R*)-**1** (20.6 mg, 0.100 mmol) were completely dissolved in DCE (1.0 mL). A portion of the obtained DCE solution (ca. 800 mL) was added to a sample tube (d=8 mm) until it was full. The tube was sealed with a screw cap and was stood at room temperature for 24 h. The obtained gel was irradiated with blue LED (7.2 W) at 25 °C (Figure 17).

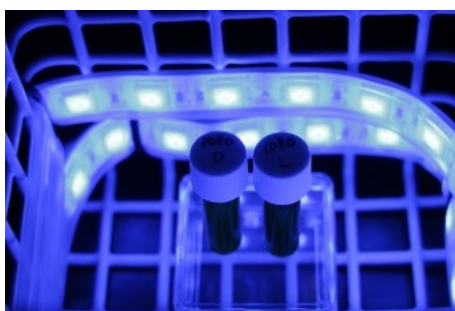


Figure 17. Experimental setup for colorimetric chiral sensing.

ESR Measurement. A mixture of **F1** (12.2 mg, 0.0100 mmol) and **M** (1.75 mg, 0.00500 mmol) in DCE (1.0 mL) was heated at 80 °C for 5 min and allowed to stand at ca. 25 °C for 24 h to obtain the organogel. A solution of (*R*)-**2** (76.0 mg, 0.500 mmol) in CH₃CN (0.5 mL) was added to the gel. After standing at 25 °C for 24 h, the resulting gel was irradiated with blue LED at 25 °C for 24 h, causing the gel's color change from yellow to green. The gel was separated from the supernatant solution, and dried under reduced pressure. Following the ESR measurement of the green xerogel (Figure 15a), the xerogel was left under O₂ (1 atm) for 3 d without light irradiation. Subsequently, the ESR measurement was also performed on the obtained xerogel whose color was changed to yellow (Figure 15b). The apparent radical signal with *g*-values 2.0041 indicated the formation of the radical flavin **F1H[•]** (Figure 15a). After standing under O₂ for 3 d, the

signal of the radical was weakened (Figure 15b), probably due to the reaction with O₂ forming **F1** (Scheme 2).

TEM Measurements. By heating at 80 °C (oil bath) for 5 min, **F1** (12.2 mg, 0.0100 mmol), **M** (1.75 mg, 0.00500 mmol), and (2*R*,3*R*)-**1** (20.6 mg, 0.100 mmol) were completely dissolved in DCE (1.0 mL). A portion of the obtained DCE solution (ca. 800 mL) was added to a sample tube (d=8 mm) until it was full. The tube was sealed with a screw cap and was stood at room temperature for 24 h. The obtained gel was irradiated with blue LED (7.2 W) at 25 °C for 5 h. The gel was diluted with DCE and cast onto a copper microgrid (200 mesh, JEOL, NO. 780111613), after which the sample was dried under a vacuum.

5-6 References and Notes

- [1] (a) Palmans, A. R. A.; Meijer, E. W. *Angew. Chem. Int. Ed.* **2007**, *46*, 8948-8968. (b) Liu, M.; Zhang, L.; Wang, T. *Chem. Rev.* **2015**, *115*, 7304-7397. (c) Yashima, E.; Ousaka, N.; Taura, D.; Shimomura, K.; Ikai, T.; Maeda, K. *Chem. Rev.* **2016**, *116*, 13752-13990. (d) Xing, P.; Zhao, Y. *Acc. Chem. Res.* **2018**, *51*, 2324-2334.
- [2] (a) Kodama, K.; Kobayashi, Y.; Saigo, K. *Chem. –Eur. J.* **2007**, *13*, 2144-2152. (b) Chen, X.; Huang, Z.; Chen, S.-Y.; Li, K.; Yu, X.-Q.; Pu, L. *J. Am. Chem. Soc.* **2010**, *132*, 7297-7299. (c) Tu, T.; Fang, W.; Bao, X.; Li, X.; Dötz, K. H. *Angew. Chem. Int. Ed.* **2011**, *50*, 6601-6605. (d) Jung, J. H.; Moon, S.-J.; Ahn, J.; Jaworski, J.; Shinkai, S. *ACS Nano* **2013**, *7*, 2595-2601. (e) Wang, X.; Duan, P.; Liu, M. *Chem. –Asian J.* **2014**, *9*, 770-778. (f) Salikolimi, K.; Praveen, V. K.; Sudhakar, A. A.; Yamada, K.; Horimoto, N. N.; Ishida, Y. *Nat. Commun.* **2020**, *11*, 2311.
- [3] (a) Jin, Q.; Zhang, L.; Cao, H.; Wang, T.; Zhu, X.; Jiang, J.; Liu, M. *Langmuir* **2011**, *27*, 13847-13853. (b) Raynal, M.; Portier, F.; van Leeuwen, P. W. N. M.; Bouteiller, L. *J. Am. Chem. Soc.* **2013**, *135*, 17687-17690. (c) Huerta, E.; van Genabeek, B.; Lamers, B. A. G.; Koenigs, M. M. E.; Meijer, E. W.; Palmans, A. R. A. *Chem. –Eur. J.* **2015**, *21*, 3682-3690. (d) Desmarchelier, A.; Caumes, X.; Raynal, M.; Vidal-Ferran, A.; van Leeuwen, P. W. N. M.; Bouteiller, L. *J. Am. Chem. Soc.* **2016**, *138*, 4908-4916. (e) Jiang, J.; Meng, Y.; Zhang, L.; Liu, M. *J. Am. Chem. Soc.* **2016**, *138*, 15629-15635. (f) Shen, Z.; Sang, Y.; Wang, T.; Jiang, J.; Meng, Y.; Jiang, Y.; Okuro, K.; Aida, T.; Liu, M. *Nat. Commun.* **2019**, *10*, 3976.
- [4] (a) Kaseyama, T.; Furumi, S.; Zhang, X.; Tanaka, K.; Takeuchi, M. *Angew. Chem. Int. Ed.* **2011**, *50*, 3684-3687. (b) Liu, J.; Su, H.; Meng, L.; Zhao, Y.; Deng, C.; Ng, J. C. Y.; Lu, P.; Faisal, M.; Lam, J. W. Y.; Huang, X.; et al. *Chem. Sci.* **2012**, *3*, 2737-

2747. (c) Kumar, J.; Nakashima, T.; Tsumatori, H.; Mori, M.; Naito, M.; Kawai, T. *Chem. –Eur. J.* **2013**, *19*, 14090-14097. (d) Yang, D.; Duan, P.; Zhang, L.; Liu, M. *Nat. Commun.* **2017**, *8*, 15727. (e) Hu, S.; Hu, L.; Zhu, X.; Wang, Y.; Liu, M. *Angew. Chem. Int. Ed.* **2021**, *60*, 19451-19457.
- [5] (a) Feng, X.; Marcon, V.; Pisula, W.; Hansen, M. R.; Kirkpatrick, J.; Grozema, F.; Andrienko, D.; Kremer, K.; Müllen, K. *Nat. Mater.* **2009**, *8*, 421-426. (b) Zhang, Y.; Chen, P.; Jiang, L.; Hu, W.; Liu, M. *J. Am. Chem. Soc.* **2009**, *131*, 2756-2757.
- [6] (a) Nakano, T.; Okamoto, Y. *Chem. Rev.* **2001**, *101*, 4013-4038. (b) Yashima, E.; Maeda, K.; Iida, H.; Furusho, Y.; Nagai, K. *Chem. Rev.* **2009**, *109*, 6102-6211. (c) Megens, R. P.; Roelfes, G. *Chem. –Eur. J.* **2011**, *17*, 8514-8523. (d) Leigh, T.; Fernandez-Trillo, P. *Nat. Rev. Chem.* **2020**, *4*, 291-310. (e) Zhou, L.; He, K.; Liu, N.; Wu, Z.-Q. *Polym. Chem.* **2022**, *13*, 3967-3974.
- [7] (a) Müller, F. *Chemistry and biochemistry of flavoenzymes*; CRC Press, 1991. (b) Massey, V. *Biochem. Soc. Trans.* **2000**, *28*, 283-296. (c) Chemistry, R. S. o.; Silva, E.; Edwards, A. M. *Flavins: Photochemistry and Photobiology*; RSC Publishing, 2006. (d) Weber, S.; Schleicher, E. *Flavins and Flavoproteins: Methods and Protocols*; 2014.
- [8] (a) Briggs, W. R.; Christie, J. M. *Trends Plant Sci* **2002**, *7*, 204-210. (b) Christie, J. M. *Annu. Rev. Plant Biol.* **2007**, *58*, 21-45.
- [9] (a) van Berkel, W. J. H.; Kamerbeek, N. M.; Fraaije, M. W. *J. Biotechnol.* **2006**, *124*, 670-689. (b) Walsh, C. T.; Wencewicz, T. A. *Nat. Prod. Rep.* **2013**, *30*, 175-200. (c) Bailleul, G.; Yang, G.; Nicoll, C. R.; Mattevi, A.; Fraaije, M. W.; Mascotti, M. L. *Nat. Commun.* **2023**, *14*, 1042.

- [10] (a) Schwechheimer, S. K.; Park, E. Y.; Revuelta, J. L.; Becker, J.; Wittmann, C. *Appl. Microbiol. Biotechnol.* **2016**, *100*, 2107-2119. (b) Averianova, L. A.; Balabanova, L. A.; Son, O. M.; Podvolotskaya, A. B.; Tekutyeva, L. A. *Front. Bioeng. Biotechnol.* **2020**, *8*.
- [11] Lee, H.; Park, H.; Ryu, D. Y.; Jang, W.-D. *Chem. Soc. Rev.* **2023**, *52*, 1947-1974.
- [12] (a) Ju, S.-Y.; Doll, J.; Sharma, I.; Papadimitrakopoulos, F. *Nat. Nanotechnol.* **2008**, *3*, 356-362. (b) Iida, H.; Iwahana, S.; Mizoguchi, T.; Yashima, E. *J. Am. Chem. Soc.* **2012**, *134*, 15103-15113. (c) Iida, H.; Miki, M.; Iwahana, S.; Yashima, E. *Chem.–Eur. J.* **2014**, *20*, 4257-4262.
- [13] (a) Busch, K. W.; Busch, M. A. *Chiral Analysis*; Elsevier Science, 2011. (b) Leung, D.; Kang, S. O.; Anslyn, E. V. *Chem. Soc. Rev.* **2012**, *41*, 448-479. (c) Zhang, X.; Yin, J.; Yoon, J. *Chem. Rev.* **2014**, *114*, 4918-4959.
- [14] (a) Torsi, L.; Farinola, G. M.; Marinelli, F.; Tanese, M. C.; Omar, O. H.; Valli, L.; Babudri, F.; Palmisano, F.; Zambonin, P. G.; Naso, F. *Nat. Mater.* **2008**, *7*, 412-417. (b) Ibanez, J. G.; Rincón, M. E.; Gutierrez-Granados, S.; Chahma, M. h.; Jaramillo-Quintero, O. A.; Frontana-Uribe, B. A. *Chem. Rev.* **2018**, *118*, 4731-4816.
- [15] (a) Hembury, G. A.; Borovkov, V. V.; Inoue, Y. *Chem. Rev.* **2008**, *108*, 1-73. (b) Chen, L.-J.; Yang, H.-B.; Shionoya, M. *Chem. Soc. Rev.* **2017**, *46*, 2555-2576.
- [16] (a) Okur, S.; Qin, P.; Chandresh, A.; Li, C.; Zhang, Z.; Lemmer, U.; Heinke, L. *Angew. Chem. Int. Ed.* **2021**, *60*, 3566-3571. (b) Zhan, K.; Jiang, Y.; Heinke, L. *Chem. Commun.* **2023**, *59*, 8704-8707.
- [17] (a) Kybert, N. J.; Lerner, M. B.; Yodh, J. S.; Preti, G.; Johnson, A. T. C. *ACS Nano* **2013**, *7*, 2800-2807. (b) Zhang, Y.; Liu, X.; Qiu, S.; Zhang, Q.; Tang, W.; Liu, H.; Guo, Y.; Ma, Y.; Guo, X.; Liu, Y. *J. Am. Chem. Soc.* **2019**, *141*, 14643-14649.

- [18] (a) Kubo, Y.; Maeda, S. y.; Tokita, S.; Kubo, M. *Nature* **1996**, *382*, 522-524. (b) Tsubaki, K.; Nuruzzaman, M.; Kusumoto, T.; Hayashi, N.; Bin-Gui, W.; Fuji, K. *Org. Lett.* **2001**, *3*, 4071-4073. (c) Folmer-Andersen, J. F.; Lynch, V. M.; Anslyn, E. V. *J. Am. Chem. Soc.* **2005**, *127*, 7986-7987. (d) Tsubaki, K.; Tanima, D.; Nuruzzaman, M.; Kusumoto, T.; Fuji, K.; Kawabata, T. *J. Org. Chem.* **2005**, *70*, 4609-4616. (e) Jung, J. H.; Lee, S. J.; Kim, J. S.; Lee, W. S.; Sakata, Y.; Kaneda, T. *Org. Lett.* **2006**, *8*, 3009-3012. (f) Maeda, K.; Mochizuki, H.; Watanabe, M.; Yashima, E. *J. Am. Chem. Soc.* **2006**, *128*, 7639-7650. (g) Leung, D.; Folmer-Andersen, J. F.; Lynch, V. M.; Anslyn, E. V. *J. Am. Chem. Soc.* **2008**, *130*, 12318-12327. (h) Lee, H.-E.; Ahn, H.-Y.; Mun, J.; Lee, Y. Y.; Kim, M.; Cho, N. H.; Chang, K.; Kim, W. S.; Rho, J.; Nam, K. T. *Nature* **2018**, *556*, 360-365. (i) Maeda, K.; Hirose, D.; Nozaki, M.; Shimizu, Y.; Mori, T.; Yamanaka, K.; Ogino, K.; Nishimura, T.; Taniguchi, T.; Moro, M.; Yashima, E. *Science Advances* **2021**, *7*, eabg5381.
- [19] Kavanagh, G. M.; Ross-Murphy, S. B. *Prog. Polym. Sci.* **1998**, *23*, 533-562.
- [20] (a) Tamura, N.; Mitsui, K.; Nabeshima, T.; Yano, Y. *J. Chem. Soc., Perkin Trans. 2*, **1994**, 2229-2237. (b) Breinlinger, E.; Niemz, A.; Rotello, V. M. *J. Am. Chem. Soc.* **1995**, *117*, 5379-5380. (c) Cooke, G. *Angew. Chem. Int. Ed.* **2003**, *42*, 4860-4870. (d) Nandwana, V.; Samuel, I.; Cooke, G.; Rotello, V. M. *Acc. Chem. Res.* **2013**, *46*, 1000-1009.
- [21] (a) Manna, S.; Saha, A.; Nandi, A. K. *Chem. Commun.* **2006**, 4285-4287. (b) Saha, A.; Manna, S.; Nandi, A. K. *Langmuir* **2007**, *23*, 13126-13135. (c) Bachl, J.; Hohenleutner, A.; Dhar, B. B.; Cativiela, C.; Maitra, U.; König, B.; Díaz, D. D. *J. Mater. Chem. A* **2013**, *1*, 4577-4588.

- [22] (a) Iida, H.; Mizoguchi, T.; Oh, S.-D.; Yashima, E. *Polym. Chem.* **2010**, *1*, 841-848.
(b) Nakade, H.; Jordan, B. J.; Xu, H.; Han, G.; Srivastava, S.; Arvizo, R. R.; Cooke, G.; Rotello, V. M. *J. Am. Chem. Soc.* **2006**, *128*, 14924-14929. (c) Ebitani, M.; In, Y.; Ishida, T.; Sakaguchi, K. i.; Flippen-Anderson, J.; Karle, I. *Acta Crystallog., Sect. B: Struct. Sci.* **1993**, *49*, 136-144.
- [23] (a) Megerle, U.; Wenninger, M.; Kutta, R. J.; Lechner, R.; König, B.; Dick, B.; Riedle, E. *Phys. Chem. Chem. Phys.* **2011**, *13*, 8869-8880. (b) Nanni, E. J., Jr.; Sawyer, D. T.; Ball, S. S.; Bruice, T. C. *J. Am. Chem. Soc.* **1981**, *103*, 2797-2802. (c) Kemal, C.; Chan, T. W.; Bruice, T. C. *J. Am. Chem. Soc.* **1977**, *99*, 7272-7286.
- [24] (a) Xu, F.; Feringa, B. L. *Adv. Mater.* **2023**, *35*, 2204413. (b) Qu, D.-H.; Wang, Q.-C.; Zhang, Q.-W.; Ma, X.; Tian, H. *Chem. Rev.* **2015**, *115*, 7543-7588.
- [25] (a) Svobodová, E.; Cibulka, R. New Applications of Flavin Photocatalysis. In *Flavin-Based Catalysis*, 2021; pp 265-291. (b) Cheng, B.; König, B. Benzylic Photooxidation by Flavins. In *Flavin-Based Catalysis*, 2021; pp 245-264. (c) König, B.; Kümmel, S.; Svobodová, E.; Cibulka, R. *Phys. Sci. Rev.* **2018**, *3*.
- [26] (a) Fukuzumi, S.; Kuroda, S.; Tanaka, T. *J. Am. Chem. Soc.* **1985**, *107*, 3020-3027.
(b) Schmaderer, H.; Hilgers, P.; Lechner, R.; König, B. *Adv. Synth. Catal.* **2009**, *351*, 163-174. (c) Feldmeier, C.; Bartling, H.; Magerl, K.; Gschwind, R. M. *Angew. Chem. Int. Ed.* **2015**, *54*, 1347-1351.
- [27] Xu, J.; Wu, G.; Wang, Z.; Zhang, X. *Chem. Sci.* **2012**, *3*, 3227-3230.
- [28] Charalambides, Y. C.; Moratti, S. C. *Synth. Commun.* **2007**, *37*, 1037-1044.
- [29] Sakai, T.; Kumoi, T.; Ishikawa, T.; Nitta, T.; Iida, H. *Org. Biomol. Chem.* **2018**, *16*, 3999-4007.

[30] Maoz, B. M.; Chaikin, Y.; Tesler, A. B.; Bar Elli, O.; Fan, Z.; Govorov, A. O.; Markovich, G. *Nano Lett.* **2013**, *13*, 1203-1209.

[31] Spartan '18; Wavefunction, CA.

List of Publications

Papers

1. “Phototropin-Inspired Chemoselective Synthesis of Unsymmetrical Disulfides: Aerobic Oxidative Heterocoupling of Thiols Using Flavin Photocatalysis”
Marina Oka, Daichi Katsube, Takeshi Tsuji, Hiroki Iida
Org. Lett. **2020**, *22*, 9244–9248.
2. “Green Aerobic Oxidation of Thiols to Disulfides by Flavin-Iodine Coupled Organocatalysis”
Marina Oka, Ryo Kozako, Hiroki Iida
Synlett **2021**, *32*, 1227–1230.
3. “Chiral Supramolecular Organogel Constructed Using Riboflavin and Melamine: Its Application in Photo-Catalyzed Colorimetric Chiral Sensing and Enantioselective Adsorption”
Marina Oka, Ryo Kozako, Yuta Teranishi, Yuta Yamada, Kazuhiro Miyake, Takuya Fujimura, Ryo Sasai, Takahisa Ikeue, Hiroki Iida
Chem. –Eur. J. **2024**, e202303353.
4. “Riboflavin-Based Photocatalysis for Aerobic Oxidative S–N Bond Formation of Thiols and Amines”
Marina Oka, Aki Takeda, Hiroki Iida
Chem. Lett. **2024**. DOI: 10.1093/chemle/upad057

Other Related Papers

1. “Non-Covalently Immobilized Chiral Imidazolidinone on Sulfated-Chitin: Reusable Heterogeneous Organocatalysts for Asymmetric Diels-Alder Reaction”
Mirai Watanabe, Takuya Sakai, Marina Oka, Yuki Makinose, Hidetoshi Miyazaki, Hiroki Iida
Adv. Synth. Catal. **2020**, *362*, 255–260.
2. “Aerobic Oxidative C–H Azolation of Indoles and One-Pot Synthesis of Azolyl Thioindoles by Flavin-Iodine-Coupled Organocatalysis”
Kazumasa Tanimoto, Hayaki Okai, Marina Oka, Ryoma Ohkado, Hiroki Iida
Org. Lett. **2021**, *23*, 2084–2088.
3. “Low-Voltage-Driven Electrochemical Aerobic Oxygenation with Flavin Catalysis: Chemoselective Synthesis of Sulfoxides from Sulfides”
Taiga Mizushima, Marina Oka, Yasushi Imada, Hiroki Iida
Adv. Synth. Catal. **2022**, *364*, 2443–2448.
4. “Aerobic cross-dehydrogenative coupling of toluenes and *o*-phenylenediamines by flavin photocatalysis for the facile synthesis of benzimidazoles”
Yuta Shiogai, Marina Oka, Hiroki Iida
Org. Biomol. Chem. **2023**, *21*, 2081–2085.
5. “Atom-Economical Syntheses of Dihydropyrroles Using Flavin-Iodine-Catalyzed Aerobic Multistep and Multicomponent Reactions”
Aki Takeda, Marina Oka, Hiroki Iida
J. Org. Chem. **2023**, *88*, 7551–7556.

Acknowledgement

The present studies have been carried out at the Department of Chemistry, Graduate School of Natural Science and Technology, Shimane University, during 2018–2024.

The author wishes to express her grateful acknowledgement to Associate Professor Hiroki Iida whose encouragement and helpful suggestions have been indispensable to the completion of the present thesis.

The author also wishes to acknowledge to Professor Takeshi Tsuji for measurement of nanosecond laser flash spectroscopy, Mr. Kazuhiro Miyake of Nara Institute of Science and Technology for SEM and STEM measurements, Dr. Takuya Fujimura and Professor Ryo Sasai for AFM and TEM measurements, Associate Professor Takahisa Ikeue for ESR measurement.

The author acknowledges Mr. Daichi Katsube, Ms. Aki Takeda, Mr. Ryo Kozako, Mr. Yuta Teranishi, Mr. Yuta Yamada for their experimental assistance. It is pleasure to express her appreciation to the colleagues of the laboratory their encouragement and friendship.

She is very grateful to Fellowship of the SU Capacity Building Project Towards a Sustainable Society (S-SPRING) during 2021–2023 and the Research Fellowship of the Japan Society for the Promotion of Science for Young Scientist during 2023–2024.

Finally, she would like to give her special thanks to Professors Yutaka Nishigaichi, Makoto Handa, and Isao Yamaguchi for serving on her dissertation committee.

January 2024

Marina OKA